



PETERSBURG NUCLEAR PHYSICS INSTITUTE NAMED BY B.P. KONSTANTINOV  
OF NATIONAL RESEARCH CENTER "KURCHATOV INSTITUTE"



# PNPI Scientific Highlights 2020





PETERSBURG NUCLEAR PHYSICS INSTITUTE NAMED BY B.P. KONSTANTINOV  
OF NATIONAL RESEARCH CENTER "KURCHATOV INSTITUTE"



# PNPI Scientific Highlights 2020

Gatchina • 2021

**Chief-editors:**

V.V. Voronin  
S.V. Sarantseva  
S.I. Vorobyov

**Proofreaders:**

E.Yu. Orobets  
N.V. Silinskaya  
A.I. Zaitseva (translation)

**Editors:**

D.N. Aristov	V.V. Sarantsev
A.A. Vorobyov	M.V. Suyasova
S.I. Vorobyov	A.V. Titov
A.L. Konevega	O.L. Fedin
A.I. Kurbakov	S.R. Friedmann
M.F. Matveev	Yu.P. Chernenkov
V.Yu. Petrov	K.A. Shabalin

**Technical editing and design:**

T.A. Parfeeva

**Layout composition:**

E.V. Veselovskaya

**Executive in charge**

S.I. Vorobyov

**PNPI Scientific Highlights 2020.** – Gatchina, Leningradskaya obl.:  
NRC “Kurchatov Institute” – PNPI Publishing, 2021. – 128 pages.

The publication is a compilation of abstracts of the most significant results of scientific research at NRC “Kurchatov Institute” – PNPI in 2020. In addition to an abstract, each scientific result in the volume features references to the full articles of leading domestic and foreign publications, where the study is described in detail and where one can get acquainted with its full content.

Copyright © 2021 NRC “Kurchatov Institute” – PNPI

# Table of contents

---

<b>5</b>	Preface
<b>9</b>	Research Divisions
<b>25</b>	Theoretical and Mathematical Physics
<b>35</b>	Research Based on the Use of Neutrons and Photons
<b>51</b>	Research Based on the Use of Protons and Ions. Neutrino Physics
<b>69</b>	Molecular and Radiation Biophysics
<b>83</b>	Nuclear Medicine (Isotope Production, Beam Therapy, Bio- and Nanotechnologies for Medical Purposes)
<b>89</b>	Nuclear Reactor and Accelerator Physics
<b>97</b>	Applied Research and Developments
<b>105</b>	Basic Installations
<b>113</b>	Management and Research

---



КОСТАДИНОВИЧ  
КОСТИЦИНОВИЧ

## Preface

Petersburg Nuclear Physics Institute named by B.P. Konstantinov of NRC “Kurchatov Institute” (hereinafter – NRC “Kurchatov Institute” – PNPI, the Institute) is a multidisciplinary research center. It conducts fundamental and applied research in the field of particle and high-energy physics, nuclear physics, condensed matter physics, molecular and radiation biophysics.

The scientific achievements of Institute’s researchers have been awarded the Lenin and State prizes, the prizes of the Government of the Russian Federation and the Academic prizes. Three employees were elected full members and eight employees – the Corresponding Members of the Russian Academy of Sciences (RAS). In 2020 the Institute employed 2 138 workers including 537 researchers, 75 Doctors of Sciences and 261 Candidates of Sciences. At the moment, two employees are the corresponding members of the RAS.

The Institute consists of five research divisions sharing a common infrastructure:

- Theoretical Physics Division;
- Neutron Research Division;
- High Energy Physics Division;
- Molecular and Radiation Biophysics Division;
- Knowledge Transfer Division.

The long-term and short-term research program of the Institute can be found in two documents, which are the program concerning the activity of the NRC “Kurchatov Institute” and the Research and Development program of the Institute in accordance with the State assignment.

Just like other institutes within the National Research Center “Kurchatov Institute”, the Institute takes an active role in various international projects and collaborates with the largest international research centers within its main research areas.

The Institute possesses a number of operating installations and designs new installations for physical research. The WWR-M research reactor built in 1959 was temporarily shut down since 31 December 2015. For a long time it was used to conduct fundamental and applied research

in the field of nuclear physics, condensed matter physics, radiation materials science, radiation biology, the production of radionuclides for medical and technical use. In 2020 the proton synchrotron CS-1000 constructed in 1970 operated only for the total of 1 497 h in experiment due to the global pandemic of coronavirus disease 2019 (COVID-19). The creation of the ophthalmological beam line with the design beam energy from 40 up to 80 MeV at the isochronous cyclotron C-80 continued. The beam line will be used for the future oncological ophthalmological center for proton radiation therapy; simulation and optimization of the beam line of variable energy proton beams at C-80 for testing the electronic component base was carried out.

Within the framework of the Kurchatov Genomics Center, measures were taken to create a material and technical base for producers screening, obtaining, analyzing and modifying target proteins, creating a research infrastructure for sample preparation and analysis of biological samples containing nucleic acids.

In 2020 works on the implementation of investment projects on modernization and renovation of engineering facilities of PIK Neutron Facility continued. This year was an important stage on the course to the creation of the instrument suite of PIK Neutron Facility. In 2020 in line with the Decree of the President of Russia No. 356 of 25.06.2019 five experimental stations in the hall of horizontal experimental channels of PIK Neutron Facility were put into operation: polarized neutron reflectometer (NERO-2), test neutron reflectometer (TNR), test neutron spectrometer (TSpectrum), texture diffractometer (TEX-3), polarized neutron diffractometer (PND). Five commissioned experimental stations ensure the implementation of a basic set of neutron techniques: diffractometry, reflectometry and spectrometry. On the grounds of this experimental suite, a unique scientific facility “International Center for Neutron Research on the basis of a high-flux reactor PIK” was registered.

Upon the favorable expert conclusion of Scientific and Technical Center for Nuclear and Radiation



Safety concerning safety in the event of introducing amendments to the terms of the facility operating license of 06.07.2017 No. GN-03-108-3378, the amendment No. 2 of 10.12.2020 to the license was made enabling the operation of the PIK Neutron Facility at the power up to 10 MW.

Although 2020 passed in the mode of restrictions on mass events, the year was still full of events in scientific and social life, both in-person and virtual ones. On the 6–7 of February the celebration of the Day of Russian Science was held in the Institute. The program prepared by the Council of Young Scientists and Specialists and the Research and Educational Center featured tours to the Institute and lessons for school children, ceremonial meeting of the Academic Council, where scholarships named after outstanding scientists who had worked in the Institute not long ago were awarded to young scientists: “V.N. Gribov scholarship” for studies in the field of theoretical physics; “S.E. Bresler scholarship” for studies in the field of biology. The Institute’s now traditional winter ball completed the program.

Late February – early March saw the traditional Winter Science Schools: 54th PNPI Winter School, 54th Winter School on Condensed Matter Physics and XXI Winter Youth School on Biophysics and Molecular Biology. The Winter Schools included lectures by famous scientists, seminars and talks by participants of the School in all key directions: nuclear physics and particle physics, reactor physics and technology, theoretical physics, condensed matter physics, biophysics and molecular biology. More than 500 scientists and researchers

representing the Institute and other major institutions of Russia and abroad contributed to the work of Winter Science Schools. In 2020 the Institute hosted 11 socially significant events (meetings, conferences, and schools). The most remarkable of them are: International Conference “Drosophila in Genetics and Medicine”, V Workshop on Inelastic Neutron Scattering “Spectrina-2020”, VII All-Russian Youth Science Forum “Open Science 2020”, IX School on Polarized Neutron Physics, and the anniversary conference “Young Talents 2020” under the program “School Environmental Initiative”.

This publication is a collection of brief descriptions of the most significant research results of NRC “Kurchatov Institute” – PNPI in 2020. This description is preceded by reviews of the heads of Institute’s scientific Divisions. The structure of Divisions is also provided. It is followed by the abstracts of papers, the presentation of which was discussed and recommended by Divisions’ academic councils. In addition to the abstract, each research result contains references to leading Russian and foreign journals, where one can read the full text of the paper.

The results of the work of the Institute’s researchers were published in 674 articles, including 473 publications indexed in the Web of Science database, and more than 380 reports were presented at 114 international and Russian conferences.

The summary contains general information about the Institute.



Director of NRC “Kurchatov Institute” – PNPI  
Sergey E. Gorchakov



**High Energy  
Physics**

**Molecular and  
Radiation Biophysics**

**Neutron  
Research**

**Knowledge  
Transfer**

**Theoretical  
Physics**



## Research Divisions

- 10** Theoretical Physics Division
- 12** Neutron Research Division
- 15** High Energy Physics Division
- 18** Molecular and Radiation Biophysics Division
- 21** Knowledge Transfer Division

## Theoretical Physics Division

Theoretical Physics Division (TPD), headed by Dr. V.Yu. Petrov, consists of 7 departments:

- Theory of Electroweak Interactions (headed by Dr. I.T. Dyatlov);
  - Theory of Strong Interactions (headed by Dr. V.Yu. Petrov);
  - Quantum Field Theory (headed by Dr. V.A. Kudryavtsev);
  - High Energy Physics (headed by Dr. V.Yu. Petrov);
  - Condensed Matter Theory (headed by Dr. D.N. Aristov);
  - Nuclei Theory (headed by Dr. M.G. Ryskin);
  - Theory of Atoms and Molecules (headed by Dr. A.I. Mikhailov)
- and the Group of Physics of Nuclear Reactors (headed by Dr. M.S. Onegin).

TPD employs 62 research staff members (26 Doctors of Sciences and 35 Candidates of Sciences).



**Dr. V.Yu. Petrov,**  
head of TPD

Research of TPD covers the great majority of areas of modern theoretical physics – from elementary particle physics and quantum field theory to physics of nuclear reactors.

High energy scattering is a traditional topic for TPD. For years, research of TPD has determined the level of world investigations in this area. In 2020 distribution amplitudes for baryon meson transitions were calculated. We suggested also generalizations of distribution amplitudes and off-forward parton distributions for nucleon.

The method to calculate non-leading double logarithmic contributions to structure functions was developed. It was possible to fix the region of validity for Regge asymptotic  $x < 10^{-6}$ .

In the area of quantum field theory we suggested the method to calculate leading infrared corrections in two-dimensional effective field theories. The new method is based only on general properties of the theory – analyticity, unitarity, crossing.

The two-loop correction in the effective string theory for Wilson loop of arbitrary form was calculated.

Theory Division is also one of the world leaders in AdS/CFT duality. Duality means that non-trivial field theory ( $N = 4$  SUSY Yang–Mills theory) in  $d = 4$  is equivalent to some string theory in anti-de-Sitter space and both theories are exactly solvable. Duality relates anomalous dimensions in SUSY theory and spectrum of the string. In 2020 we suggested and solved exactly the new theory in  $d = 3$  with AdS/CFT duality (so-called fish net). It is important that this is the first solvable theory which does not have SUSY symmetry. In spite of the fact that it does not obey unitarity, the solved theory is very close to SYK theories that are now very popular in condensed matter physics.

Confinement of quarks still remains the most interesting phenomenon in quantum chromodynamics. According to the present belief, confinement is related to the linear potential (string) which appears between quark and antiquark introduced to the vacuum of Yang–Mills theory. The essential progress was achieved in the SUSY theories and the “instead-of-confinement” mechanism manifesting in these theories was investigated in details. The quarks behavior of quarks was also considered and it was shown that in the theory the color-flavor locking appears, which can be observed in nature at large density of matter.

We continue with investigation of the nuclear matter on the basis of quantum chromodynamics (QCD) sum rules. In 2020 three particle forces were taken into account. It was shown that energy minimum with three-forces is close to the experimental value.

A new approach to calculate corrections to the double logarithmic approximation to QCD structure functions at small  $x$  was proposed. For non-leading contributions to the structure function  $F_1(x, Q^2/\mu^2)$  a new expression was obtained. This expression appeared to be quite similar to the contribution of Regge pole (in particular, BFKL pomeron). One has to account for this contribution on the same footing as Regge pole contributions. It is possible to fix region of validity for Regge theory at  $x < 10^{-6}$ .

In 2019 LHCb Collaboration discovered two pentaquark states on Large Hadron Collider (LHC). In the series of papers of M. Eides, V. Petrov, and M. Polyakov the interpretation of these resonances as bound state of excited charmonium and proton was suggested. The alternative suggestion is a weakly bound state of two hadrons with the open charm. We analyzed both scenarios and calculated properties of pentaquarks. Also new pentaquarks were predicted. In 2019 LHCb Collaboration reported about new, more accurate where measured properties of pentaquarks were essentially reconsidered. In the TPD paper of 2020 published in this volume it was demonstrated that it is simpler to describe new pentaquark properties in the model proposed by authors in the previous papers.

Another series of papers of 2019–2020 in TPD is closer to classical nuclear theory. In these papers, with account of inter-nucleon correlations and nucleon pairing the calculations of the properties for odd-odd isotopes of indium from  $^{130}\text{In}$  to  $^{138}\text{In}$  (far from stability line) were performed.

In atomic physics in 2020 we calculated the ionization of internal electrons at  $\alpha$ -decays of the nuclei for different isotopes. Probabilities of ionizations  $P_i(Q_\alpha)$  were calculated for  $K$ -,  $L$ - and  $M$ -electrons. Results obtained are important for spectra of super-heavy elements.

TPD papers of 2020 in condensed matter theory are represented in this volume by investigations of O. Utiosov and A. Syromyatnikov. They considered specific models of frustrated antiferromagnetic (in particular with dipole forces) in the magnetic field. Two scenarios of phase transitions in such a system are well-known. However, it was demonstrated in this paper, that three more scenarios are possible. Moreover, one of them was already observed in the experiment. It would be very interesting to find other examples of proposed new scenarios of phase transitions.

For a number of years in TPD the theory of one-dimensional quantum wires has been developed. In 2020 it was shown that this theory is closely related to the theory of boundary states in topological isolators. The properties of this boundary states were determined but they definitely require further investigation. Also some new results for exact solutions in quantum wires were published.

In 2020 we continued the investigation of strongly correlated fermi-systems, in particular, systems with heavy fermions in graphene. It was shown that in the magnetic field the resistance of such a system should sharply reduce in accordance with experimental data.

Nuclear reactors theory in TPD in 2020 was mainly related to the PIK reactor. The burnup of PIK was studied and its influence on the reactor reactivity. The work on SERPENT code for operative calculations of PIK reactivity was continued. The production of a few typical isotopes on the PIK reactor was calculated. Fuel burning was taken into account.

The following statistics describe research of TPD in 2020:

- 109 research publications from journals in Web of Science, Scopus;
- 37 talks are presented on international conferences and workshops;
- 8 lecture courses in universities of Saint Petersburg, 2 international conferences were organized;
- 2 post-graduate students were hired as a staff members of TPD.

## Neutron Research Division

Neutron Research Division (NRD), headed by Dr. A.I. Kurbakov, consists of 4 departments.

Neutron Physics Department (headed by Corresponding Member of the RAS Prof. A.P. Serebrov) consists of 4 laboratories:

- Neutron Physics Laboratory (headed by Corresponding Member of the RAS Prof. A.P. Serebrov);
- X- and  $\gamma$ -Ray Spectroscopy Laboratory (headed by Prof. V.V. Fedorov);
- Nuclear Spectroscopy Laboratory (headed by Dr. I.A. Mitropolsky);
- Molecular and Atomic Beams Laboratory (headed by Dr. V.F. Ezhov)

and 2 groups:

- Weak Interaction Research Group (headed by Dr. A.N. Pirozhkov);
- Nuclear Fission Physics Group (headed by A.M. Gagarsky).

Condensed Matter Research Department (headed by Dr. I.A. Zobkalo) consists of 4 laboratories:

- Disordered State Physics Laboratory (headed by Dr. V.V. Runov);
- Crystal Physics Laboratory (headed by Dr. Yu.P. Chernenkov);
- Material Research Laboratory (headed by Dr. A.I. Kurbakov);
- Neutron Physical and Chemical Research Laboratory (headed by Dr. V.T. Lebedev)

and Condensed Matter Electrodynamics Group (headed by Dr. O.V. Gerashchenko).

Semiconductor Nuclear Detectors Department (headed by Dr. A.V. Derbin).

Operation of Neutron Stations at the PIK Reactor Department (headed by Dr. V.V. Tarnavich).

NRD employs 121 research staff members (9 Doctors of Sciences and 48 Candidates of Sciences).



**Dr. A.I. Kurbakov,**  
head of NRD

The main directions of NRD scientific activity are fundamental studies in the field of nuclear physics, elementary particle physics, and condensed matter physics. The neutron is a very convenient research tool because it is involved in all types of interactions currently known. The purpose of the research carried out in NRD is the development and widespread introduction of methods and technical resources primarily using neutron radiation to study the composition, structure and fundamental properties of matter, create and analyze the properties of new materials and new physical phenomena in them, develop domestic unique experimental

facilities and analytical techniques for neutron research.

The establishment of the International Center for Neutron Research based on the PIK reactor is currently at the forefront. Unique physical installations are being developed, designed and created.

NRD is the main executor at NRC “Kurchatov Institute” – PNPI of the thematic area No. 7 “Research in the field of neutron physics” of the Program of activities of the NRC “Kurchatov Institute”. The employees of the division participate as performers in the implementation of some other areas of this Program.

2020 was a successful year as far as the scientific results are concerned. Four works performed by NRD employees, one in the field of scientific research and three students’ works were among the winners of the 2019 Kurchatov Prize Competition, the results of which were announced in 2020. The team that developed the project of an ultracold neutron source based on superfluid helium for the PIK Research Facility received the

2020 Aleksandrov Prize. At the competition for the best scientific works of NRC “Kurchatov Institute” – PNPI, research teams, in which the main performers were scientists from the NRD, received one first, three second and two third places. During 2020, NRD employees carried out work under 5 RSF and 10 RFBR projects, in which scientists from NRD were the leaders.

In the field of studies of the fundamental properties of matter using neutrons, new important results were obtained over the past year.

Experiments on the search for the electric dipole moment (EDM) and measurement of the neutron lifetime in magnetic and gravitational traps of ultracold neutrons, as well as studies of the fundamental properties and interactions of the neutron by crystal diffraction methods, continue. The neutron lifetime is a key physical quantity, both for determining the parameters of the weak interaction and for describing the process of primary nucleosynthesis in astrophysics. From the data obtained in the experiment on measuring the EDM of a neutron by the rotation of the neutron spin while passing near the Bragg reflection through a perfect crystal without a center of symmetry, a better restriction on the coupling constant of the new interaction is obtained within the framework of the extension of the Standard Model  $g_A^2 \leq 4.5 \cdot 10^{-24} (g^2 + 1/\lambda_A^2)$  (V.V. Fedorov Laboratory).

The angular distributions of fragments were measured during fission of  $^{240}\text{Pu}(n, f)$  in a wide range of neutron energies 1–200 MeV for the first time. A software package has been developed to describe the obtained data. With the help of it, it was possible to describe the energy dependence of the angular anisotropy of fission fragments in a model with a small number of parameters. Thus, the promising nature of the method for obtaining new information on the fission process has been shown. It has been established that during the fission of nuclei, in addition to neutrons emitted from fission fragments, there is also an insignificant fraction of “bursting” neutrons, whose emission mechanism is still unknown. At the same time, the angular distribution of “prompt” neutrons is not isotropic in the center-of-mass system of each of the fission fragments (A.M. Gargarsky Group).

It was shown for the first time that spectroscopic experiments with chiral molecules are sensitive to a pseudovector field. Such a field plays the role of dark matter in some modern cosmological models. With the right choice of a molecule, one can increase the sensitivity to such a field by two to three orders of magnitude and explore a previously inaccessible region of the space of parameters of boson models of dark matter (M.G. Kozlov Group).

The electron and vibrational spectra for a molecule containing a short-lived radioactive atom have been studied for the first time. Based on the studies carried out, the possibility of effective laser cooling of the RaF molecule was confirmed. The results obtained are a decisive step towards the use of short-lived radioactive molecules in fundamental physics experiments to search for new physics beyond the Standard Model (V.F. Ezhov Laboratory).

In the field of condensed matter physics, there is now an increased interest of researchers in the prediction, detection and study of new unusual magnetic phenomena and in the search for new exotic magnetic structures. Much attention is paid to objects such as low-dimensional systems in which quantum nature manifests itself at the level of macroscopic collective phenomena. Unusual states demonstrate systems in which frustrations of various nature and anisotropy of magnetic interactions exist.

Experimental studies by neutron powder diffraction of the  $\text{Li}_2\text{MnTeO}_6$  compound made it possible to describe a new physical phenomenon: a hidden magnetic order in triangular-lattice frustrated magnetism. The magnetic susceptibility  $\chi(T)$  demonstrates very unusual behavior. It is described by the Curie–Weiss law at high temperature with Curie–Weiss temperature of  $\Theta = -74$  K and exhibits no obvious anomaly indicative of a long-range magnetic ordering at low magnetic fields. At high magnetic fields, however, the character of  $\chi(T)$  changes showing a maximum at about 9 K. The magnetic structure of  $\text{Li}_2\text{MnTeO}_6$ , determined by neutron powder diffraction measurements at 1.6 K, is described by the  $120^\circ$  noncollinear spin structure with the propagation vector  $\mathbf{k} = (1/3, 1/3, 0)$ . The spin-exchange interactions evaluated by density functional calculations are dominated by the nearest-neighbor antiferromagnetic exchange within each triangular

spin lattice. It was determined that this spin lattice is strongly spin frustrated with  $f = |\Theta|/T_N \approx 8$  and exhibits a two-dimensional magnetic character in a broad temperature range above  $T_N$  (A.I. Kurbakov Laboratory).

A number of new results have been obtained in the study of multiferroics. For the first time, neutron diffraction, measurements of magnetization and dielectric permittivity revealed electric polarization induced by a helicoidal magnetic order in the compound  $^{160}\text{Gd}_2\text{BaCuO}_5$ . Magnetoelectric interactions in both commensurate and incommensurate phases are due to two-spin and single-spin contributions of magnetic ions located in off-center positions. It is shown that new multiferroics with complex  $4f$ - $3d$  couplings can be a platform for the search and synthesis of new magnetoelectric materials with practical application. A series of phase transitions and interesting magneto-electric properties were found in the multiferroic ferroborate  $\text{HoFe}_3(\text{BO}_3)_4$ . It is shown that the peculiarities of the magnetic properties of ferrobates are determined by the energy levels of the ground multiplet in the crystal field (I.V. Golosovsky Group).

At the Condensed Matter Research Department of NRD, several groups are investigating the fractal organization of nanomaterials, polymers and biological objects by small-angle neutron scattering and synchrotron radiation, in particular, the study of the structural organization of chromatin in the nucleus of a biological cell and switch of fractal properties of DNA in chicken erythrocytes nuclei by mechanical stress (G.P. Kopitsa and S.V. Grigoriev Group).

With the active participation of many NRD employees, five research experimental stations were installed on neutron beams and put into operation

in the hall of horizontal experimental channels of the PIK reactor. These are polarized neutron reflectometer NERO-2, test neutron reflectometer TNR, test neutron spectrometer T-Spectrum, neutron texture diffractometer TEX-3 and polarized neutron diffractometer DPN. The commissioned five experimental stations ensure the implementation of a basic set of neutron techniques: diffraction, reflectometry and spectrometry.

An important scientific area at NRD is neutrino physics. The data accumulated at the SM-3 reactor allow us to speak about the observation of the oscillatory effect of reactor antineutrinos in a sterile state with a reliability of the order of three standard deviations (A.P. Serebrov Laboratory). According to the Physics World editors, the top ten world scientific studies of 2020 includes the discovery of the Borexino Collaboration with the participation of scientists from the NRC “Kurchatov Institute” – PNPI and the “Kurchatov Institute” for the detection of neutrinos emitted in the reactions of the so-called CNO (carbon–nitrogen–oxygen) cycle on the Sun. For the first time it was experimentally proven that the Sun “draws” a part of the energy in thermonuclear processes of the CNO cycle (A.V. Derbin Laboratory).

The following statistics demonstrates the results obtained by NPD employees during 2020:

- 76 research papers published in reviewed journals (including 55 papers published in foreign editions); 88 research reports presented at international and Russian events (49 oral presentations, mostly on-line);
- 1 certificate of state registration of specialized programs obtained;
- 1 Doctor of Sciences dissertation and 3 Candidate of Sciences dissertations defended.

## High Energy Physics Division

High Energy Physics Division (HEPD), science headed by Corresponding Member of the RAS Prof. A.A. Vorobyov, headed by Prof. O.L. Fedin, consists of 10 laboratories:

- Elementary Particle Physics Laboratory (headed by Prof. G.D. Alkhazov);
- Relativistic Nuclear Physics Laboratory (headed by Prof. V.M. Samsonov);
- Short-Lived Nuclei Laboratory (headed by Dr. V.N. Panteleev);
- Meson Physics Laboratory (headed by Dr. S.I. Vorobyov);
- Few Body System Laboratory (headed by Prof. S.L. Belostotski);
- Crystal Optics of Charged Particles Laboratory (headed by Dr. Yu.M. Ivanov);
- Hadron Physics Laboratory (headed by Dr. O.L. Fedin);
- Physics of Exotic Nuclei Laboratory (headed by Prof. Yu.N. Novikov);
- Baryonic Physics Laboratory (headed by Dr. A.A. Dzyuba);
- Cryogenic and Superconductive Techniques Laboratory (headed by Dr. A.A. Vasilyev)

and 4 technical departments:

- Radio Electronics Department (headed by Dr. V.L. Golovtsov);
- Tracking Detector Department (headed by Prof. A.G. Krivshich);
- Computing Systems Department (headed by A.E. Shevel);
- Muon Chambers Department (headed by V.S. Kozlov).

HEPD employs 114 research staff members (15 Doctors of Sciences and 65 Candidates of Sciences).



**Prof. A.A. Vorobyov,**  
Corresponding Member  
of the RAS,  
science head of HEPD



**Prof. O.L. Fedin,**  
head of HEPD

HEPD activity is mainly aimed at the experimental research in the field of elementary particle physics and nuclear physics. In addition, the development of innovative methods for obtaining radioisotopes for medical applications and studies of magnetic properties of materials with the use of the  $\mu$ SR-method are being performed. As in previous years, research works were conducted at facilities of NRC “Kurchatov Institute” – PNPI and at accelerators of the world’s leading nuclear centers.

In 2020, the following experiments were carried out.

1. Experiments at the NRC “Kurchatov Institute” – PNPI synchrocyclotron:
  - Production and studies of short-lived nuclei with the isotope mass separator on-line facility IRIS;
  - Studies of polarization effects in proton quasi-elastic scattering off nuclei;
  - Studies of magnetic properties of materials with  $\mu$ SR-method.
2. Experiments in the European Center for Nuclear Research (CERN):
  - Participation in CMS, ATLAS, LHCb and ALICE experiments at the Large Hadron Collider (LHC);



- Production and studies of short-lived nuclei with the isotope mass separator on-line facility ISOLDE;

- Studies of possibilities to use crystal collimation of the LHC beams (experiment UA9).

3. Experiment at the electron accelerator at Bonn University (Germany):

- Study of nucleon structure by  $\gamma$ - $p$ -scattering.

High precision studies of muon capture on deuteron (experiment MuSun) at the Paul Scherrer Institute meson factory (Switzerland) were completed, the data analysis being continued.

New projects:

- Preparations of experiment "Proton" for measurements of the proton charge radius in elastic electron-proton scattering at the electron accelerator MAMI (Mainz, Germany);

- Preparations of experiment AMBER/NA66 for measurements of the proton charge radius in elastic muon-proton scattering on the SPS beam at CERN;

- Preparations for experiments R3B, MATS, PANDA and CBM at the accelerator complex FAIR (Helmholtz Center for Heavy Ion Research, Germany);

- Preparation for the SHiP experiment at CERN for search of new particles from hidden sector;

- Preparation of the experiment for search of muon-catalyzed  $d^3\text{He}$  fusion at the Paul Scherrer Institute meson factory (Switzerland);

- Preparation of the MPD experiment for study quark-gluon plasma (QGP) at the NICA collider which is under construction now in Dubna;

- Project IRINA for production and studies of short-lived nuclei at the high flux neutron reactor;

- Project PITRAP for precision mass measurements of short-lived nuclei at the high flux neutron reactor;

- Project RIC-80 for production of radioisotopes for medical applications.

One of the main activities of the HEPD was the participation in fundamental research at unique accelerator facilities in world scientific centers, such as the LHC at the CERN and at the new generation accelerator research complex at the European Facility for Antiproton and Ion Research (FAIR).

At the CERN HEPD participated in the LHC experiments CMS, ATLAS, LHCb, and ALICE from the

initial stages of design and construction of these detectors with a significant intellectual and instrumental contribution to the various subsystems of these detectors. After the LHC start-up, HEPD physicists and engineers, along with other participants in the experiments, shared responsibilities in maintenance and operation of these detectors and took part in the analysis of the experimental data. The analysis of the experimental data collected in Run 2 (2015–2018) continues to yield a great amount of new results. The most significant of them are the setting new stricter upper limits on the production cross section of new heavy Higgs bosons in the ATLAS experiment, the search for new asymptotic effects of Lipatov–Fadin–Kuraev–Balitsky (BFKL) evolution in di-jet processes with a large separation in rapidity, in the first measurements of diffraction processes of proton scattering by nuclei in the CMS experiment, the discovery of the double-Cabibbo suppressed decay  $\Xi_c^+ \rightarrow p\phi$  and the discovery of a particle with double charm  $\Xi_c^{++}$  in the LHCb experiment, as well as the study in the ALICE experiment of the energy dependence of the cross section for the exclusive hard photo-production of heavy quarkonium in a wide energy range, which made it possible to extract from the data the density of soft gluons in nucleons and nuclei, which is responsible for the formation of QGP in central ion-ion collisions.

In 2020, the activities of the HEPD groups participating in the LHC experiments were focused on the detectors upgrade to be prepared for operation during Run 3 with the increased LHC luminosity. As an example, in the framework of the ATLAS upgrade program, the work on the creation of 36 quadruplets of the thin-gap chambers for the ATLAS muon spectrometer was successfully completed.

The study of the properties of QGP is the one of the fundamental research direction in the HEPD which started in the 80s in the PHENIX experiment (Brookhaven National Laboratory, USA) and continued in the ALICE experiment (CERN). After the launch of the FAIR accelerator complex, the study of QGP will be carried out in the CBM experiment and in the multipurpose MPD experiment at the NICA collider which is under construction now in Dubna.

HEPD is also involved in the design development of the concept and physics research program for the second SPD detector at the NICA collider, to study collisions of polarized particle and the spin structure of the nucleon.

The following statistics demonstrate scientific activity of the HEPD in 2020:

- 217 research papers published in reviewed journals (including 212 papers published in foreign editions);
- 22 research reports presented at international and Russian events.

## Molecular and Radiation Biophysics Division

**Molecular and Radiation Biophysics Division (MRBD), headed by Dr. A.L. Konevega, consists of 13 laboratories:**

- Biophysics of Macromolecules (headed by Dr. V.V. Isaev-Ivanov);
- Genetics of Eukaryotes (headed by Dr. V.G. Korolev);
- Protein Biosynthesis (headed by Dr. A.L. Konevega);
- Biopolymers (headed by Dr. A.L. Timkovsky);
- Human Molecular Genetics (headed by Dr. S.N. Pchelina);
- Enzymology (headed by Dr. A.A. Kulminskaya);
- Experimental and Applied Genetics (headed by Dr. S.V. Sarantseva);
- Medical Biophysics (headed by Prof. Dr. L.A. Noskin);
- Medical and Bioorganic Chemistry (headed by Dr. F.M. Ibatullin);
- Proteomics (headed by Dr. S.N. Naryzhny);
- Cryoastrobiology (headed by Dr. S.A. Bulat);
- Molecular and Cellular Biophysics (headed by Dr. G.N. Rychkov);

**3 centers:**

- Center for Preclinical and Clinical Research (headed by Dr. A.P. Trashkov);
  - Resource Center (headed by Dr. N.A. Verlov);
  - Kurchatov Genome Center (headed by Dr. A.Yu. Konev)
- and Engineering Support Department (headed by P.A. Sotnikov).

MRBD employs 139 research staff members (15 Doctors of Sciences and 55 Candidates of Sciences).



**Dr. A.L. Konevega,**  
head of MRBD

The studies of MRBD are dedicated to the most significant branches of molecular biology, biophysics, molecular and medical genetics.

The department is actively researching a new area at the intersection of molecular biology and bioinformatics – proteomics. The human proteome consists of a diverse and heterogeneous range of gene products/proteoforms/types of proteins. The rapidly growing volume of information about proteoforms generated by various methods requires the creation of an approach for data inventory. The work of S.N. Naryzhny (Proteomics Laboratory) presents a database of proteoforms based on information obtained

by separating proteoforms using two-dimensional electrophoresis (2DE) followed by ESI LC-MS/MS analysis. The principles and structure of the database are described.

For several years, MRBD has been conducting interlaboratory work on the study of extracellular vesicles (EVs), which play an important role in many biological processes. For example, EVs are involved in important processes in the development of glioblastoma multiforme (GBM), including malignant transformation and invasion. EVs secreted by glioblastoma cells can cross the blood-brain barrier and carry the molecular load obtained from the tumor into the peripheral circulation. The determination of the molecular profile of EVs (exosomes) released by glioblastoma cells seems to be a promising approach for the development of non-invasive methods for the detection of specific markers of exosomal proteins in peripheral blood.

The aim of the study conducted by T.A. Shtam (Laboratory of Protein Biosynthesis) and S.N. Naryzhny (Proteomics Laboratory) was to determine

common exosomal proteins present in preparations from different cell lines and to search for potential glioblastoma biomarkers in exosomes. A correlation was found between the increased level of glial cell proteins and their presence in exosomes. Thus, the presence of many potential glioblastoma biomarkers in exosomes was confirmed.

In addition, EVs play an important role in the pathogenesis of Parkinson's disease (PD). Currently, it is believed that the formation of  $\alpha$ -synuclein fibrils is a key link in the pathogenesis of this disease, and the aggregates of this protein are transmissible and are able to spread from cell to cell via EVs. It has been shown that the size and morphology of EVs can affect the diffusion properties of vesicles and, possibly, the spread of  $\alpha$ -synuclein pathology in PD.

In a study carried out by A.K. Emelyanov (Laboratory of Human Molecular Genetics), EVs isolated from the cerebrospinal fluid (CSF) of patients with PD were used as the object of study. This work is the first to describe the morphological diversity of human CSF EVs, including a group of patients with PD, and it is assumed that there are EVs subpopulations in human biological fluids that potentially have different specific functions.

Another important observation was made in the work of S.N. Pchelina (Laboratory of Human Molecular Genetics), where the phenomenon of increased size and changes in the morphology of EVs obtained from the blood plasma of patients with Gaucher disease (GD) was first discovered. In this disease, the accumulation of neurotoxic forms of  $\alpha$ -synuclein in blood plasma, caused by mutations in the gene of the lysosomal enzyme glucocerebrosidase (*GBA*), and an inverse correlation of their level with the activity of this enzyme were shown. Mutations in the *GBA* gene increase the risk of PD by 6–7 times, and since the function of lysosomes is critical for the secretion of exosomes by cells, it was suggested that the dysfunction of lysosomes, which occurs due to a decrease in *GBA* activity, may affect the EVs pool of blood plasma.

In the work of T.A. Shtam in the study of EVs isolated from plasma and whole blood of patients with breast cancer (BC) and healthy women, the morphology of EVs was described in detail. It was shown that some of the exosomes circulating

in the blood are associated with the surface of the formed elements; their role in the dissemination of the tumor process remained unclear. An *in vitro* study demonstrated the effect of a pool of human whole blood exosomes on the main stages of breast cancer development: angiogenesis, the ability of cells to migrate, invade, and form intercellular contacts. Some molecular participants in these processes have been identified. In addition to fundamental research on EVs, new, original methods for their isolation from various biological sources are being developed.

In another study by T.A. Shtam, a comparative analysis of four methods for isolating EVs from human blood plasma was carried out: 1) sequential ultracentrifugation, 2) ultracentrifugation using a sucrose "pillow", 3) agglutination of vesicles with plant lectins, 4) immunoprecipitation on latex particles. In addition, a new method for the isolation of EVs from blood plasma using the SubX™ reagent has been developed and tested. The method is based on the creation of large conglomerates of vesicles due to the interaction of phosphate groups of membrane phospholipids, which occurs in the presence of SubX™. These large aggregates can be sedimented by centrifugation at relatively low speeds, which greatly simplifies the procedure for the extraction of EVs. The addition of an excess of salt to the resulting precipitate leads to the release of individual vesicles from the aggregates.

Research into microbiology and biotechnology is traditional for MRBD. In the work of A.A. Kulminskaya and coworkers (Laboratory of Enzymology), together with the NRD, the questions of induction of nucleation, growth and aggregation of biogenic crystals of  $\text{CaCO}_3$  were investigated. Microorganism-induced precipitation and crystallization of  $\text{CaCO}_3$  are considered an alternative "green" technology for self-healing cementitious materials and represent the basis for the development of new biomaterials. The aim was to search for ureolytic calcifying microorganisms and analyze their ability to biomineralize calcium carbonate during their growth in media with and without urea. Several microorganisms were found with a high level of specific activity of urease, while a sharp increase in the pH of the medium containing urea led to the effective

biomineralization of  $\text{CaCO}_3$ . These microorganisms completely restore microcracks in cement samples. It has been suggested that ureolytic microorganisms retain their ability to induce  $\text{CaCO}_3$  biomineralization regardless of the origin of carbonation in the cellular environment, switching between the mechanisms of urea degradation and dissimilation of organic calcium salts.

Another example of the development of new biomaterials is the example of biodegradable bacterial cellulose (BC). BC synthesized by the *Gluconacetobacter hansenii* strain was first treated with cellobiohydrolase from the yeast *Scytalidium candidum* 3C. Enzymatic hydrolysis significantly affected the crystal and supramolecular structures of native BC. Experiments *in vitro* and *in vivo* did not reveal a cytotoxic effect from the addition of the enzyme to BC dressings and showed a generally positive effect on the treatment of extensive III degree burns, significantly accelerating wound healing in rats. The results obtained can serve as a basis for the further development of effective biodegradable dressings for wound healing based on hydrolyzed BC.

The work on the repair of genetic damage is traditional for MRBD. In eukaryotes the tolerance to DNA damage is determined by two repair pathways: homologous recombination repair and the pathway controlled by the RAD6-epistatic group of genes. Monoubiquitination of PCNA mediates an error-prone pathway, while polyubiquitination stimulates an error-free pathway. The error-free pathway includes components of recombination repair, however, the factors that act in this pathway remain largely unknown. In the work of E.A. Alekseeva (Laboratory of Genetics of Eukaryotes) a new participant in the error-free pathway of tolerance to DNA damage, a product of the *HIM* gene, was identified, and the mechanism of the error-free pathway of bypassing DNA damage in the *him1* mutant acts through the recruitment of highly

erroneous Pol $\eta$  polymerase to carry out reparative DNA synthesis during post-replicative genome repair.

The work of the Protein Biosynthesis Laboratory deserves special attention. In the work of D.S. Vinogradova, a system of sensitive, fast and accurate analysis of the interactions of biomolecules in the process of translation initiation was developed, as a result of which a new direction in the mechanism of a strict response was determined. The inhibitory effect of the ppGpp molecule on the process of translation initiation was shown, and the key role of the messenger RNA molecule in this process was revealed. In addition, it was shown for the first time that at an increased concentration of the ppGpp molecule under unfavorable conditions, the cell can use pppGpp to initiate the process of protein biosynthesis.

In the work of E.V. Poleskova, using cryo-EM, the structure of the ribosome-antibiotic complex was obtained with a resolution of 2.1 Å, which is currently the best among the published cryo-EM structures of ribosomal complexes. It was shown that the more pronounced inhibition of protein biosynthesis by dirithromycin, compared with its precursor erythromycin, is a consequence of the location of the hydrophobic radical dirithromycin: it is directed into the lumen of the exit tunnel, partially closes it, which leads to disruption of the normal passage of the growing peptide through the tunnel, and inhibits the synthesis of polypeptide chains.

In 2020, MRBD employees published more than 110 papers in peer-reviewed journals (48 in foreign ones), made more than 57 reports at international scientific conferences.

A new generation of scientists is being actively prepared; more than 30 postgraduate students are carrying out research projects in the laboratories of the Division (including 23 under the postgraduate program of the NRC "Kurchatov Institute" – PNPI).

## Knowledge Transfer Division

Knowledge Transfer Division (KTD), headed by Dr. A.V. Titov, consists of 3 laboratories:

- Holographic Information and Measuring Systems (headed by Dr. B.G. Turukhano);
- Quantum Chemistry (headed by Dr. A.V. Titov);
- Chemistry and Spectroscopy of Carbon Materials (headed by Dr. A.A. Borisenkova)

and 3 departments:

- Acceleration Division (headed by Dr. E.M. Ivanov), which includes also Laboratory of Acceleration Physics and Techniques (headed by Dr. S.A. Artamonov);
- Applied Nuclear Physics (headed by Dr. V.A. Solovei), which includes 2 laboratories:
  - Laboratory of Radiation Physics (headed by Dr. A.V. Vorobyev);
  - Laboratory of Electronic and Software Supply (headed by V.A. Solovei);
- Informational Technologies and Automatization (headed by S.B. Oleshko), which also includes Laboratory of Informational and Computational Systems (headed by S.B. Oleshko);

KTD employs 67 research staff members (9 Doctors of Sciences and 25 Candidates of Sciences).



Dr. A.V. Titov,  
head of KTD

The basic accelerator facilities of the Institute are concentrated in the KTD. First of all, it is a unique synchrocyclotron with an energy of 1000 MeV,

SC-1000, with a current of 1  $\mu\text{A}$  of the output beam. It allows one to conduct a wide range of scientific and applied studies in various fields – from nuclear physics to medicine.

Its main distinguishing features are:

- Highly efficient output system (30%), which is five times higher than the efficiency of a standard regenerative system;
- The system of time stretching of the derived proton beam, which allows you to increase the time filling coefficient of the beam from 2 to 85%.

For a number of physical and applied studies, proton beams of other energies are required. For this purpose, proton beams of variable energy from 60 to 1000 MeV were created at the SC-1000 of NRC “Kurchatov Institute” – PNPI by the Accelerator Department (AD) staff. The diame-

ter of the obtained beams is  $\sim 30\text{--}80$  mm,  $\Delta\rho/\rho$  is in the range of 1.3–14%, and the intensity varies in the range of  $10^7\text{--}10^{12}$   $\text{s}^{-1}$ .

In addition to the main proton beam, there is the second one of “low” intensity, about 1% of the main beam, which is output from the synchrocyclotron chamber simultaneously with the main beam. The beam can be used for both physical and applied purposes, in particular, for the proton radiation therapy, which can significantly reduce the cost of irradiation of patients.

For scientific research, there are secondary beams of  $\pi^\pm$  and  $\mu^\pm$  mesons obtained on the external meson-forming target. In the accelerator chamber, neutrons with energies from 0.01 eV to 950 MeV are generated as a result of a single-turn discharge of a proton beam onto an internal neutron-forming lead target.

The improvement of space and aviation technology is largely associated with the use of micro- and nanoelectronics elements. One of the main conditions for their successful use is the ability to function reliably for a long time in the radiation fields of outer space and the upper atmosphere. Currently, the regulations of Russia and the standards of the leading countries of the world include mandatory tests of the radiation resistance of modern radio-electronic equipment used in aviation and space technology, relative to the effects

of various types of radiation. In 2015, a specialized center for proton radiation testing with an energy of 60–1 000 MeV, including two stands with beam diagnostics systems, modern dosimetry devices, an automated results processing system and a modern infrastructure for users, began operating at the synchrocyclotron of the NRC “Kurchatov Institute” – PNPI.

The standards of the leading countries of the world provide for mandatory tests of the radiation resistance of radio-electronic equipment used in aviation and space technology, relative to the effects of neutron fluxes. The international regulatory document JEDEC STANDARD prescribes testing of electronic components and radio products in neutron fluxes with a spectrum that is similar to the atmospheric spectrum of neutrons. In 2015, the Nuclear Fission Physics Group of NRD and the AD of KTD completed the creation of the ISNP/GNEIS neutron test bench at the GNEIS neutron source of the SC-1000 synchrocyclotron.

The high intensity of the neutron beam allows for accelerated testing of electronics – one hour of exposure of the product on the beam is equivalent to 125 thousand hours of stay at flight altitudes of 10–12 km. Thus, since 2015 the universally valid center for radiation-resistance testing of electronic components has been in operation at NRC “Kurchatov Institute” – PNPI, which is now capable of fully testing the electronics on beams of variable-energy protons as well as on neutron beams with the range repeating that of atmospheric neutrons.

A multi-purpose cyclotron complex based on the constructed isochronous cyclotron C-80 with a variable proton energy of 40–80 MeV and a beam output current of up to 100  $\mu\text{A}$  is being launched in the KTD by the AD NRC “Kurchatov Institute” – PNPI and the D.V. Efremov Scientific Research Institute of Electrophysical Apparatus. The high energy of the accelerated beam combined with the high intensity will allow the production of high-quality radioisotopes and radiopharmaceuticals that are not available for commercial cyclotrons, in particular generator isotopes. Generator isotopes open the way for positron emission tomography in medical centers far from the cyclotron. The project also provides for the development of a method for creating

ultrapure medical isotopes using a magnetic separator. The energy range of the proton beam (60–70 MeV) of the C-80 cyclotron makes it possible to create the only ophthalmological center in Russia for proton therapy of oncological diseases of the visual organs. The development of this project has long been carried out by the AD together with the A.I. Alikhanov Institute of Theoretical and Experimental Physics (NRC “Kurchatov Institute” – ITEP).

The vast experience gained at NRC “Kurchatov Institute” – ITEP, where about 1 400 patients underwent proton therapy sessions until 2010, will be used to create equipment for the ophthalmology and radiation planning office.

The Holographic Information and Measuring Systems Laboratory (HIMSLab) of KTD is one of the world leaders in the field of precision measurements at the nanometer scale. To conduct these studies, HIMSLab has a modern unique underground vibration-free holographic laboratory. The laboratory and unique stands for the synthesis of linear and radial holographic diffraction gratings produced 15 types of nano technological devices and systems, including: photoelectric encoders of linear and angular displacements, length encoder, two-, three-, four- or more coordinate measuring machines, radiusmeter, planometer, rotary tables for the measurement with 10 nm resolution and hundredths of a second. In 2015, for the first time in the world, HIMSLab created a linear holographic grating with a length of 1 300 mm and a resolution of 1 nm. Works of HIMSLab were marked at the exhibition “Army 2015”.

The main direction of the work of the Quantum Chemistry Laboratory (QCL) of KTD is the development of methods for calculating the electronic structure of molecules containing heavy elements. This activity was stimulated already in the early 1980s due to the necessity to calculate *P*- and *CP*-odd effects in heavy diatomic molecules. The two-step method developed in the laboratory became the basis for the calculations and allowed us to divide the calculation of such molecules into two sequential calculations in the valence region and in the region of the core. Up to date, the accuracy attained in these calculations has become a record in the world. The laboratory staff did not limit

themselves to calculating  $P$ - and  $CP$ -odd effects; they went over to more complex structures. The development of methods, algorithms, and software packages for accurate modeling of the electronic structure and properties of compounds of heavy elements allowed us to start a systematic study of the properties of superheavy elements, go to calculations in solid-state systems and implement a study of the chemical properties of superheavy elements from the “stability island” synthesized in Dubna and Darmstadt. One more direction of the laboratory research is the development of the theory of electronic structure and calculations of the properties of laser-cooled molecules. Such molecules have a very interesting property – the ability to rescatter hundreds and even thousands of photons without a “population leak”, which allows one to apply very well-developed methods for laser cooling of atoms to such molecules. The laboratory also participates in the development of a new direction in molecular spectroscopy – laser spectroscopy of compounds of radioactive elements. This direction is founded on the methods of the ISOL (Isotope Separation On-Line) spectroscopy, which proved themselves to be good in the spectroscopy of unstable atomic isotopes. However, the transfer of these methods to radioactive molecules became possible only after a series of theoretical studies in which QCL staff took an active part.

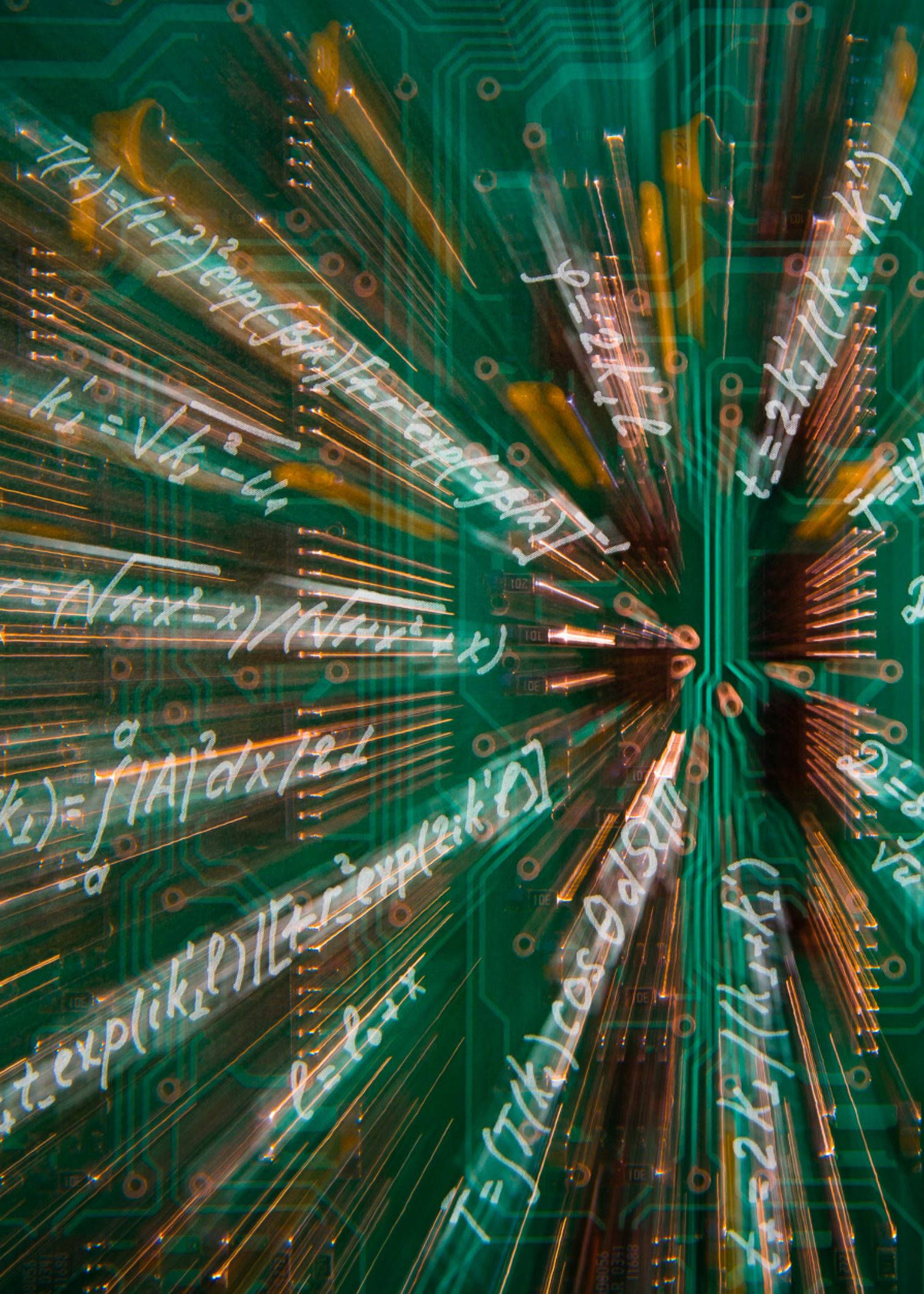
In the Laboratory of Radiation Physics the following investigations are conducted:

- Investigations of the interactions of neutron and high energy particles with a substance and modification of the structure and properties of solids under irradiation;
- Investigation of the proton and neutron induced radiation effects in electronic components and devices, and development of techniques of the measurements and radiation testing procedures;
- Investigation of the interaction of neutrons with atomic nuclei at different energies and measurement of nuclear constants;
- Development and construction of the new nuclear physics experimental installations.

The main research trend of the Laboratory of Chemistry and Spectroscopy of Carbon Materials (LCSCM) of KTD is the development of new fullerene and endometallofullerene derivatives, the study of their physical and chemical properties, radiation resistance and self-assembly in aqueous solutions. One of the most important scientific and practical tasks of the LCSCM is the development of new endometallofullerene derivatives which are promising as systems for targeted drug delivery. Commonly used radiopharmaceuticals contain a radioisotope in combination with a chelating agent that binds the radioactive atom firmly enough and prevents its binding to blood components and other body tissues. However, the stability of such a chelate complex is not absolute and therefore small amounts of toxic radioactive metal can be released into the body. For this purpose, the laboratory studies the radiation resistance of endometallofullerenes and their derivatives under irradiation.

In 2020, the KTD staff published 45 papers indexed by Web of Science and Scopus, made more than 40 reports at Russian and international scientific conferences and scientific seminars, also, 13 patents were obtained.





$$\Psi(x) = (1-r)^2 \exp(-\beta x) / (1+r) \exp(\beta x)$$

$$k_1 = \sqrt{k_2^2 - 4}$$

$$r = (\sqrt{1+x^2} - x) / (\sqrt{1+x^2} + x)$$

$$k_1 = \int_{-a}^a |A|^2 dx / 2L$$

$$t \exp(ik_1 l) / [r r^2 \exp(2ik_1 l)]$$

$$L = 2L + x$$

$$\phi = 2k_1 l$$

$$x = 2k_1 / (k_1 + k_2)$$

$$T = \int T(k) \cos \theta \sin \theta dk$$

$$x = 2k_1 / (k_1 + k_2)$$

# Theoretical and Mathematical Physics

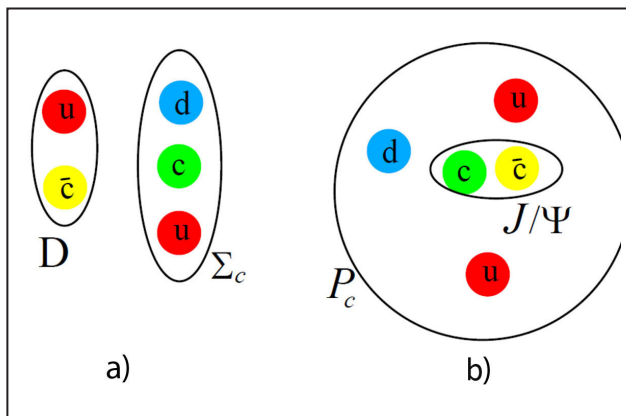
- 26 More about strange exotics of LHCb
- 28 Calculation of the properties of narrow optical transitions in highly charged ions for optical frequency standards
- 29 String baryon of the  $N = 2$  supersymmetric quantum chromodynamics from the  $2D-4D$  correspondence
- 30 Phase competition in frustrated anisotropic antiferromagnets in strong magnetic field
- 31 Fock space relativistic coupled cluster method: a new level of accuracy in predicting the properties of heavy element compounds
- 32 Universal scaling of energy consumption in biological systems with variable mass

## More about strange exotics of LHCb

M.I. Eides, V.Yu. Petrov, M.V. Polyakov  
Theoretical Physics Division of NRC “Kurchatov Institute” – PNPI

Recently LHCb discovered two new exotic strange states: the  $ccsu$  tetraquark and the anti- $c$   $csud$  pentaquark. By common wisdom they were recognized as expected strange partners of already known exotic particles: non-strange tetraquark and pentaquark.

This paper is aimed to make it clear that the discovery of the strange pentaquark witnesses in favor of hadrocharmonium scenario. There are two scenarios proposed to describe heavy LHCb pentaquarks: deuteron-like scenario (Fig. a) and hadrocharmonium scenario (Fig. b).



Two scenarios for pentaquarks (a, b)

In the first scenario exotic particles come as flavor multiplets which can be either octets or decuplets. Strange quark mass is considered as a small perturbation splitting these multiplets. In the first order in the strange mass we obtain Gell-Mann–Okubo formulae. The concrete model allows also determining coefficients in Gell-Mann–Okubo formulae and calculating the mass of strange partners. Predictions of the strange partners masses were made in the first paper devoted to the hadrocharmonium

scenario and were corrected later according to the fresh LHCb data.

However, the new strange LHCb pentaquarks do not correspond to the predictions made in these papers – they are too heavy. Hence, they cannot be the strange partners of known exotic pentaquarks but should enter the multiplets with heavier non-strange pentaquarks. Indeed, the typical effect of the strange quark mass considered as a perturbation is that strange members of multiplet are 150–250 MeV heavier than non-strange ones. Hence, non-strange partners of the newly discovered LHCb strange pentaquarks should have masses around 4 600–4 700 MeV and are not known yet.

One can try to interpret these heavier states in hadrocharmonium scenario. Then they are part of some octet with corresponding non-strange pentaquark. In this scenario it is possible to have strange partners of the discovered mass but it should be with excited states of a number of hadron states in the sectors with parity plus, not minus. Therefore unambiguous prediction of this scenario is parity plus of new pentaquarks and relatively wide particles which appear as a combination of large number of overlapping narrow states.

In the deuteron-like scenario it is very doubtful that hadrons come in flavor octets. Deuteron-like states are a result of fine tuning of attraction and repulsion which is completely broken down by mass of the strange quark. This mass is rather large on the scale of the deuteron well. By the way, this is the reason why there is no strange partner of deuteron itself. If, nevertheless, non-strange partner of discovered strange particle exists it is much heavier than known states and not discovered yet. They can be some excited states of known pentaquarks

with parity minus. Let us pay attention to the fact that different scenarios predict opposite values of parities.

The situation is much worse for discovered tetraquarks. Neither hadrocharmonium nor deuteron scenario can be applied here. It is highly improbable that heavy quarks are on the large distances. Quarks will attract each other to form a small size colored diquark. This diquark can be in a six- or anti-three-color state. This particle is in the center of large size colored "meson". However, the interaction of these two particles is completely unknown

and cannot be calculated by known methods. Correspondingly, the spectrum of these tetraquarks cannot be predicted and they cannot be interpreted as strange partners of any known exotics.

To summarize: common wisdom that new strange exotics are flavor partners of known exotic hadrons is unjustified. It can be true for strange pentaquarks in the hadrocharmonium scenario. However, strange tetraquarks are not partners of any known particles and there are no methods at the moment which are able to describe their properties.

## Calculation of the properties of narrow optical transitions in highly charged ions for optical frequency standards

M.G. Kozlov, I.I. Tupitsyn, A.I. Bondarev, S.G. Porsev

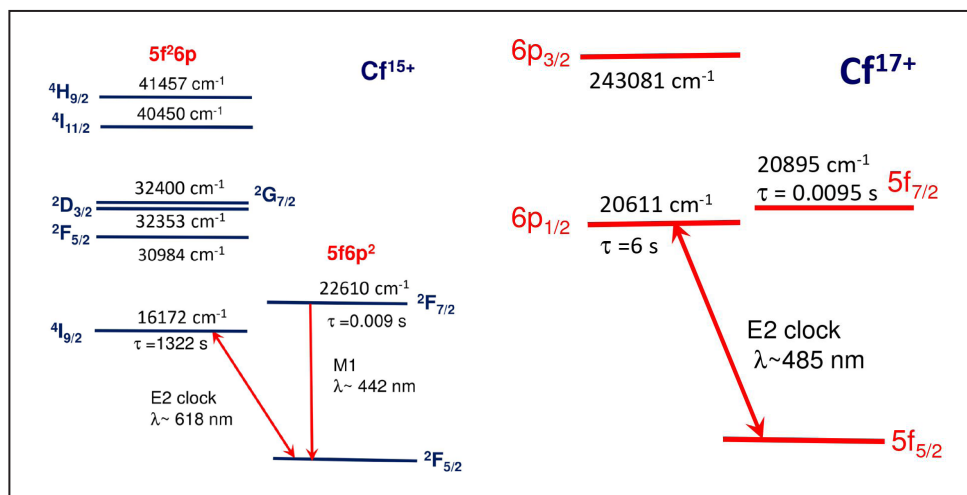
Neutron Research Division, Theoretical Physics Division of NRC “Kurchatov Institute” – PNPI

Using optical clock on atoms and singly charged ions allowed reaching relative accuracy in frequency measurements at the level of  $10^{-18}$ . Such clock can be used not only for the development of new technologies, but also as very sensitive tools for the search of new physics beyond the Standard model. Recently a plethora of narrow optical transitions have been predicted for the highly charged ions (HCI). At the same time cooling and trapping of HCI has been demonstrated experimentally. All this opens ways to use HCI for building new generation of optical clock. A small size and low sensitivity of HCI to the external perturbations potentially allow increasing accuracy and sensitivity to new physics by one, or two orders of magnitude.

Information on the spectra of HCI is sparse and experimental search for narrow optical transitions is very difficult. Therefore, it is essential to predict positions of such transitions with highest possible accuracy. We developed new methods of

calculations for complex many-electron ions and calculated properties of ions  $\text{Ir}^{17+}$ ,  $\text{Cf}^{15+}$  and  $\text{Cf}^{17+}$ . For  $\text{Ir}^{17+}$  we calculated properties of the “clock” transition, as well as a large number of  $M1$  and  $E1$  transitions. For the  $M1$  transitions we obtained a good agreement with the existing experimental data. We also explained why  $E1$  transitions were not detected experimentally and predicted several strong transitions, which can be potentially observed.

We calculated wavelengths of the narrow transitions in  $\text{Cf}^{15+}$  and  $\text{Cf}^{17+}$  ions, which can be used for the optical clock and estimated all main sources of the systematic effects. These estimates showed that both ions are perspective candidates for building optical clock. The ion  $\text{Cf}^{17+}$  looks slightly better because it has simpler level structure and there is “magic” frequency of the trapping field. At this frequency the systematic effects caused by the micromotion of the ion are suppressed.



Calculated spectra of  $\text{Cf}^{15+}$  and  $\text{Cf}^{17+}$  ions. The arrows indicate possible “clock” transitions. Lifetime is shown for metastable levels.

1. Porsev S.G., ..., Bondarev A.I., Kozlov M.G., Tupitsyn I.I. et al. // Phys. Rev. A. 2020. V. 102. P. 012802-1-9.
2. Cheung C., ..., Porsev S.G., Kozlov M.G., Tupitsyn I.I., Bondarev A.I. // Phys. Rev. Lett. 2020. V. 124. P. 163001-1-6.

## String baryon of the $N = 2$ supersymmetric quantum chromodynamics from the $2D-4D$ correspondence

E.A. Ievlev, A.V. Yung

Theoretical Physics Division of NRC “Kurchatov Institute” – PNPI

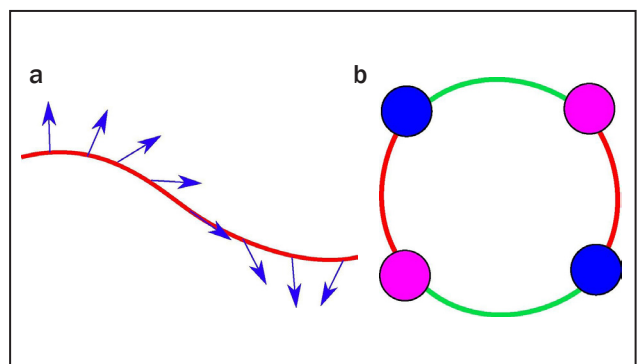
Confinement problem in quantum chromodynamics (QCD) is one of the major unsolved problems in theoretical high energy physics. QCD is a strongly coupled theory, and in the course of many years the analytical methods of investigation had faced serious obstacles. One promising approach that nevertheless can help us to understand the strong coupling physics is to consider supersymmetric analogs of QCD.

Non-Abelian strings (flux tubes) were discovered in the  $N = 2$  supersymmetric QCD in 2003 by A. Yung with K. Konishi and his research group, and also independently by Hanani and Tong. These non-Abelian strings are distinguished by the presence of orientational zero modes that rotate the string flux inside a group  $SU(N)$  (Fig. a). The theory of such non-Abelian strings has been developed for several years by A. Yung and M. Shifman. Non-Abelian strings turn out to be an alternative to Abrikosov–Nielsen–Olesen strings. They are responsible for non-Abelian confinement of monopoles.

In 2015 it was shown that in four dimensional  $N = 2$  supersymmetric QCD with the gauge group  $U(N = 2)$ , four quark flavors and Fayet–Iliopoulos  $D$ -term, the non-Abelian string behaves as a critical superstring. This happens because four translational modes together with the six orientational string modes combine to form a ten dimensional space necessary for the superstring to become critical. This superstring theory was subsequently studied. In particular, the low-lying string spectrum was described. Closed string states appearing in four dimensions are identified with hadrons of the four dimensional  $N = 2$  supersymmetric QCD.

In this string theory approach a massless state has been found that was interpreted as a baryon of the  $N = 2$  QCD (Fig. b). In the present work we confirm its presence using purely field theory methods. To this end we study the two dimensional conformal theory on the non-Abelian string world sheet – so-called weighted  $N = (2,2)$  supersymmetric WCP(2,2) model. Its target space is a six dimensional non-compact Calabi–Yau manifold, the so-called conifold. Using the  $2D-4D$  correspondence we show that the conifold complex structure deformation corresponds to an emerging Higgs branch in the four dimensional  $N = 2$  QCD. The modulus on this Higgs branch turns out to be the vacuum expectation value of the massless BPS baryon found previously in the string theory approach.

These results are an important contribution to a solution of one of the fundamental problems of theoretical high energy physics, namely, calculation of the hadron spectrum from the first principles.



Oriental modes of the non-Abelian string (schematically) (a); string baryon can be represented as a closed string with four monopoles (b)

## Phase competition in frustrated anisotropic antiferromagnets in strong magnetic field

O.I. Utesov, A.V. Syromyatnikov

Theoretical Physics Division of NRC "Kurchatov Institute" – PNPI

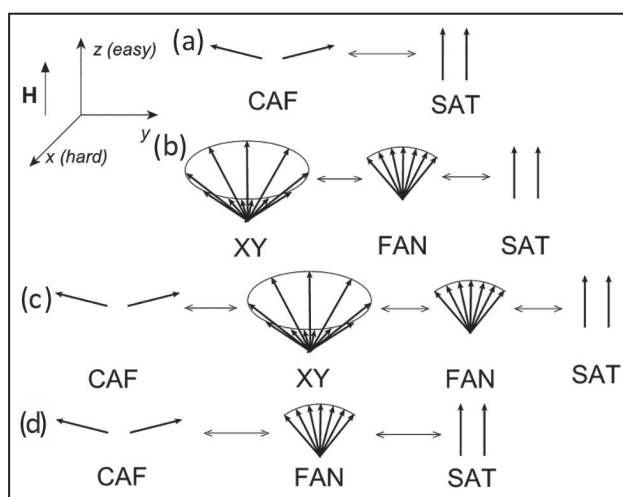
Multiferroics are compounds that possess several orderings in one phase (for example, magnetic and ferroelectric ordering). They are one of the most popular topics of investigation in contemporary condensed matter physics. From the applied point of view, such materials can be used for the creation of future electronic devices. So-called multiferroics of the spin origin, where electric polarization emerges in certain magnetic phases, can be highlighted. In particular, in such compounds giant magnetoelectric effect was observed.

In this context, noncollinear magnetic phases (e. g., spiral) with broken inversion symmetry, where the emergence of electric polarization is allowed, are of prime importance. Spiral magnetic ordering may arise, in particular, due to the frustrated exchange interactions. This makes further research on phase transitions involving helical phases an important problem.

In the present work properties of frustrated (with the minimum of exchange interaction in incommensurate vector) anisotropic antiferromagnets at low temperature in strong magnetic fields, close to the saturation one, were studied. This research extends the results of our previous work, where sequences of phase transitions in the same model, but in weak fields, were investigated.

On the level of classical energy, we show that in the studied model standard for antiferromagnets spin-flip transition (Fig. a) cannot be realized, even if perpendicular to the field anisotropy is large enough, to make canted antiferromagnetic phase (CAF) more preferable in comparison with conical spiral (XY). It is shown that in the considered model

with perpendicular to the field anisotropy XY phase becomes unstable near the saturation field, and the Ising type phase transition to the fan (FAN) phase takes place. Depending on the model parameters three possible sequences of phase transitions are denoted as (Figs. b–d). In all of them, before the transition to the saturated phase (SAT), the system passes through the fan phase. We derive analytical results for the transitions fields. They showed excellent correspondence with the results of numerical modeling with the use of Monte-Carlo method. Moreover, it was shown, that the developed theory allows describing all five phase transitions on the magnetic field applied along the easy axis and both transitions on magnetic field along the middle axis in multiferroic  $\text{MnWO}_4$ .



Phase transitions scenarios in frustrated anisotropic antiferromagnets with biaxial anisotropy ( $z$  axis is the easy magnetization direction,  $x$  axis – the hard one) in strong fields (close to the saturation one) along the  $z$  axis

## Fock space relativistic coupled cluster method: a new level of accuracy in predicting the properties of heavy element compounds

A.V. Zaitsevskii, A.V. Oleynichenko, N.S. Mosyagin, A.V. Titov  
Knowledge Transfer Division of NRC “Kurchatov Institute” – PNPI

The current level of accuracy and reliability in first-principle based predicting of energetic, radiative, electrical, and other properties of atoms, molecules and clusters does not fully correspond to the rapidly growing capabilities of modern experimental techniques. At the same time, it is just the accuracy level that determines the prospects for the development of many fields of science, including the production of matter at ultralow temperatures, high-resolution spectroscopy and the search for new physics in low-energy (“tabletop”) experiments as well as spectroscopic registration of superheavy elements and the creation of new materials.

At the Quantum Chemistry Laboratory (QCL) in NRC “Kurchatov Institute” – PNPI, work is underway to create tools for simulating systems comprising heavy atoms, aiming to raise the accuracy of predicting properties to a qualitatively new level. These tools are based on the Fock space relativistic coupled cluster (FS RCC) theory which is well-defined, physically transparent and in principle offers the possibility (up to now only in principle) to systematically improve the results.

The new QCL developments allow

- Radically extending the range of molecular systems accessible for modeling due to the elimination

of numerical instabilities (the technique of adjustable shifts of energy denominators and extrapolation to the zero-shift limit),

- Predicting the “non-energetic” properties of electronic transitions (radiative transition probabilities, off-diagonal hyperfine interaction matrix elements) that were previously unavailable or required unacceptable costs for FS RCC modeling,

- Raising the accuracy of the calculated properties to an unprecedented level by expanding the representation of the cluster operator (taking into account more complex independent electron-electron scattering processes).

One could notice the following successful applications of the new developments:

- Determination of changes in the magnetic dipole hyperfine interaction constants due to the formation of chemical bond,

- Calculation of the probabilities of electronic transitions in optical cycles in molecules of compounds of heavy elements, promising for direct laser cooling,

- Reproduction of the energies of electronic transitions in atoms of heavy elements (Tl, Pb) with the accuracy which creates a real possibility to model spectroscopic experiments with their superheavy homologues.



## Universal scaling of energy consumption in biological systems with variable mass

A.M. Makarieva, A.V. Nefiodov

*Theoretical Physics Division of NRC "Kurchatov Institute" – PNPI*

The relationship between energy consumption and order in complex systems has recently acquired great relevance in connection with the discussed strategies for changing the main energy sources used by civilization. In the literature, one can find statements that in the process of evolution of living organisms the rate of their energy consumption per unit mass increased, that this increase is a measure of the progressive development of living systems, and that modern civilization with its growing energy consumption is a special example of such progress.

On the other hand, a high rate of energy consumption is characteristic of unstable, decaying objects that explosively destroy their environment. Since the main property of life is sustainability, evolutionary progress can manifest itself at the level of ecosystems not as an increase in energy consumption but as an increase in the efficiency of the regulation of the environment, which life maintains in a state optimal for itself.

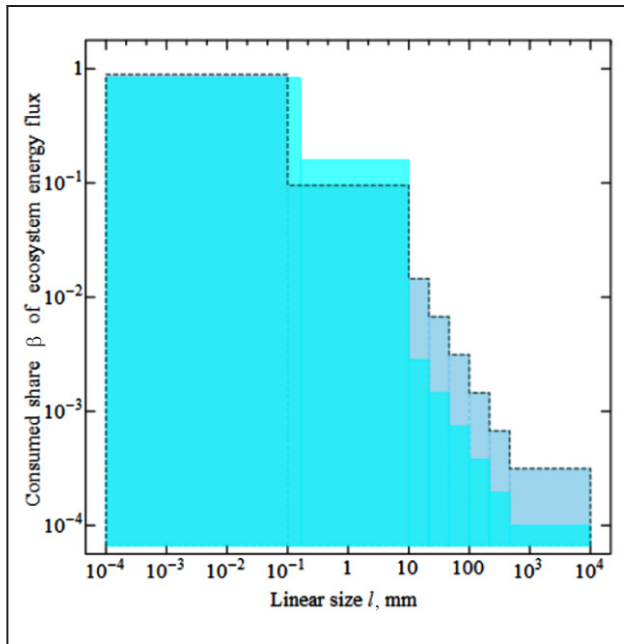
In the fundamental works of V.G. Gorshkov in 1980 and 1981, the basic universal principles of energy consumption of biological systems were identified. Living organisms that appeared at different stages of the evolutionary process, from bacteria to mammals, consume approximately the same power per unit mass, of the order of several watts per kilogram. Subsequently, this statement was confirmed on the example of the analysis of several thousand biological species. In sustainable ecosystems, by contrast, the energy consumption per unit area of organisms decreases with increasing size of the organisms. The smallest organisms (bacteria and fungi) consume the largest share of ecosystem productivity.

The development of these fundamental ideas led to the formulation of a new understanding of

the role of increasing the body size of organisms in the evolution of life. While in larger organisms the volume-specific rate of energy consumption is approximately universal, their rate of energy consumption per unit area of their body surface grows proportionally to the linear size of the body. At large body sizes, this rate can exceed the rate of energy production in the process of photosynthesis supported by solar radiation by an order of magnitude or more. Thus, large animals act as local destroyers of the ecosystem biomass, and their evolutionary appearance can be interpreted as a sign of decay (aging) of the life algorithm as a whole.

It turns out that the distribution of energy consumption over the body size of heterotrophs, which is characteristic of stable terrestrial ecosystems, is also preserved in ocean ecosystems. This indicates the universal nature of this distribution, since the biomass of terrestrial ecosystems (mainly wood) exceeds the biomass of the ocean, where photosynthesis is carried out mainly by unicellular phytoplankton, by at least two orders of magnitude (Fig.). When a major part of ecosystem productivity is consumed by the smallest organisms, the stability of the organization of the ecosystem is achieved due to the operation of the law of large numbers.

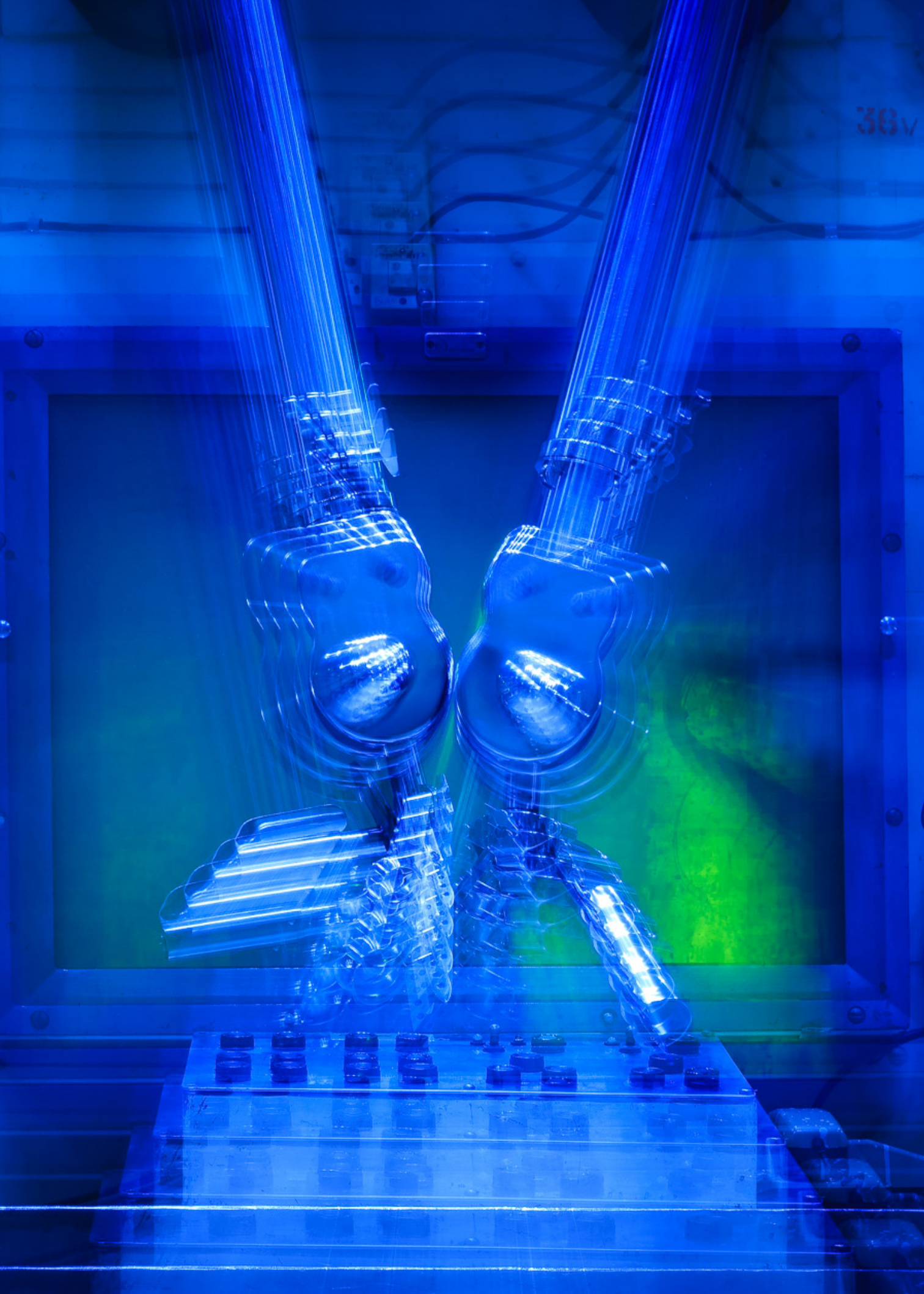
These results contribute to the solution of one of the fundamental interdisciplinary problems of modern science – the determination of the principles of maintaining the stability of living systems in the face of environmental and climatic cataclysms that increase in frequency on a global scale. The relative fluctuations introduced by the huge number of tiny organisms that process most of the energy flow are small. Large organisms, dictated by their body size to destroy living biomass, are allocated a low share of the energy flow. This smallness limits their potential destructive effects.



Share  $\beta$  of ecosystem energy flux consumed by heterotrophs from a given body size interval in stable ecosystems on land (*dashed contour histogram*) and in the ocean (*solid contour histogram*). Total area of the histogram equals unity

Civilization consumes about 10% of the primary productivity of the biosphere, that is, ten times more than is allocated to large animals. The biosphere and environment are rapidly deteriorating. To continue its existence, our civilization must

return to the range of stability, reducing the anthropogenic impact on natural ecosystems (primarily, the intact forests that perform climate-regulating functions) by at least one order of magnitude.



## Research Based on the Use of Neutrons and Photons

- 36 Seven order diffraction enhancement of the Stern–Gerlach effect for a neutron in a crystal
- 38 New experiment searching for solar axions with  $\text{Tm}_3\text{Al}_5\text{O}_{12}$  cryogenic bolometer
- 39 Investigation of angular distributions of fission fragments of  $^{240}\text{Pu}$  by neutrons with energies of 1–200 MeV
- 40 Investigation of the structure of the fission barrier and properties of transition states in neutron resonances
- 41 Peculiarities of magnetic ordering in novel chiral magnet  $\text{MnSnTeO}_6$
- 43 Structure and kinetics of anion exchange in layered double hydroxides
- 45 Dzyaloshinsky–Moriya interaction in multiferroics  $\text{NdMn}_2\text{O}_5$
- 46 Onset of a skyrmion phase by chemical substitution in  $\text{MnGe}$  chiral magnet
- 47 Switch of fractal properties of DNA in chicken erythrocytes nuclei by mechanical stress
- 49 1D ceric hydrogen phosphate aerogels: noncarbonaceous ultraflyweight monolithic aerogels

## Seven order diffraction enhancement of the Stern–Gerlach effect for a neutron in a crystal

V.V. Voronin, S.Yu. Semenikhin, D.D. Shapiro, Yu.P. Braginets, V.V. Fedorov – Neutron Research Division of NRC “Kurchatov Institute” – PNPI,  
V.V. Nesvizhevsky, M. Jentschel – Institut Laue–Langevin,  
A.I. Ioffe – Jülich Centre for Neutron Science,  
Ya.A. Berdnikov – Peter the Great Saint Petersburg Polytechnic University

A study of the diffraction enhancement of effects of small forces, acting on the neutron at diffraction angles close to the right one was carried out within the preparation of the new experiment to test the equivalence principle for neutrons by the crystal-diffraction method. The spatial splitting of a neutron beam into two components with opposite spin directions in a small magnetic field gradient ( $\sim 3$  G/cm) was measured at the Laue diffraction in a crystal (analogous to the Stern–Gerlach experiment). The experiment was performed in the two-crystal scheme (total crystal size is  $130 \times 130 \times 218$  mm) where the external force  $\pm F_w$ , acting on the diffracting neutron in the crystal, slightly changes the direction of its motion (and/or wavelength), and so the parameter of deviation from the Bragg condition. As a result the amplitudes of the direct wave and the wave reflected by crystallographic planes will change as well as the direction of the neutron current in the crystal.

In Figure 1 we show by *solid* and *dotted* lines the two Kato trajectories of neutrons with opposite spin projection “weakly absorbed” inside the crystal (which correspond to one of two branches of the neutron dispersion surface in crystal). Under experimental conditions (large thickness of the crystals and large Bragg angles) the neutrons of other diffracting branch are almost completely absorbed due to the Bormann effect by the silicon crystal (Si) and the according Kato trajectories disappear.

The result is a significant change in the direction of the neutron current in the crystal and a curvature of the neutron Kato trajectory, which leads to a spatial shift of the neutron beam at the exit face of the second crystal.

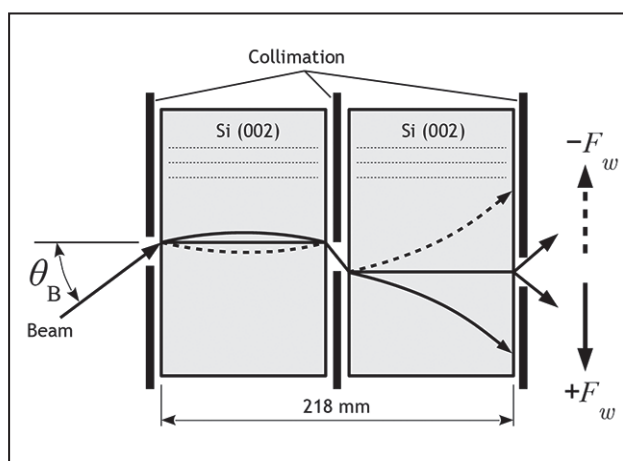


**Fig. 1.** A two-crystal scheme of an experiment with direct collimation of a neutron beam (top view), where  $\pm F_w$  is an external force acting on a neutron in a crystal acting

The diffraction enhancement of the deflection of the neutron direction inside the crystal is well known and can reach  $\sim 10^5$ – $10^6$ . However, in our experiment we used an additional gain related to large diffraction angles. As the diffraction angle increases, the residence time of the neutron in the crystal, and so the time of the force's impact on it, increases proportionally to  $\tan \theta_B$ . Thus, there is a new possibility to amplify the diffraction enhancement and to get higher sensitivity to external forces acting on the neutron in the crystal. In our case, for the (220) silicon crystal plane, the total diffraction enhancement is  $K_e^{(220)} = 2.1 \cdot 10^5 \cdot \tan^2 \theta_B$ , which gives a value of  $1.1 \cdot 10^7$  at the maximum Bragg angle of  $82^\circ$  in the experiment.

The experiment was conducted at the PF1b cold neutron beam in Institut Laue–Langevin (Grenoble, France). The measurement results are shown in Fig. 2. Since the incident neutron beam is not

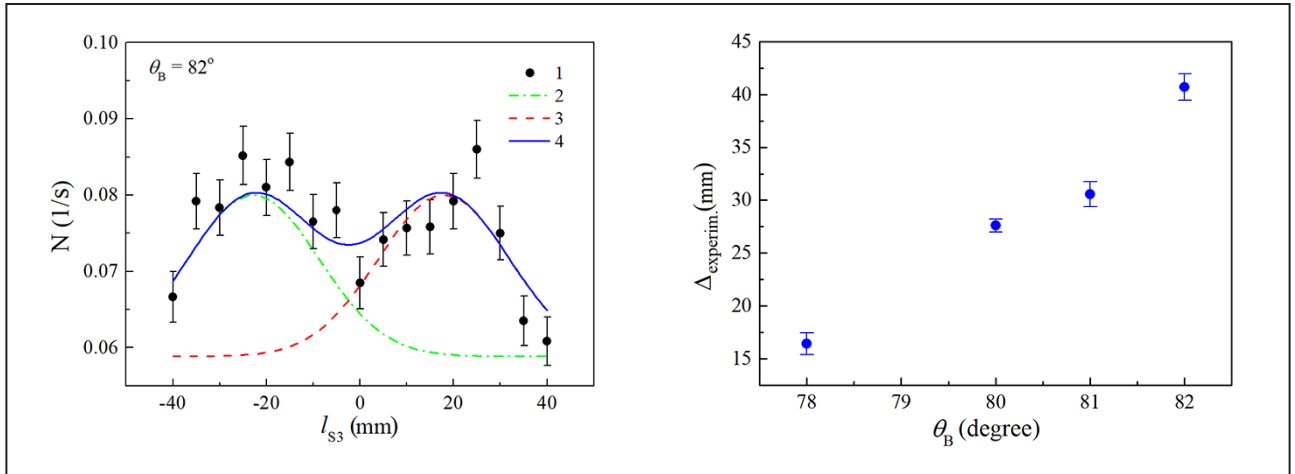


**Fig. 2.** The spatial intensity distribution on the output surface of the working crystal at a gradient of 3 G/cm in the neutron beam area and a diffraction angle of 82° (on the left); the distance between the positions of the maxima of the two-crystal lines for the two spin projections (on the right)

polarized, the diffracting beams will shift in opposite directions for different projections of the neutron spin relative to the center of the original beam. In the Fig. 2 on the left, the black dots show the experimental data, curves 2 and 3 are the fitting curves (Gauss) for two reflexes with different spin projections, and 4 is their sum. The right Fig. 2 shows the dependence of the distance between the positions of the maxima of the two-crystal lines (curves 2 and 3 of the left Fig. 2) for the two spin projections on the diffracting angle. At maximum measured angle of 82°, the splitting reaches  $4.1 \pm 0.1$  cm. For comparison, the spatial splitting

for neutrons with a wavelength 3.8 Å (corresponding to a Bragg angle of 82°), moving in free space under the same field gradient through the same 3-slit collimator without crystal (removed from the setup) at a path length of 21.8 cm (the total length of the working crystal) is easily calculated as  $3.9 \cdot 10^{-7}$  cm. The average value of the field gradient along the neutron beam was  $3.12 \pm 0.09$  G/cm, which is consistent with estimates based on magnetometer (Fig. 3).

Thus, the measured value of enhancement was  $K_{exp} \sim 2 \cdot 10^5 \cdot \tan^2 \theta_B$ , which is in good agreement with the theory.

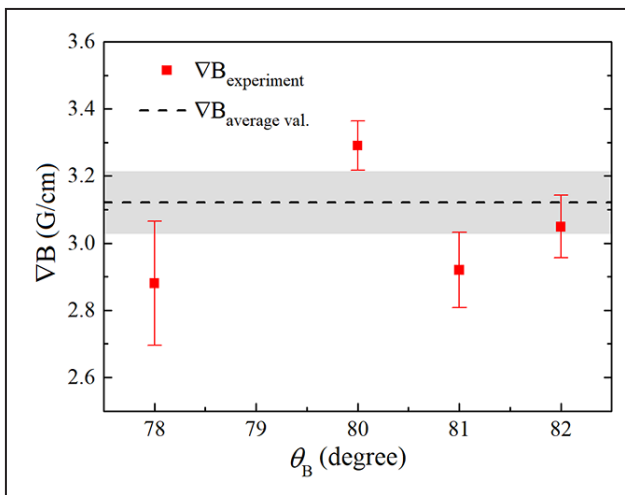


**Fig. 3.** The field gradient as function of diffraction angle  $\theta_B$  (red squares) and calculated average value of the field gradient (the dashed line)

## New experiment searching for solar axions with $\text{Tm}_3\text{Al}_5\text{O}_{12}$ cryogenic bolometer

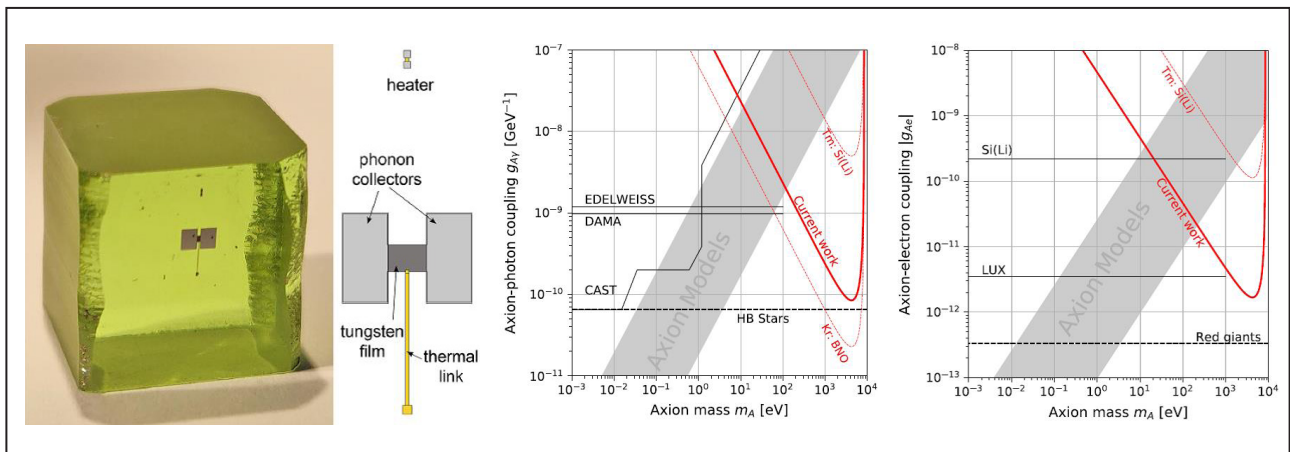
S.V. Bakhlanov, A.V. Derbin, I.S. Drachnev, A.M. Kuzmichev, I.S. Lomskaya, V.N. Muratova, D.A. Semenov, M.V. Trushin, E.V. Unzhakov  
Neutron Research Division of NRC "Kurchatov Institute" – PNPI

Intensive experimental searches for axions and axion-like particles (ALPs) are currently supported by two main circumstances: first, axions solve the strong  $CP$  problem and, second, axions are well-motivated candidates for the role of dark matter particles. Moreover, the existence of axions and ALPs could explain too rapid cooling of some classes of stars and the anomalous transparency of the Universe for  $\gamma$ -quanta with energies of the order of 1 TeV.

The search for the resonant absorption of solar axions by  $^{169}\text{Tm}$  nuclei was proposed by authors and was carried out in collaboration of Russian and foreign institutes. The new approach is to use the

$\text{Tm}_3\text{Al}_5\text{O}_{12}$  crystal as a bolometric cryogenic detector to search for resonant excitation of the first nuclear level of the  $^{169}\text{Tm}$  isotope (8.4 keV) by solar axions:  $A + ^{169}\text{Tm} \rightarrow ^{169}\text{Tm}^* \rightarrow ^{169}\text{Tm} + \gamma$  (8.41 keV). Measurements carried out with 8 g crystal for 6.6 days allowed establishing new limits on the coupling constants of the axion with photons  $g_{A\gamma}$  and electrons  $g_{Ae}$ :  $|g_{A\gamma}(g_{0AN} + g_{3AN})| \leq 1.44 \cdot 10^{-14} \text{ GeV}^{-1}$  and  $|g_{Ae}(g_{0AN} + g_{3AN})| \leq 2.81 \cdot 10^{-16}$ . The obtained restrictions excluded a new range of possible values of the coupling constants  $g_{A\gamma}$  and electrons  $g_{Ae}$  and axion masses  $m_A$  (Fig.).

The work was supported by the RFBR grant No. 17-02-00305.



$\text{Tm}_3\text{Al}_5\text{O}_{12}$  crystal with deposited TES thermistor (left). Constraints on the coupling constants  $g_{A\gamma}$  and  $g_{Ae}$  in comparison with the results of other experiments and the predictions of the theoretical KSVZ and DFSZ axion models (center and right)

## Investigation of angular distributions of fission fragments of $^{240}\text{Pu}$ by neutrons with energies of 1–200 MeV

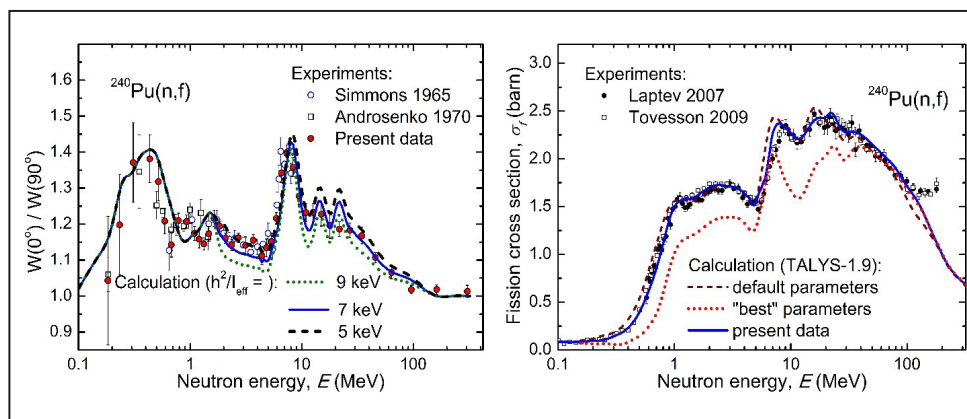
A.S. Vorobyev, A.M. Gagarski, O.A. Shcherbakov, L.A. Vaishnene – Knowledge Transfer Division, Neutron Research Division, High Energy Physics Division of NRC “Kurchatov Institute” – PNPI,  
A.L. Barabanov – NRC “Kurchatov Institute”

To date, quite extensive data have been accumulated on the total fission cross-sections of many nuclei in low and intermediate neutron energies, up to 200 MeV. However, systematic studies of differential fission cross-sections in the same wide range of neutron energies began only in the last decade. This is primarily due to the fact that increasingly accurate fission data is needed for the design of modern and future nuclear reactors, as well as for the design of accelerator-driven systems (ADS) installations, including powerful neutron sources. No less important is that the development of existing and new theoretical approaches to the description of fission process is impossible without their verification using a variety of high-precision experimental data on complete and differential fission cross-sections that are sensitive to various aspects of the fission mechanism.

We performed measurements for a wide set of target nuclei:  $^{233}\text{U}$ ,  $^{235}\text{U}$ ,  $^{238}\text{U}$ ,  $^{232}\text{Th}$ ,  $^{237}\text{Np}$ ,  $^{239}\text{Pu}$ ,  $^{240}\text{Pu}$ ,  $^{209}\text{Bi}$  and  $^{\text{nat}}\text{Pb}$ , and also proposed a method for the theoretical description of the results obtained. For the actinide nuclei  $^{233}\text{U}$ ,  $^{237}\text{Np}$ ,  $^{239}\text{Pu}$ , and  $^{240}\text{Pu}$  measurements in the region above 20 MeV were performed for the first time, while for  $^{209}\text{Bi}$  and  $^{\text{nat}}\text{Pb}$ , such measurements were not previously performed at all on neutron sources with a continuous spectrum.

A comparison of experimental data and model calculations (Fig.) suggests that the proposed approach can be used to obtain new information about both reactions at intermediate energies and the fission process (fission barriers, characteristics of nuclei at barriers, parameters of transition states).

The work was supported by the RFBR grant No. 18-02-00571.



Anisotropy of the angular distributions of the fragments (*left*) and the fission cross section  $^{240}\text{Pu}$  (*right*) in comparison with the calculation results

1. Barabanov A.L., Vorobyev A.S., Gagarski A.M., Shcherbakov O.A., Vaishnene L.A. // Bull. Rus. Acad. Sci: Phys. 2020. V. 84. No. 4. P. 397.
2. Vorobyev A.S., Gagarski A.M., Shcherbakov O.A., Vaishnene L.A., Barabanov A.L. et al. // Bull. Rus. Acad. Sci: Phys. 2020. V. 84. No. 10. P. 1245.
3. Vorobyev A.S., Gagarski A.M., Shcherbakov O.A., Vaishnene L.A., Barabanov A.L. // JETP Lett. 2020. V. 112. Iss. 6. P. 323.



## Investigation of the structure of the fission barrier and properties of transition states in neutron resonances

O.A. Shcherbakov, A.S. Vorobyev, A.M. Gagarski, L.A. Vaishnene  
 Knowledge Transfer Division, Neutron Research Division, High Energy Physics Division  
 of NRC "Kurchatov Institute" – PNPI

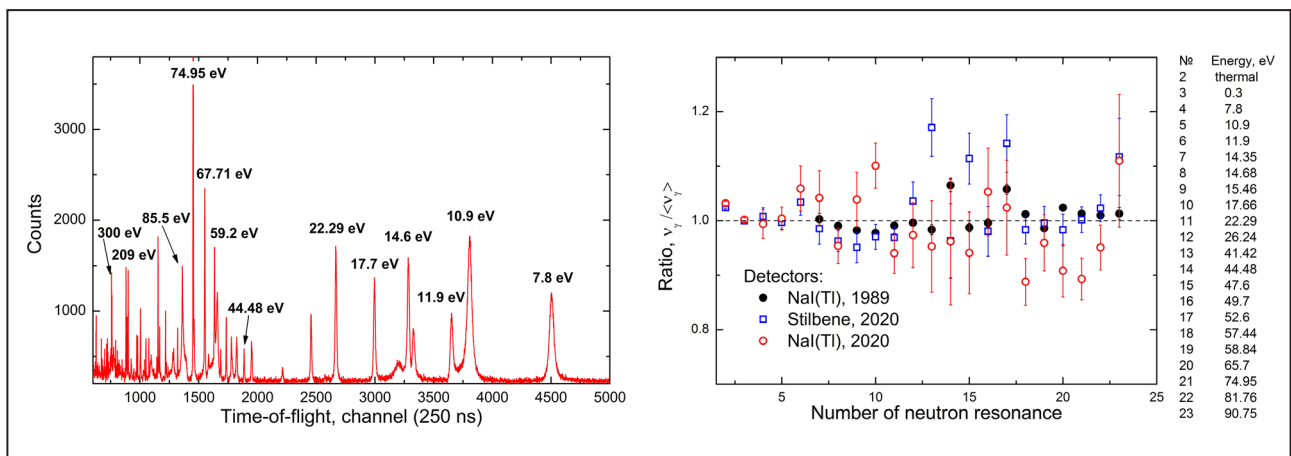
The properties of the highly excited states of heavy nuclei resulting from the absorption of low-energy resonant neutrons can be obtained by analyzing experimental data on the  $(n, \gamma f)$  reaction. The density and structure of levels near and below the neutron binding energy, the type and multipole nature of radiation transitions between them, the structure of fission barriers and transition states – this is a far from complete list of physical quantities of interest.

Experimental studies of the  $(n, \gamma f)$  reaction in this work were carried out by measuring the multiplicity of  $\gamma$ -quanta and fission neutrons, as well as the energy spectra and total energy of the  $^{235}\text{U}$  and  $^{239}\text{Pu}$  fission gamma  $\gamma$ -rays by resonant neutrons with an energy of 1–300 eV. The measurements were carried out on the 45-meter flight base of beam No. 2 of the GNEIS neutron time-of-flight spectrometer operating on the basis of the SC-1000 synchrotron, NRC "Kurchatov Institute" – PNPI.

The figure shows the results of measurements of the  $\gamma$ -quanta multiplicity of  $^{239}\text{Pu}$  fission obtained using various detectors.

In the analysis of the data measured, the experimental evaluation of the width of the  $(n, \gamma f)$  reaction for 1+ resonances  $^{239}\text{Pu}$  was obtained, which is within the achieved statistical data accuracy consistent with the best estimates, which were made earlier by other authors. At the same time, theoretical calculations of the widths of the  $(n, \gamma f)$  reaction and the spectra of the pre-fission  $\gamma$ -quanta for the  $^{239}\text{Pu}$  nucleus were also performed using various variants of the radiation function model. To obtain an unambiguous reliable conclusion about the mechanism of pre-fission  $\gamma$ -transitions, it is necessary to increase the statistical accuracy of the data, so the measurements will be continued.

The work was supported by the RFBR grant No. 19-02-00116.



The time-of-flight spectrum from  $^{239}\text{Pu}(n, f)$  fission fragments in the energy range 0.7–300 eV (left) and the multiplicity of  $\gamma$ -quanta for well-resolved resonances at  $^{239}\text{Pu}(n, f)$  fission (right)

## Peculiarities of magnetic ordering in novel chiral magnet $\text{MnSnTeO}_6$

A.I. Kurbakov, M.D. Kuchugura

Neutron Research Division of NRC “Kurchatov Institute” – PNPI

The discovery of skyrmion phases has focused attention on the interplay between complex magnetism and crystal symmetries, in particular, the coupling of structural and magnetic chiralities. Over the past few years, the chiral antiferromagnet  $\text{MnSb}_2\text{O}_6$  (sp. gr.  $P321$ ), which is of great interest to the manifestation of the magnetoelectric effect – the creation and switching of electric polarization by a magnetic field, has been actively studied. The unusual physical properties of  $\text{MnSb}_2\text{O}_6$  stimulate interest in the preparation and investigation of its structural analogues. However, it turns out that in the  $\text{MSb}_2\text{O}_6$  series, all  $\text{M}^{2+}$  cations larger than  $\text{Mn}^{2+}$  ( $M = \text{Cd}, \text{Ca}, \text{Sr}, \text{Pb}, \text{and Ba}$ ) give rise to the rosielite structure type, whereas all stable compounds with  $\text{M}^{2+}$  cations smaller than  $\text{Mn}^{2+}$  ( $M = \text{Mg}, \text{Co}, \text{Ni}, \text{Cu}, \text{and Zn}$ ) belong to the trirutile structure type. Both rosielite and trirutile types are centrosymmetric and, thus, less interesting than chiral  $\text{MnSb}_2\text{O}_6$ . To find structural analogs of  $\text{MnSb}_2\text{O}_6$ , we carried out heterovalent substitutions. The most similar to  $\text{MnSb}_2\text{O}_6$  should be its isoelectronic counterpart,  $\text{MnSnTeO}_6$ .

In this work, a new layered oxide  $\text{MnSnTeO}_6$  with the rarest combination of magnetic properties is studied in detail. It possesses two-dimensional magnetism, multiferroism, and the coupling of the crystal and magnetic chirality. This unique set of properties makes the new compound promising for future electronics based on quantum effects. The structure and its static and dynamic magnetic properties were studied comprehensively both experimentally (through X-ray and neutron powder diffraction, magnetization, specific heat, dielectric permittivity, and ESR techniques) and theoretically by means of *ab initio* DFT calculations within the spin-polarized generalized gradient approximation.

$\text{MnSnTeO}_6$  is isostructural with  $\text{MnSb}_2\text{O}_6$  (sp. gr.  $P321$ ) and does not show any structural transition

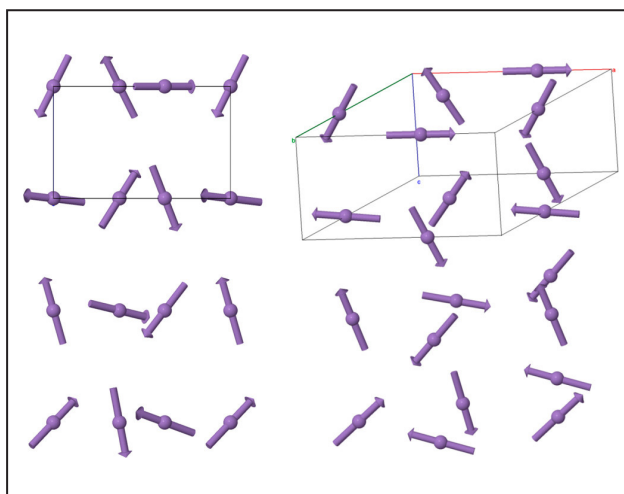


**Fig. 1.** Model of the magnetic structure. The 2D distribution of the Mn spins in the  $ac$  plane (left); the 3D spatial spins distribution (right). The crystallographic unit cell is also shown

between 3 and 300 K. Magnetic manganese ions form a layered structure from a distorted triangular lattice in the  $ab$  plane. The magnetic susceptibility and specific heat measurements reveal two anomalies. The first at  $T_N \sim 9.8$  K, is related to formation of long-range magnetic order, which was shown by means of neutron diffraction to have a propagation vector  $\mathbf{k} = (0, 0, 0.183)$ . The magnetic ground state of  $\text{MnSnTeO}_6$  has a complex nature, is formed as a result of frustrations and is described by a set of cycloids (Fig. 1).

The thermodynamic parameters demonstrate an additional anomaly on the temperature dependences of  $\chi(T)$ ,  $C_p(T)$  and  $\varepsilon(T)$  at  $T^* \sim 4.9$  K, which is characterized by significant temperature hysteresis, but cannot be associated with any change in structure and corresponding first-order phase transition. Clear enhancement of the dielectric permittivity at  $T^*$  is most likely to reflect the coupling of dielectric and magnetic subsystems leading to development of electric polarization. *Ab initio* calculations

demonstrate that in contrast to naive expectations the largest exchange coupling is not between Mn ions in the same triangular plane but between planes along diagonals. Exchange couplings behave differently in the two types of domains (chirality) due to the difference in super-superexchange interactions. There are two oxygen ions on the

exchange path along one diagonal, while there is nothing between the Mn ions forming paths along the other diagonal. These two oxygen ions act as an effective media and provide their 2p orbital for the exchange interaction. Summarizing the data of all studies, a magnetic phase diagram of a new chiral magnet  $\text{MnSnTeO}_6$  was constructed (Fig. 2).

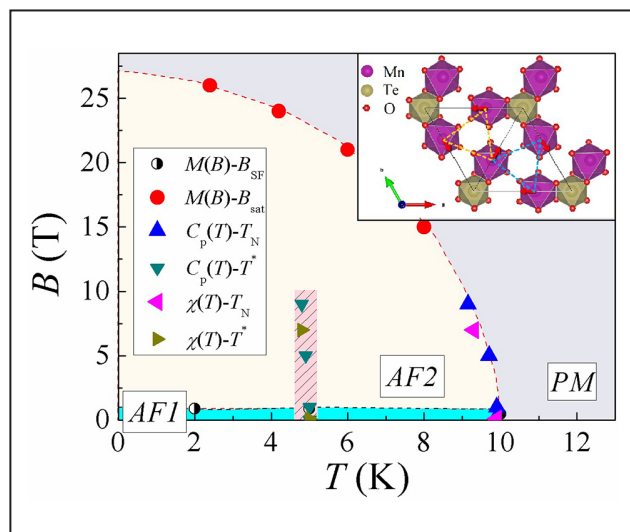


**Fig. 2.**  $\text{MnSnTeO}_6$  magnetic phase diagram. *The inset shows a polyhedral view of the first layer in the crystal structure of  $\text{MnSnTeO}_6$ , formed by  $\text{MnO}_6$  and  $\text{TeO}_6$  octahedra, purple and yellow, respectively. The arrows show the directions of the magnetic moments. A parallelogram formed by straight lines shows a crystallographic unit cell*

## Structure and kinetics of anion exchange in layered double hydroxides

M.H. Iuzviuk, I.A. Zobkalo

Neutron Research Division of NRC “Kurchatov Institute” – PNPI

Layered double hydroxides (LDHs) are layered compounds based on the brucite structure ( $\text{Mg}[\text{OH}]_2$ ) with anion exchange capacity. Due to the ability to anion exchange, LDHs act as nanocontainers or nanoreservoirs for storing and releasing various compounds in their anionic form (organic, inorganic, biomolecules). One of the promising applications of LDHs is the field of corrosion protection. LDHs can store corrosion inhibitors and release them “on demand”: depending on environmental conditions (for example, pH, presence of aggressive particles), *i. e.* serve as new non-toxic protective materials.

*In situ* synchrotron studies of the crystal structure of Zn–Al layered double hydroxides obtained on a metal substrate (aluminum alloy AA2024, Zn), as well as the processes of anion exchange in them, have been carried out. The experiments were performed at the X-Ray radiation source PETRA III at the DESY synchrotron center (Hamburg). Anion exchange occurred between the “parental”  $\text{NO}_3^-$  anion and the “guest”  $\text{Cl}^-$ ,  $\text{SO}_4^{2-}$  (corrosion accelerators) and  $\text{VO}_x^{y-}$  (corrosion inhibitor). It was shown that, as a result of the exchange reaction of nitrate anions ( $\text{NO}_3^-$ ) for chlorides ( $\text{Cl}^-$ ) in LDHs, the space group remains unchanged ( $R3m$ ) on both types of substrates. During the nitrate – sulfate ( $\text{SO}_4^{2-}$ ) exchange, the space group changes from  $R3m$  to  $P3$  both on Zn and on AA2024. Anion exchange nitrate – vanadate ( $\text{VO}_x^{y-}$ ) leads to the formation of two crystalline phases of LDHs– $\text{VO}_x$  on the zinc surface. Presumably, these are LDHs with the  $\text{V}_2\text{O}_7^{4-}$  and  $\text{V}_4\text{O}_{12}^{4-}$  anions.

In Figure 1 the complete reaction of nitrate–sulphate anion exchange is shown based on the intensity variation of the basal reflections.

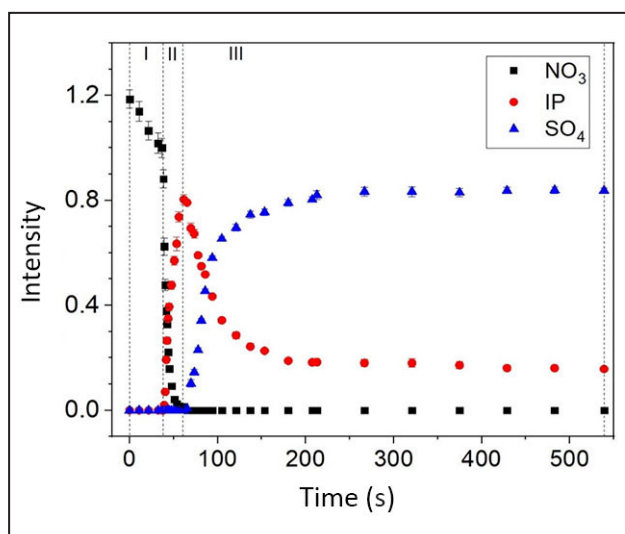


**Fig. 1.** Time evolution of integral intensity of basal peaks: decay of the initial phase Zn-LDH- $\text{NO}_3$  (squares), formation and decrease of IP (circles) and formation of Zn-LDH- $\text{SO}_4$  (triangles).

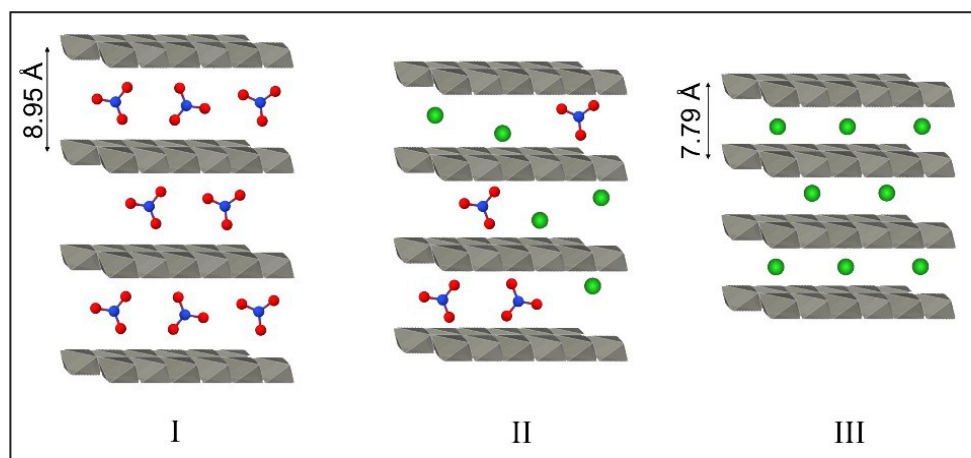
The anion exchanges were studied using a universal approach to describing the proceeding of solid-state reactions – the Avrami–Erofeev model. As a result, such reaction parameters as the rate constant, the start time of the reaction were obtained, as well as conclusions about the type of exchange reactions were made.

Nitrate–chloride and nitrate–sulfate anion exchanges proceed in two stages with the formation of an intermediate crystalline phase, which is LDHs with parental and guest anions simultaneously (Fig. 2). The first stage is characterized by a two-dimensional, the second one by a one-dimensional diffusion-controlled reaction with a deceleration of nucleation. This means that the reaction rate is determined by the rate at which the guest anions –  $\text{Cl}^-$  and  $\text{SO}_4^{2-}$  – penetrate into the inter-

layer galleries, with the effect of slowing down the nucleation at the edges of the layers. As a result of the exchange, in both cases the parental crystal phase of LDHs- $\text{NO}_3$  completely disappears, but the intermediate phase is retained until the end of the reaction. The nitrate–vanadate exchange reaction, unlike those described above, proceeds in one stage, but with the formation of two final crystalline phases, presumably, these are the LDHs- $\text{V}_2\text{O}_7$

and LDHs- $\text{V}_4\text{O}_{12}$  phases. The reactions are characterized by two-dimensional processes with instant nucleation. This exchange does not end with the complete release of nitrate anions, in contrast to the two previous ones.

The analysis shows that LDHs effectively absorb aggressive anions ( $\text{Cl}^-$ ,  $\text{SO}_4^{2-}$ ) from the environment, and can also serve as nanocontainers for corrosion inhibitors ( $\text{VO}_x$ ).



Schematic representation of anion exchange process via intermediate phase (I–III)

## Dzyaloshinsky–Moriya interaction in multiferroics $\text{NdMn}_2\text{O}_5$

I.A. Zobkalo, A.N. Matveeva, S.V. Gavrilov

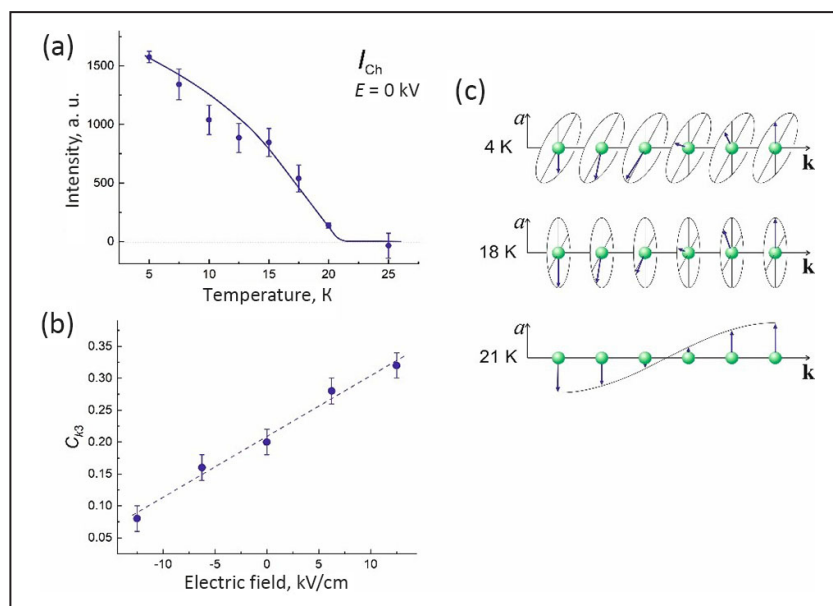
Neutron Research Division of NRC “Kurchatov Institute” – PNPI

Multiferroics are substances where two spontaneous ordered phases of different nature are simultaneously present. Such functional materials can be used to solve problems in energy- and resource-saving technologies, for lossless energy transmission, and energy storage systems. The fundamental problem, which is associated with the unique properties of multiferroics is the origin of the mechanisms of magnetoelectric coupling in magnetically induced ferroelectrics.

Rare-earth manganates  $\text{RMn}_2\text{O}_5$  ( $R$  – rare-earth element) demonstrate the most impressive examples of the coupling between magnetic and electrical properties. Despite numerous experimental and theoretical studies, the mechanism(s) of the origin of ferroelectric polarization in these substances cannot be unambiguously determined.  $\text{NdMn}_2\text{O}_5$  has been studied using polarized neutron diffraction methods, which directly indicate the presence of antisymmetric interactions, previously only assumed.

It is shown that in  $\text{NdMn}_2\text{O}_5$ , the antisymmetric Dzyaloshinsky–Moriya (DM) interaction is clearly manifesting itself in those magnetic phases in which ferroelectric polarization is observed. In magnetic phases where there is no DM, there is also no polarization. It allows us to make an assumption that DM induces ferroelectric polarization in the  $\text{RMn}_2\text{O}_5$  compounds.

The obtained dependences of the neutron chiral scattering on the external electric field also allow us to conclude that the antisymmetric interactions and the ferroelectric polarization in  $\text{RMn}_2\text{O}_5$  are closely coupled (Fig.). The performed theoretical analysis at the qualitative level confirmed the possibility of the existence of a non-zero interaction of DM in  $\text{RMn}_2\text{O}_5$ . It is shown that the structure of  $\text{RMn}_2\text{O}_5$  compounds has a certain “softness”, which leads to the appearance and coexistence of several magnetic structures with similar wave vectors in a single crystal.



Temperature dependence of the chiral scattering in single crystal  $\text{NdMn}_2\text{O}_5$  (a); dependence of the average chirality on the applied electric field in the FC mode (b); schematic representation of the temperature transformation of a chiral structure of the “elliptical spiral” type into a non-chiral structure of the “spin wave” type (c)

## Onset of a skyrmion phase by chemical substitution in MnGe chiral magnet

E.V. Altynbaev, S.V. Grigoriev

Neutron Research Division of NRC “Kurchatov Institute” – PNPI

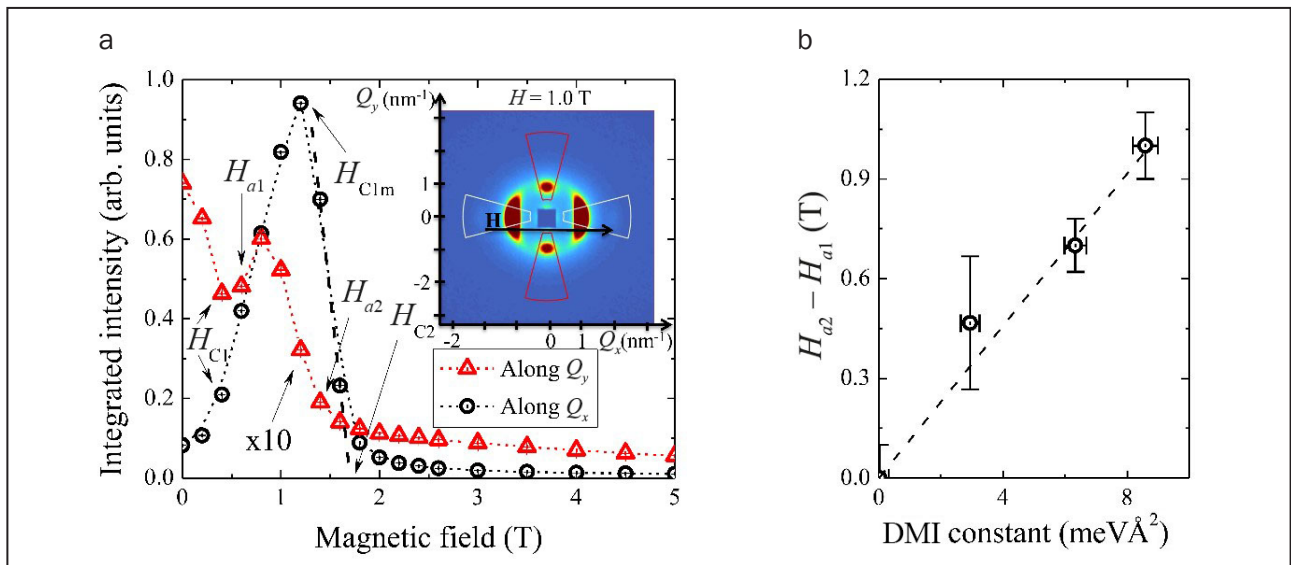
The evolution of the magnetic phase diagram ( $H$ - $T$ ) of  $\text{Mn}_{1-x}\text{Fe}_x\text{Ge}$  with  $x = 0.0; 0.1; 0.2$  and  $0.3$  was studied using small-angle neutron scattering (SANS).

SANS experiments were carried out on the SANS-1 instrument at the Heinz Maier-Leibnitz Institute (MLZ, Garching, Germany; research reactor FRM-II) and on the PA20 instrument at the Leon Brillouin Laboratory (LLB, Saclay, France; research reactor Orphée). The example of the SANS map measured at  $T = 100$  K and  $H = 0.8$  T is presented on the inset of Figure. The field dependence of the neutron scattering intensity along and perpendicular to the field direction is presented in Fig. a.

As a result, we have observed the absence of a regular skyrmion lattice or A-phase in MnGe and

its onset under a small substitution of Mn for Fe. The A-phase is observed over a wide temperature range  $30 < T < 140$  K, perhaps thanks to the inherent fluctuations and metastable character of  $\text{Mn}_{1-x}\text{Fe}_x\text{Ge}$ . Its field range increases linearly starting from zero with the Fe concentration and calculated DMI constant (Dzyaloshinsky–Moriya) as presented in Fig. b.

These results emphasize that DMI and helical fluctuations are the main ingredients for the stabilization of a skyrmion lattice in B20 magnets, and indicate a way to fine-tune the properties of dense skyrmion lattice using controlled chemical substitution.



Neutron scattering intensity deduced from the small-angle neutron scattering maps of  $\text{Mn}_{0.7}\text{Fe}_{0.3}\text{Ge}$ , integrated in directions along (black circles) and perpendicular (red triangles) to the external field,  $H$ , at  $T = 100$  K (a). A map measured at 100 K and 0.8 T is shown in the inset with the white (red) integration sector for the direction along (perpendicular to) the magnetic field. Field extension of the A-phase (averaged over temperature for each sample) versus the calculated DMI constant for connections  $\text{Mn}_{1-x}\text{Fe}_x\text{Ge}$  (b)

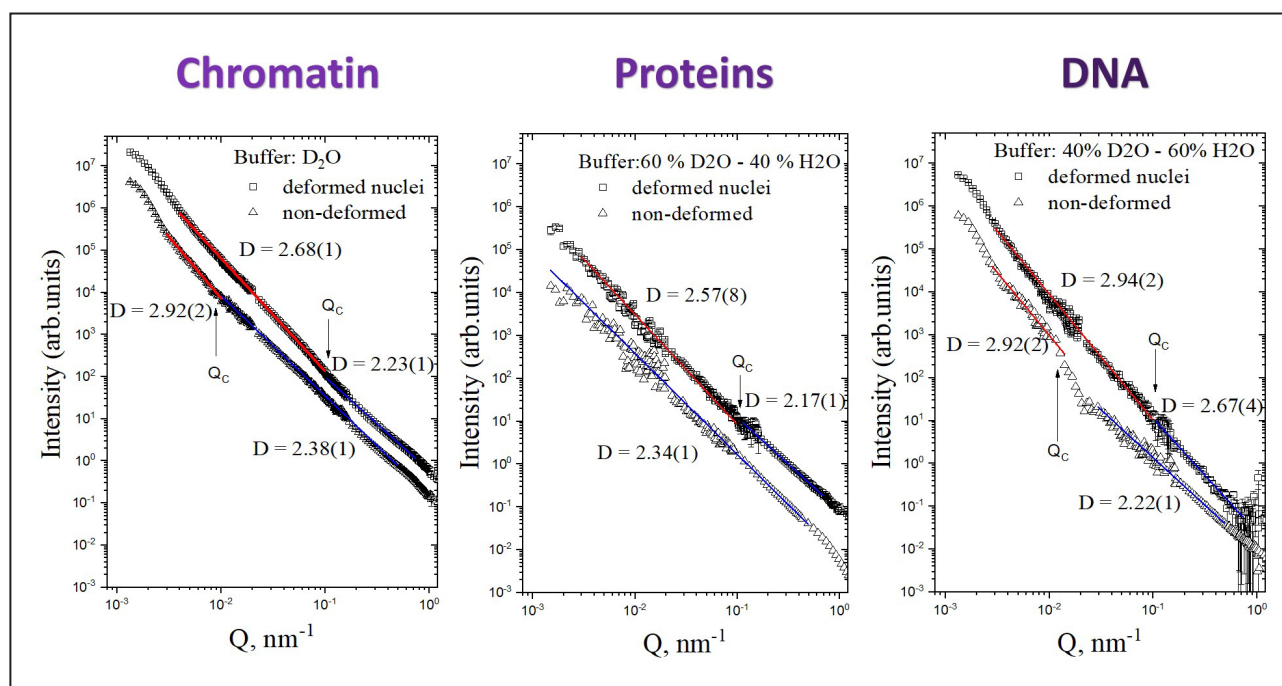
## Switch of fractal properties of DNA in chicken erythrocytes nuclei by mechanical stress

S.V. Grigoriev, E.G. Iashina, V.Yu. Bairamukov, M.V. Filatov, R.A. Pantina, E.Yu. Varfolomeeva  
Neutron Research Division, Molecular and Radiation Biophysics Division  
of NRC "Kurchatov Institute" – PNPI

Everyone knows that the cell is the basic structural, functional, and biological unit of all known living organisms. The cell nucleus acts like the brain of the cell. A complex of macromolecules found in cells, consisting of DNA and protein is called the chromatin. All the information about a biological organism is written in the double-helix DNA consequence. One of the most exciting questions that scientists are trying to answer is how meters of DNA are packed inside the 5- $\mu\text{m}$  diameter nucleus of a cell. Work is part of a project that is dealing with the search for universal principles of large-scale organization of chromatin and the study of its physical properties and changes under various influences.

The small-angle neutron scattering (SANS) on the chicken erythrocyte nuclei demonstrates the bifractal nature of the chromatin structural organization (Fig.). The use of the contrast variation

( $\text{D}_2\text{O}-\text{H}_2\text{O}$ ) in SANS measurements reveals the differences in the DNA and protein arrangements inside the chromatin substance. It is the DNA that serves as a framework that constitutes the bifractal behavior showing the mass fractal properties with  $D = 2.22$  at a smaller scale and the logarithmic fractal behavior with  $D \approx 3$  at a larger scale. The protein spatial organization shows the mass fractal properties with  $D \approx 2.34$  throughout the whole nucleus. The borderline between two fractal levels can be significantly shifted toward smaller scales by centrifugation of the nuclei disposed on the dry substrate, since nuclei suffer from mechanical stress transforming them to a disklike shape. The height of this disk measured by atomic force microscopy (AFM) coincides closely with the fractal borderline, thus characterizing two types of the chromatin with the soft (at larger scale) and rigid



Small-angle neutron scattering on non-deformed (open squares) and deformed (open triangles) nuclei of chicken erythrocytes in heavy water  $\text{D}_2\text{O}$  (chromatin), in 60%  $\text{D}_2\text{O}$  (proteins only), and in 40%  $\text{D}_2\text{O}$  (DNA only) in 60%  $\text{D}_2\text{O}$  (proteins only)



(at smaller scale) properties. The combined SANS and AFM measurements demonstrate the stress induced switch of the DNA fractal properties from the rigid, but loosely packed, mass fractal to the soft, but densely packed, logarithmic fractal.

In this work we have shown that spatial organization of chromatin in the nucleus of chicken erythrocytes is described by the bifractal model that is originated from the bifractal nature of the DNA large-scale arrangement. The DNA is arranged as a low density mass fractal ( $D = 2.2$ ) for the smaller scale and it is able to condense into the logarithmic fractal at the larger scale. The logarithmic fractal

implies a hierarchical branched structure similar to a three-dimensional spherically symmetric tree of folds, which ensures the maximum availability of any section from the outside and the most compact, dense structure. Apparently, such a structure is characteristic for living systems.

We have shown that with the mechanical stress we are able to switch the DNA inside nuclei from the mass fractal state to the logarithmic fractal state. This experiment shows the relation between mechanical and structural properties of the DNA at large scale and paves a way for manipulations of these properties.

## 1D ceric hydrogen phosphate aerogels: noncarbonaceous ultraflyweight monolithic aerogels

G.P. Kopitsa – Neutron Research Division of NRC “Kurchatov Institute” – PNPI,  
I.V. Grebenshchikov Institute of Silicate Chemistry of the RAS,  
T.O. Kozlova, A.E. Baranchikov, D.A. Kozlov, A.V. Gavrikov, A.D. Yapryntsev, K.B. Ustinovich,  
V.K. Ivanov – N.S. Kurnakov Institute of General and Inorganic Chemistry of the RAS,  
T.O. Kozlova, D.A. Kozlov – Lomonosov Moscow State University,  
A. Chennevière – Paris–Saclay University, Leon Brillouin Laboratory

Aerogels are unique materials possessing a specific spatial structure, which gives rise to a high specific surface area, ultrahigh porosity, adjustable density ranges, low thermal conductivity and permittivity, low speed of sound propagation, and so forth. To date, many aerogel materials have been obtained, with the greatest attention in recent years focused on ultralight carbonaceous aerogels (density 1–10 mg/cm<sup>3</sup>), primarily graphene or graphene oxide-based aerogels, as well as ultralight renewable and biodegradable aerogel materials obtained from plant cell biomass.

Inorganic aerogels usually possess a higher density than carbonaceous aerogels. Typical examples are silica aerogels and aerogels based on other metal oxides (Al<sub>2</sub>O<sub>3</sub>, SnO<sub>2</sub>, TiO<sub>2</sub>, etc.). In most cases, the structure of inorganic aerogels obtained using template-free approaches (e. g., using a conventional sol-gel method) represents a three-dimensional open network assembled using metal oxide NP<sub>s</sub>.

In this study, we have further analyzed the conditions for the formation of ultralight monolithic ceric hydrogen phosphate (CeP) lyogels due to the aggregation of flexible inorganic fibers into a strong network using a conventional one-pot,

template-free method sol-gel process without the use of any organic gelators. Optimal conditions were established for obtaining monolithic CeP lyogels, depending on the type of the inorganic gelator and the ratio “CeP solution: gelator solution”. We have demonstrated that the CeP framework is capable of retaining a huge amount of liquid (in the wet gels, up to 20 000 water molecules per cerium atom) and serves as a perfect starting material for the production of ultralight aerogels. Supercritical drying of lyogels synthesized using threemolecular (3M) aqueous solutions of HNO<sub>3</sub> and H<sub>3</sub>PO<sub>4</sub> results in the formation of monolithic cerium-containing phosphoric aerogels. The fibrous 1D structure of the obtained aerogels was confirmed by a set of analytical methods, which also revealed that the total pore volume in the final product increased several times with an increase in the ratio of “CeP solution: gelator solution”. It was found that using 3M orthophosphoric acid as the gelator with a ratio of CeP solution: 3M H<sub>3</sub>PO<sub>4</sub> solution = 1 : 50 at CeP concentration = 0.1 M makes it possible to obtain a purely inorganic CeP aerogel with a density as low as 1 mg/cm<sup>3</sup>.



# Research Based on the Use of Protons and Ions. Neutrino Physics

- 52 Branching fraction measurement of the decay  $\Xi_c^0 \rightarrow \pi^- \Lambda_c^+$
- 53 A precision measurement of the Higgs boson mass in the diphoton decay channel at CMS experiments
- 54 First observation of production of three electroweak bosons at  $\sqrt{s} = 13$  TeV by CMS experiments
- 55 Search for new heavy neutral Higgs boson decaying to four lepton in the ATLAS experiment
- 56 Observation of four-top-quark production in the ATLAS experiment
- 57 Femtoscopy in proton-proton interactions at the Large Hadron Collider: a new method to study the interaction potentials of unstable baryons
- 59 First observation of spin-orbit effects in quark-gluon plasma at the Large Hadron Collider
- 60 Coherent photoproduction of  $\rho^0$  mesons in ultraperipheral collisions of nuclei at the Large Hadron Collider
- 61 The effect of Glauber-Gribov nuclear shadowing in incoherent photoproduction of  $\rho^0$  mesons in ultraperipheral collisions of nuclei at the Large Hadron Collider
- 62 Observation of structure in polarization of scattered protons in inclusive  $(p, p')$  reaction with  ${}^9\text{Be}$  nucleus at 1 GeV
- 63 Direct observation of the long-lived highly excited atomic metastability
- 64 Hyperfine anomaly and magnetic moments of gold isotopes
- 65 Nuclear-matter distributions in the neutron-rich carbon isotopes  ${}^{14-17}\text{C}$  from intermediate-energy proton elastic scattering in inverse kinematics
- 66 Detection of solar CNO-neutrino in the Borexino experiment
- 67 Emission of high-energy protons and photons and production of subthreshold pions in heavy-ion collisions in a hydrodynamic approach with a nonequilibrium equation of state

## Branching fraction measurement of the decay $\Xi_c^0 \rightarrow \pi^- \Lambda_c^+$

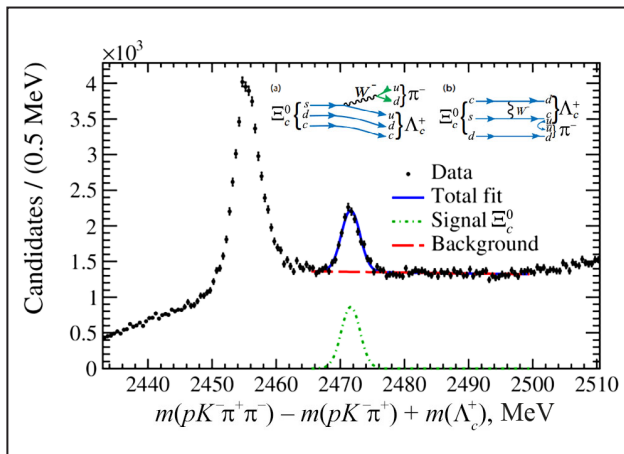
G.D. Alkhazov, A.V. Andreianov, N.F. Bondar, A.A. Vorobyev, N.I. Voropaev, A.A. Dzyuba, K.A. Ivshin, D.S. Ilin, A.G. Inglessi, S.N. Kotriakhova, P.V. Kravchenko, O.E. Maev, D.A. Maisuzenko, N.R. Sagidova, A.N. Solovjev, I.N. Solovyev, A.D. Chubykin, V.V. Chulikov  
High Energy Physics Division of NRC “Kurchatov Institute” – PNPI,  
LHCb Collaboration

Weak decays of the ground states of  $\Xi_c$  baryons usually go via channels, which do not contain charm quarks in their final states. However, a heavy quark baryons decay, which conserve charm quantum number is possible. An example is  $\Xi_c^0 \rightarrow \pi^- \Lambda_c^+$ . Such transition can be described by s quark decay or by weak scattering process. Corresponding quark diagrams are presented in Figure. For the  $\Xi_b^-$  baryons a decay of similar type with a conservation of beauty quantum number is also possible. However, due to the structure of weak interaction at the quark sector of the Standard Model (absence of the flavor changing neutral currents at the tree level of theory) only s quark decay amplitude plays role for the  $\Xi_b^{--} \rightarrow \pi^- \Lambda_b^0$  decay. Comparison of branching fractions for the  $\Xi_c^0 \rightarrow \pi^- \Lambda_c^+$  and  $\Xi_b^{--} \rightarrow \pi^- \Lambda_b^0$  decays will help to establish a role of the exchange diagram.

In 2020 LHCb Collaboration has published an analysis devoted to the measurements of the  $\Xi_c^0 \rightarrow \pi^- \Lambda_c^+$  decay branching fraction. This decay has

been observed for the first time in a Large Hadron Collider (LHC) data by an analysis group of the NRC “Kurchatov Institute” – PNPI. The data from the first run of LHC collected at the center-of-mass energies of 7 and 8 TeV for colliding protons were used. The branching fraction measurement is done at 13 TeV using the Run 2 data. An event selection procedure using multivariate machine learning techniques allows obtaining  $6320 \pm 230$  candidates for this decay (see Fig.). Decays of  $\Lambda_c^+$  and  $\Xi_c^+$  baryons with known absolute branching fractions were used as normalization channels. In addition, an assumption about symmetries of heavy quark baryon production processes is used.

The first measurement of the branching fraction of the suppressed  $\Xi_c^0 \rightarrow \pi^- \Lambda_c^+$  decay has been performed, giving  $B = (0.55 \pm 0.02 \text{ (stat.)} \pm \pm 0.18 \text{ (syst.)}) \cdot 10^{-2}$ . This result can be theoretically explained assuming constructive interference between s quark decay and weak scattering amplitudes.



Reconstructed  $\pi^- \Lambda_c^+$ -mass distribution for selected candidates. Lines demonstrate a spectrum description in the region, which corresponds to the  $\Xi_c^0 \rightarrow \pi^- \Lambda_c^+$  decay. The Figure also contains quark diagram describing s quark decay (a); weak scattering amplitudes (b)

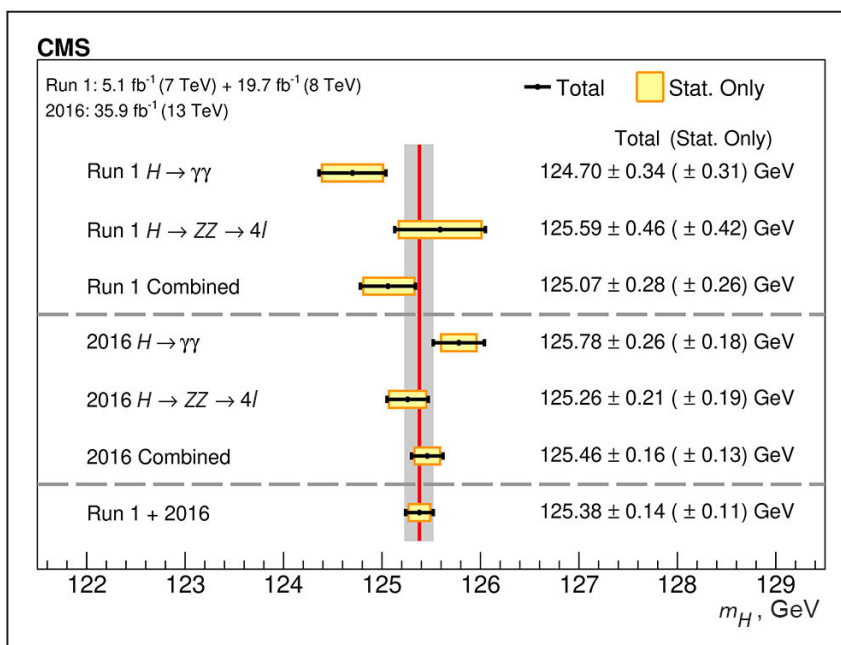
## A precision measurement of the Higgs boson mass in the diphoton decay channel at CMS experiments

A.A. Vorobyev, V.L. Golovtsov, Yu.M. Ivanov, V.T. Kim, E.V. Kuznetsova, P.M. Levchenko, V.A. Murzin, V.A. Oreshkin, I.B. Smirnov, D.E. Sosnov, V.V. Sulimov, L.V. Uvarov, L.A. Chtchipounov  
 High Energy Physics Division of NRC “Kurchatov Institute” – PNPI,  
 CMS Collaboration

After the discovery of Higgs boson of Standard Model by ATLAS and CMS experiments at Large Hadron Collider in 2012, one of the most important goals for further research is to study its properties. The dataset 2016 with  $35.9 \text{ fb}^{-1}$  of data collected by CMS experiment has been analyzed for Higgs boson for decay channel  $H \rightarrow \gamma\gamma$ . New analysis techniques have been introduced at CMS to improve the precision of the measurement along with a new method to estimate the systematic uncertainty of ECAL. The measured value of the Higgs boson mass in the diphoton decay channel is found to be  $m_H = 125.78 \pm 0.26 \text{ GeV}$ . This measurement has been combined with a recent measurement by CMS of the same quantity in the  $H \rightarrow ZZ \rightarrow 4l$

decay channel to obtain a value of  $m_H = 125.46 \pm 0.16 \text{ GeV}$ . Furthermore, when the Run 2 result with the 2016 data set is combined with the same measurement performed in Run 1 at 7 and 8 TeV the value of the Higgs boson mass is found to be  $m_H = 125.38 \pm 0.14 \text{ GeV}$ . This is currently the most precise measurement of the mass of the Higgs boson.

NRC “Kurchatov Institute” – PNPI has made the large contribution to the development and construction of endcap muon detector of the CMS experiment which plays an important role in the Higgs boson properties study. NRC “Kurchatov Institute” – PNPI team is actively participating in CMS physics analysis.



A summary of the measured Higgs boson mass in the  $H \rightarrow \gamma\gamma$  and the  $H \rightarrow ZZ \rightarrow 4l$  decay channels, and for combinations of the two is presented here

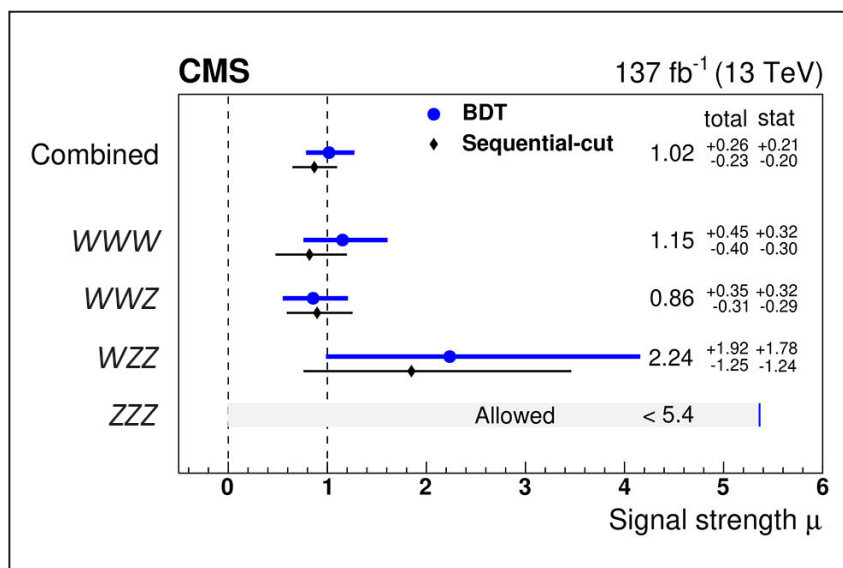
## First observation of production of three electroweak bosons at $\sqrt{s} = 13$ TeV by CMS experiments

A.A. Vorobyev, G.E. Gavrilov, V.L. Golovtsov, Yu.M. Ivanov, V.T. Kim, E.V. Kuznetsova, P.M. Levchenko, V.A. Murzin, V.A. Oreshkin, I.B. Smirnov, D.E. Sosnov, V.V. Sulimov, L.V. Uvarov  
High Energy Physics Division of NRC “Kurchatov Institute” – PNPI,  
CMS Collaboration

The first observation of the combined production of three massive gauge bosons ( $VWV$  with  $V = W, Z$ ) in  $pp$  collisions at 13 TeV was reported. The production process is interesting because the predictions of the Standard Model (SM) for these processes involve the non-Abelian character of the theory. It is sensitive to physics beyond the SM. The analysis is based on CMS data with an integrated luminosity of  $137 \text{ fb}^{-1}$ . The observed (expected) significance of the combined  $VWV$  production signal is 5.7 (5.9) standard deviations. The searches for individual  $WWW$ ,  $WWZ$ ,  $WZZ$ , and  $ZZZ$  production are performed in the final states with three, four, five and six leptons ( $e, \mu$ ) or with two leptons of the same sign and one or two jets, and the corresponding

measured cross section relative to the SM prediction is  $1.02 \pm 0.23$  (0.26). The significances of the individual  $WWW$  and  $WWZ$  production are 3.3 and 3.4 standard deviations, respectively. Measured production cross sections for the individual three-boson processes are also in a good agreement with the SM predictions (Fig.).

NRC “Kurchatov Institute” – PNPI has made a large contribution to the development and construction of endcap muon detector of the CMS experiment which plays an important role in the study of electroweak boson properties. NRC “Kurchatov Institute” – PNPI team is actively participating in CMS physics analysis.



Best fit values of the signal strength for boosted tree decision (BDT)-based and the sequential-cut analyses. For  $ZZZ$  production, a 95% CL upper limit is shown

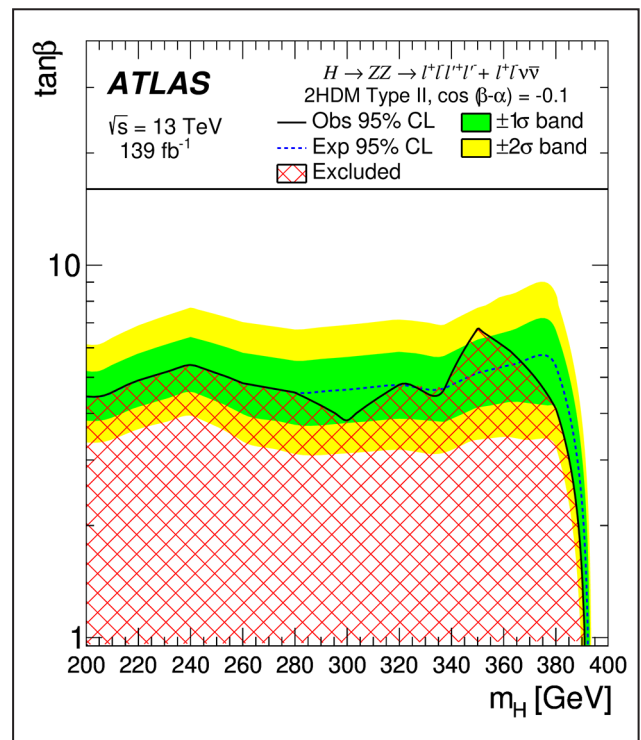
## Search for new heavy neutral Higgs boson decaying to four lepton in the ATLAS experiment

O.L. Fedin, S.G. Barsov, A.E. Ezhilov, M.P. Levchenko, V.P. Maleev, Yu.G. Naryshkin, D. Pudzha, V.M. Solovyev V.A. Schegelsky  
High Energy Physics Division of NRC "Kurchatov Institute" – PNPI,  
ATLAS Collaboration

Searches for new physics beyond the Standard Model (SM) is one of the main goals of the ATLAS experiment at the Large Hadron Collider (LHC). Some of SM extensions (BSM models) such as two Higgs doubled model (2HDM) predict new resonances in the extended Higgs sector. A search of one of these resonances – new neutral heavy Higgs boson in the decay into a pair of Z bosons with  $4l$  or  $2l2\nu$  in the final states (where  $l$  stands for either an electron or a muon) was performed in ATLAS. The invariant mass of four leptons for the  $4l$  final state and transverse mass for the  $2l2\nu$  final state was used as a discriminating variable. Two production mechanisms of new resonance were studied: gluon-gluon fusion (ggF) and vector-boson fusion (VBF). Two different hypotheses for the heavy scalar width were used: narrow width approximation (NWA) and the large width approximation (LWA). The interference between the heavy scalar and the SM Higgs boson as well as between the heavy scalar and the  $gg \rightarrow ZZ$  background was taken into account.

The search uses proton-proton collision data at a centre-of-mass energy of  $\sqrt{s} = 13$  TeV collected during LHC Run 2 (2015–2018) with the integrated luminosity of  $139 \text{ fb}^{-1}$ . No significant excess is observed with respect to the predicted SM background. In the NWA hypothesis the upper limits for cross section at 95% CL were found to be in the range from 200 fb at  $m_H = 240$  GeV to 2.6 fb at  $m_H = 2$  TeV for the ggF production mode and from 87 fb at  $m_H = 250$  GeV to 1.9 fb

at  $m_H = 1.8$  TeV for the VBF production mechanism. The results were interpreted with 2HDM scenario and the limits on the model's parameters were derived. Figure shows exclusion limits as a function of the heavy Higgs boson mass  $m_H$  and the parameter  $\tan\beta$  – the ratio of the two vacuum expectation values.



The exclusion contour in the 2HDM Type-II models shown as a function of the heavy scalar mass  $m_H$  and the parameter  $\tan\beta$  at 95% CL, obtained in the ATLAS experiment



## Observation of four-top-quark production in the ATLAS experiment

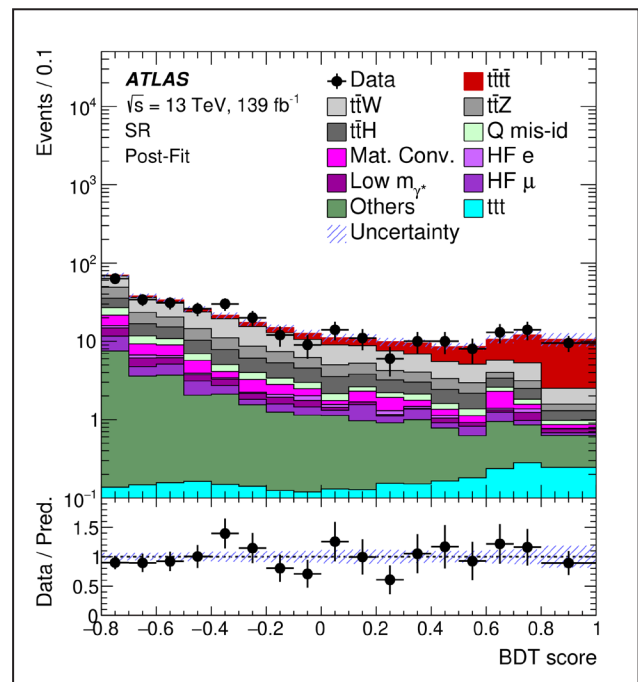
S.G. Barsov, A.E. Ezhilov, M.P. Levchenko, V.P. Maleev, Yu.G. Naryshkin, D. Pudzha, V.M. Solovyev, O.L. Fedin, V.A. Schegelsky  
High Energy Physics Division of NRC “Kurchatov Institute” – PNPI,  
ATLAS Collaboration

Top quark ( $t$ ) is the heaviest known elementary particle of the Standard Model (SM). Hence, it has a large coupling to the SM Higgs boson and is predicted to have large couplings to hypothetical new particles in many models beyond the SM. In that respect, rare processes involving the top quark are particularly relevant to study. One of such processes is the production of four top quarks ( $t\bar{t}t\bar{t}$ ) which is predicted by the SM but has not been observed yet.

In the SM, the top quark is expected to decay into a  $W$  boson and a  $b$  quark with a branching ratio of approximately 100%. Thus, in events with  $t\bar{t}t\bar{t}$  production the decay  $t\bar{t}t\bar{t} \rightarrow W^+W^-W^+W^-b\bar{b}b\bar{b}$  will be observed, which will then produce different final states depending on the hadronic or leptonic decay mode of the  $W$  bosons.

A search for four-top-quark production using an integrated luminosity of  $139 \text{ fb}^{-1}$  of proton-proton collision data at a centre-of-mass energy of 13 TeV was performed in the ATLAS detector at the Large Hadron Collider. Events with exactly two leptons with the same electric charge or events with at least three leptons were considered in the search. Only electrons and muons were considered as leptons. To separate signal events from background events a multivariate discriminant (BDT score) was used, which was obtained with boosted decision tree (BDT) technique. The  $t\bar{t}t\bar{t}$  production cross section was determined via a fit to the BDT score distribution (Fig.) in data. The observed (expected)

signal significance is found to be 4.3 (2.4) standard deviations, providing evidence for this process assuming the SM four-top-quark production properties. The four-top-quark production cross section is measured to be  $24^{+7}_{-6} \text{ fb}$ , which is consistent within 1.7 standard deviations with the SM expectation of  $12.0 \pm 2.4 \text{ fb}$ .



Comparison between data and prediction after the fit (“Post-Fit”) for the distribution of the BDT score. The band includes the total uncertainty of the post-fit computation. The ratio of the data to the total post-fit computation is shown in the lower panel

## Femtoscopy in proton-proton interactions at the Large Hadron Collider: a new method to study the interaction potentials of unstable baryons

M.B. Zhalov, V.V. Ivanov, E.L. Kryshen, M.V. Malaev, V.N. Nikulin, A.Yu. Ryabov, V.G. Ryabov, Yu.G. Ryabov, A.V. Khanzadeev, V.M. Samsonov  
High Energy Physics Division of NRC “Kurchatov Institute” – PNPI,  
ALICE Collaboration

In 2020 the ALICE Collaboration published in “Nature” the results of studies of low-energy interactions of  $\Xi^-(dss)$  and  $\Omega^-(sss)$  hyperons with protons. The knowledge of baryon-baryon potentials is one of the key problems of nuclear physics, physics of neutron stars, and a more global challenge to construct the fundamental theory of strong interactions, quantum chromodynamics (QCD), in the non-perturbative region. In terms of quarks and gluons, the fundamental degrees of freedom of QCD, significant progress in this area has been achieved in the determination of baryon-baryon potentials on the lattice with their subsequent verification using a comparison to experimental data.

The traditional method of experimental studies of the interaction potential of low-energy protons and neutrons using their elastic scattering is not applicable in the case of unstable baryons because of their short lifetime. In the ALICE experiment, a new approach to this problem based on the method of femtoscopy has been proposed. Formulated by analogy with the Hanbury Brown and Twiss (HBT) effect of interferometry in astrophysics, in high-energy nuclear physics this method is actively used to determine the size of proton-proton and nucleus-nucleus interactions in events with a high multiplicity of produced particles.

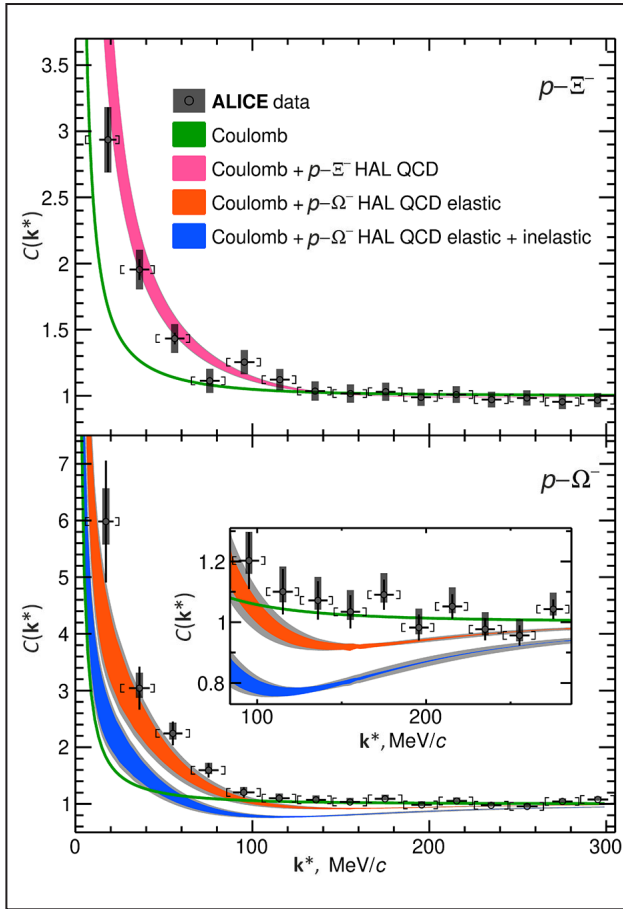
The method is based on a comparison of the experimental correlation function  $C^{\text{exp}}(\mathbf{k}^*)$  of pairs of particles with the relative momentum  $|\mathbf{k}^*|$  with the theoretically modelled correlation function  $C^{\text{theor}}(\mathbf{k}^*) = \int S(\mathbf{r}) |\Psi(\mathbf{k}^*, \mathbf{r})|^2 d\mathbf{r}$ . From the comparison one determines the source function of  $S(\mathbf{r})$ , which describes the spatial distribution of the particle emission region in a parametric form provided that the wave function  $\Psi(\mathbf{k}^*, \mathbf{r})$  of the pair of correlated particles is known. In ultrarelativistic proton-proton

collisions with a high multiplicity of produced particles, correlations between protons and hyperons at relatively low energies originate out of their final-state interactions.

In the ALICE experiment, using the large volume of data on proton-proton collisions at  $\sqrt{s} = 13$  TeV, events with  $pp$ ,  $p\Xi^-$  and  $p\Omega^-$  pairs with the relative momenta  $|\mathbf{k}^*|$  in the  $20 < |\mathbf{k}^*| < 300$  MeV/c interval were selected and the experimental correlation functions of  $C_{pp}^{\text{exp}}(\mathbf{k}^*)$ ,  $C_{p\Xi}^{\text{exp}}(\mathbf{k}^*)$  and  $C_{p\Omega}^{\text{exp}}(\mathbf{k}^*)$  were determined. Knowledge of the potential of the proton-proton interaction allows one to find  $\Psi_{pp}(\mathbf{k}^*, \mathbf{r})$  by solving the Schrödinger equation and to extract the source function of  $S_{pp}(\mathbf{r})$  from the femtoscopy analysis of  $C^{\text{exp}}(\mathbf{k}^*)$ .

Figure shows a comparison of measured  $C_{p\Xi}^{\text{exp}}(\mathbf{k}^*)$  and  $C_{p\Omega}^{\text{exp}}(\mathbf{k}^*)$  with the theoretical correlation functions for  $p\Xi^-$  and  $p\Omega^-$  pairs, which were obtained using this  $S_{pp}(\mathbf{r})$  source function and the wave functions of correlated  $p\Xi^-$  and  $p\Omega^-$  pairs obtained by solving the Schrödinger equation with the Coulomb interaction and the hyperon-proton potentials from the HAL QCD (Hadron to Atomic nuclei from Lattice QCD) lattice calculations. These calculations predict strong attraction for the  $p\Omega^-$  interaction, which may lead to formation of a bound state with the binding energy of 2.5 MeV. The similarly strong attraction is predicted for  $p\Xi^-$  in the  $0.5 < r < 2$  fm region; however, for  $r < 0.2$  fm, the attraction is charged to repulsion. This behavior of the potentials is reflected in the behavior of the calculated correlation functions presented in Figure. *The green line* shows the correlations due to Coulomb attraction only, while *the magenta and orange lines* also include the strong interaction.

Besides the  $p\Xi^-$  and  $p\Omega^-$  potential interaction, inelastic channels ( $p\Xi^- \rightarrow \Lambda$ ,  $p\Omega^- \rightarrow \Xi\Lambda$ , ...) were



Comparison of the correlation function measured by ALICE with that theoretically modelled using the HA HAL QCD lattice calculations of the hyperon-proton potentials

also considered. Their effect has turned out to be negligible for  $p\Xi^-$ , while leading to deviations from the data for  $p\Omega^-$  (compare *the blue and orange lines*). This behavior of the experimental correlation functions confirms the attraction in the strong interaction of  $\Xi^-$  and  $\Omega^-$  hyperons with protons predicted by HAL QCD, but does not agree with the existence of a bound state in the  $p\Omega^-$  system, which is realized as a local minimum of  $C_{p\Omega}^{\text{theor}}(\mathbf{k}^*)$  at  $100 < |\mathbf{k}^*| < 300$  MeV/c. Such

a minimum is absent in the measured correlation function  $C_{p\Omega}^{\text{exp}}(\mathbf{k}^*)$  in the entire momentum range  $|\mathbf{k}^*| < 300$  MeV/c.

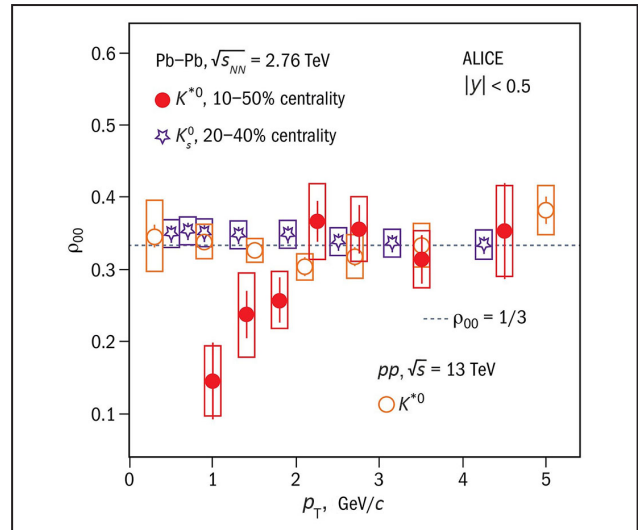
These results demonstrate the potential of the femtoscopy method to study strong baryon-baryon interactions at low energies and to reconstruct baryon-baryon potentials down to distances of the order of  $10^{-14}$  cm using data on ultrarelativistic proton-proton collisions at the Large Hadron Collider.

## First observation of spin-orbit effects in quark-gluon plasma at the Large Hadron Collider

M.B. Zhalov, V.V. Ivanov, E.L. Kryshen, M.V. Malaev, V.N. Nikulin, V.G. Ryabov, Yu.G. Ryabov, V.M. Samsonov, A.V. Khanzadeev  
High Energy Physics Division of NRC "Kurchatov Institute" – PNPI, ALICE Collaboration

The main goal of the ALICE experiment is to study properties of the strongly interacting quark-gluon plasma (QGP) formed in the interaction region of colliding ultrarelativistic nuclei. In semi-central collisions, the non-uniform distribution of nucleons in the nuclei and the non-zero impact parameter may result in the orbital angular momentum  $L$  of quarks in the quark-gluon lump formed in the interaction region, which is perpendicular to the reaction plane. The spin-orbit interaction of quarks in the QGP may lead to their polarization along  $L$  and, in the transition of the QGP into the hadron gas, to polarization of hadrons in the processes of recombination or fragmentation of the polarized quarks.

The ALICE Collaboration has analyzed the data on the yield of short-lived  $K^*(892)^0$  vector mesons in hadronization of the QGP to measure the orientation of the spin of  $K^*(892)^0$  with respect to the reaction plane in semi-central Pb-Pb collisions at  $\sqrt{s_{NN}} = 2.76$  TeV and pp collisions at  $\sqrt{s_{NN}} = 13$  TeV. For an unpolarized vector meson, the probabilities of the spin projections of 1, 0, and  $-1$  are the same and equal to  $1/3$ , and the angular distribution of  $K^*(892)^0$  decay products should be isotropic with respect to the quantization axis. The angular distribution asymmetry allows one to measure the value of the  $\rho_{00}$  spin density matrix element, which determines the probability for  $K^*(892)^0$  to be in the state with the spin-zero projection. The deviation of  $\rho_{00}$  from  $1/3$  indicates polarization of  $K^*(892)^0$ . The results of the analysis are presented in Figure. In Pb-Pb collisions, the magnitude of  $\rho_{00}$  is noticeably smaller than  $1/3$  for small transverse momenta  $p_T \sim 1$  GeV/c. In pp scattering, where the



Dependence of measured  $\rho_{00}$  on the vector meson transverse momentum

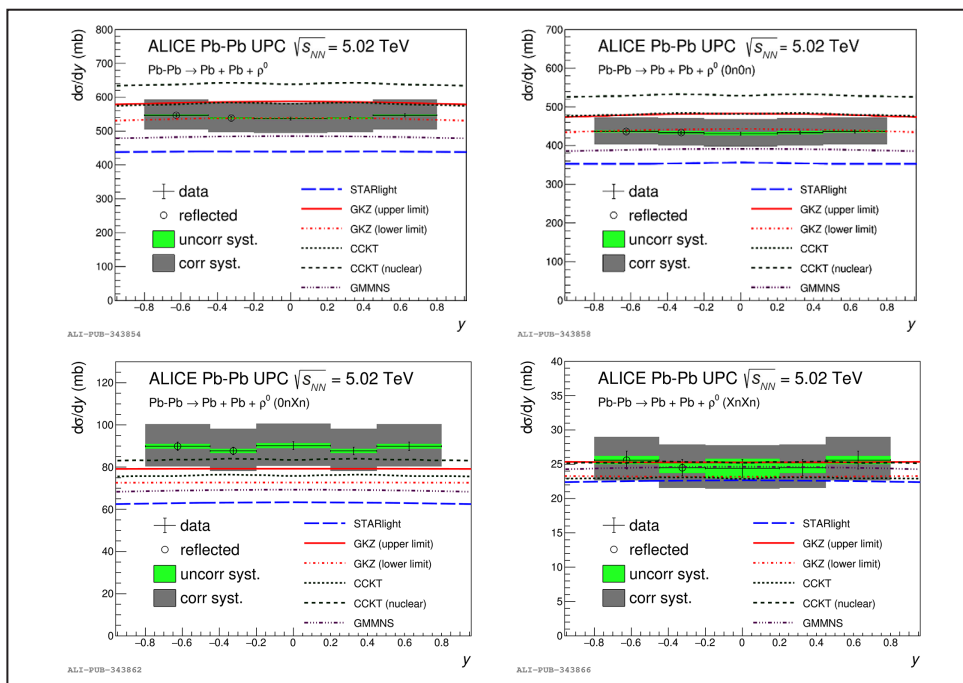
probability to have a large angular momentum is small, the measured values of  $\rho_{00}$  agree with  $1/3$  in the entire range of the transverse momentum. The polarization of  $\Lambda$  hyperons produced in Pb-Pb interactions, which was measured earlier in similar conditions, has turned out to be close to zero within  $1\sigma$ . Taking this into account, the effect of vector meson polarization observed at a  $3\sigma$  level can be considered not only as evidence of noticeable spin-orbit interactions in the evolution of the QGP formed in semi-central heavy-ion interactions at the Large Hadron Collider energies, but also as an indication of the possibility of different hadronization mechanisms in formation of vector mesons and baryons in the process of the QGP transition into the hadron phase.

## Coherent photoproduction of $\rho^0$ mesons in ultraperipheral collisions of nuclei at the Large Hadron Collider

V.A. Guzey, M.B. Zhalov, V.V. Ivanov, E.L. Kryshen, M.V. Malaev, V.N. Nikulin,  
V.G. Ryabov, Yu.G. Ryabov, V.M. Samsonov, A.V. Khanzadeev  
High Energy Physics Division of NRC “Kurchatov Institute” – PNPI,  
ALICE Collaboration

The cross section of coherent photoproduction of  $\rho^0$  mesons in ultraperipheral collisions of lead nuclei at  $\sqrt{s_{NN}} = 5.02$  TeV has been measured by the ALICE Collaboration in the  $y < |0.8|$  rapidity interval. Since the large value of the electric charge of the nucleus ( $Z = 82$ ) largely compensates the smallness of the  $\alpha_{em}$  fine-structure constant, the process of coherent photoproduction can be accompanied by excitation of the nuclei due to an additional exchange of one or several photons of relatively low energies with the subsequent decay via neutron emission. It allows one to measure the photoproduction cross section in the channels with a different number of neutrons: OnOn denotes the case without additional photon exchanges; OnXn refers to the excitation of only one of the colliding nuclei

decaying with the emission of one or several photons; the XnXn channel corresponds to the situation, when both colliding nuclei become additionally excited. The results of the measurement are presented in Figure along with theoretical predictions for these cross sections obtained in different models for the description of coherent photoproduction of light vector mesons on nuclei. A comparison of the theoretical models with the data shows that the approach developed at NRC “Kurchatov Institute” – PNPI (*the red lines* labeled Guzey–Kryshen–Zhalov), which is based on the use of the Gribov–Glauber model for photon-nucleus scattering and a modified model of vector meson dominance for the hadron structure of the photon, describes the experimental data with a reasonable accuracy.



Comparison of the ALICE measurements of the coherent  $\rho^0$  mesons photoproduction in ultraperipheral collisions of lead nuclei at  $\sqrt{s_{NN}} = 5.02$  TeV with theoretical predictions

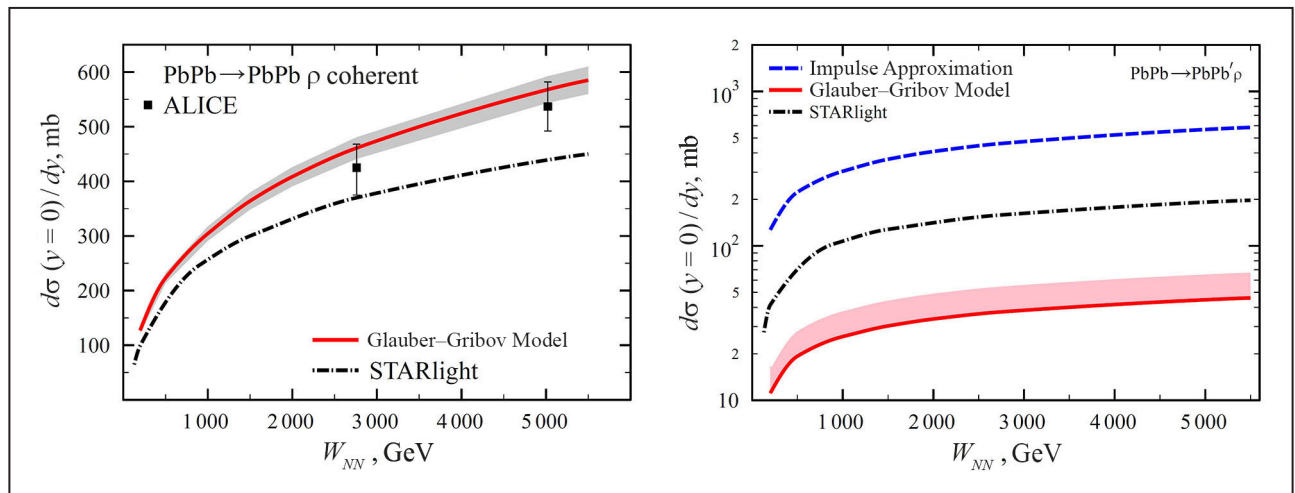
# The effect of Glauber–Gribov nuclear shadowing in incoherent photoproduction of $\rho^0$ mesons in ultraperipheral collisions of nuclei at the Large Hadron Collider

V.A. Guzey, M.B. Zhalov, E.L. Kryshen

High Energy Physics Division of NRC “Kurchatov Institute” – PNPI

Recently our group at NRC “Kurchatov Institute” – PNPI developed an approach based on the Glauber–Gribov model for photon-nucleus scattering and a modified model of vector meson dominance for the hadronic structure of the photon, which describes with reasonable accuracy the ALICE data on coherent photoproduction of  $\rho^0$  mesons in ultraperipheral collisions (UPCs) of nuclei at the Large Hadron Collider (LHC), see *the right panel* of Figure. This makes it reasonable to use an analogous approach for predictions of the cross section of incoherent photoproduction of  $\rho^0$  mesons in Pb-Pb UPCs in the LHC kinematics. *The left panel* of Figure demonstrates that the effect of nuclear shadowing in this process is significant and leads

to a factor of 10 suppression of the  $\sigma_{\gamma A \rightarrow \rho A'}$  cross section of incoherent photoproduction of  $\rho^0$  mesons on nuclei compared to its estimate in the impulse approximation giving  $\sigma_{\gamma A \rightarrow \rho A'} = A \sigma_{\gamma N \rightarrow \rho N}$ . In particular, while approximately 70% of the suppression effect come from the elastic Glauber rescattering, the remaining 30% of the effect originate from the Gribov inelastic shadowing. A comparison of the cross sections predicted in our study with those calculated within the STARlight framework, which is commonly used in the data analysis, shows that the approximations used in STARlight overestimate the cross section of incoherent photoproduction of  $\rho$  on nuclei by a factor of 4 compared to the Glauber model calculations.



A comparison of the calculation results of the cross sections of  $\rho^0$  meson photoproduction in Pb-Pb ultraperipheral collisions in the Glauber–Gribov model with those of STARlight, the impulse approximation, and the ALICE data

## Observation of structure in polarization of scattered protons in inclusive $(p, p')$ reaction with ${}^9\text{Be}$ nucleus at 1 GeV

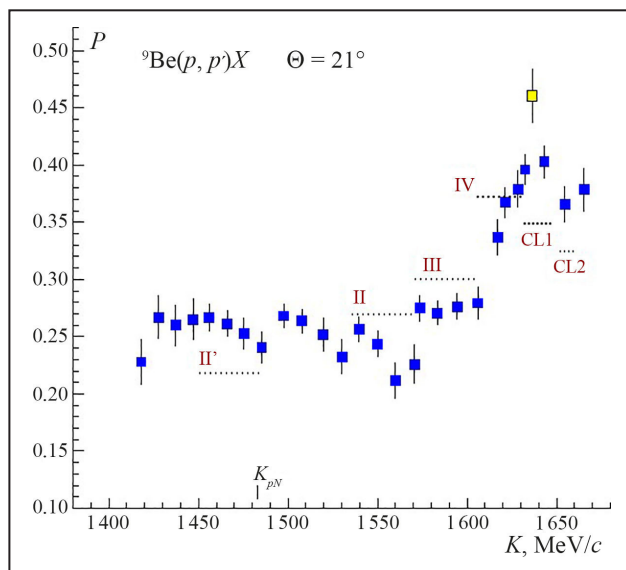
G.M. Amalsky, V.A. Andreev, S.G. Barsov, G.E. Gavrilov, A.A. Zhdanov, A.A. Izotov, D.S. Ilyin, A.Yu. Kisselev, N.G. Kozlenko, P.V. Kravchenko, D.A. Maysuzenko, O.V. Miklukho, V.I. Murzin, D.V. Novinskiy, A.V. Shvedchikov  
High Energy Physics Division of NRC “Kurchatov Institute” – PNPI

The polarization ( $P$ ) in the inclusive reaction as a function of the scattered proton momentum ( $K$ ) was measured on the proton beam of the synchrocyclotron of NRC “Kurchatov Institute” – PNPI. The measurements were carried out using a precision magnetic spectrometer equipped with a polarimeter on proportional chambers.

Description of the structure in polarization observed at a scattering angle  $\Theta = 21^\circ$  (Fig.): momentum intervals II, III, and IV, indicated by the dotted line segments, correspond predominantly to quasi-elastic scattering  ${}^9\text{Be}(p, p'NC)X$  on dense two-nucleon, three-nucleon, and four-nucleon correlations (NC) inside the  ${}^9\text{Be}$  nucleus, which are similar to light nuclei  ${}^2\text{H}$ ,  ${}^3\text{He}$  ( ${}^3\text{H}$ ) and  ${}^4\text{He}$ . In the interval II', a significant contribution is made by quasi-elastic scattering by the two-nucleon correlation,

followed by its decay into two nucleons with equal and oppositely directed momenta exceeding the Fermi momentum ( $K_F \sim 250 \text{ MeV}/c$ ). The momentum interval CL1 corresponds to quasi-elastic scattering  ${}^9\text{Be}(p, p'X)Y$  by residual nuclei ( $X$ )  ${}^7\text{Li}$ ,  ${}^6\text{He}$  ( ${}^6\text{Li}$ ), and  ${}^5\text{He}$  in the above reactions. In this interval, a broad peak is observed in the momentum distribution of scattered protons. In interval CL2, a narrower peak in the momentum distribution is observed, which corresponds to quasi-elastic scattering  ${}^9\text{Be}(p, p'{}^8\text{Be})n$  by an eight-nucleon cluster ( ${}^8\text{Be}$ ).

The discovery of this peak confirms the model of the  ${}^9\text{Be}$  nucleus, in which the nucleus consists of a solid core, similar to the  ${}^8\text{Be}$  nucleus, and a neutron ( $n$ ) weakly bound to it. The polarization of secondary protons in the proton elastic scattering off this core has been measured for the first time.



Blue squares are the result of measuring the polarization of secondary protons in the  $(p, p')$  reaction with the  ${}^9\text{Be}$  nucleus. The yellow square corresponds to the measured polarization in the proton elastic scattering by the  ${}^4\text{He}$  nucleus.  $K_{pN}$  is the momentum corresponding to the maximum of the quasi-elastic peak in the scattering of beam protons by nuclear nucleons

## Direct observation of the long-lived highly excited atomic metastability

S.A. Eliseev, Yu.N. Novikov, P.E. Filianin –  
High Energy Physics Division of NRC “Kurchatov Institute” – PNPI,  
Collaboration of Max Planck Institute for Nuclear Physics of the Max Planck Society  
in Heidelberg, Ruprecht Karl University of Heidelberg and Sorbonne University

In the Max Planck Institute for Nuclear Physics in Heidelberg with the PENTATRAP installation in collaboration with NRC “Kurchatov Institute” – PNPI, very high (202 eV) and long-lived ionic state in  $^{187}\text{Re}^{29+}$  has been discovered. This state has been seen in the cyclotron frequencies measurements that directly depend on the ionic masses. Careful theoretical analysis showed that observed energy and lifetime of this state can be explained by the hit of the spin of the external electron in the “spin trap”, which significantly suppresses the level de-excitation (Fig. 1). Observation of the similar long-lived isoelectronic state in  $^{187}\text{Os}^{30+}$  with the energy of  $207 \pm 3$  eV supports the assumption made.

This experiment marks the beginning of a new direction – long-lived high-energy atomic spectrometry. On the one hand, it can be of interest in physics beyond the Standard Model through its component – quantum electrodynamics, which is very sensitive to processes with a very high de-excitation hindrance. On the other hand, the metastability found attracts attention due to its practical application, since the frequency factor of the discharge (the ratio of the transition frequency to its width) exceeds this value by many orders of magnitude for all known frequency standards (Fig. 2, where the frequency factor for different nuclides is shown as a function of the wavelength).

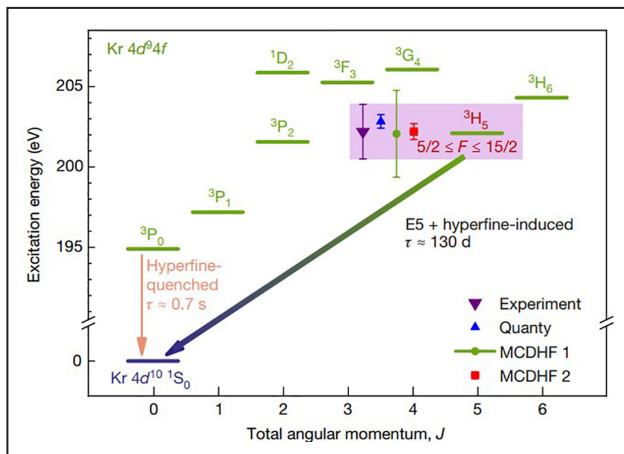


Fig. 1. E5-transition with a high hindrance

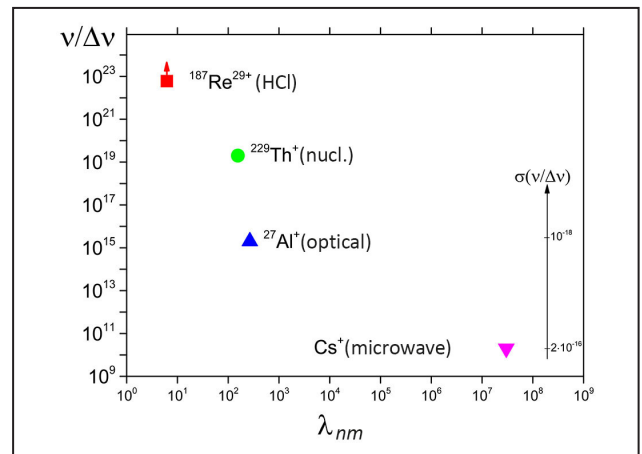


Fig. 2. Comparison of the frequency qualities

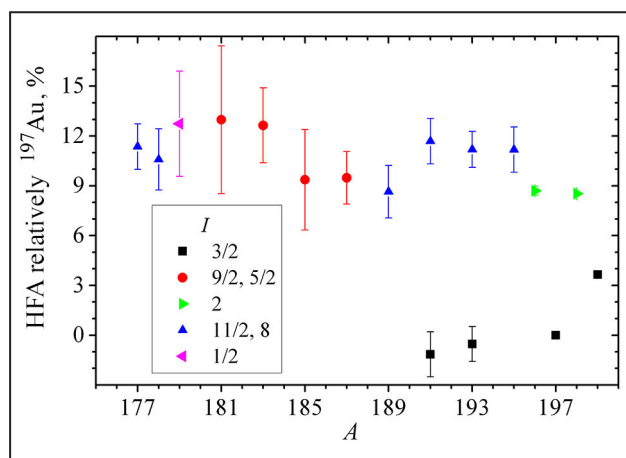


## Hyperfine anomaly and magnetic moments of gold isotopes

A.E. Barzakh, D.V. Fedorov, P.L. Molkanov, M.D. Seliverstov, M.G. Kozlov, Yu.A. Demidov  
High Energy Physics Division, Knowledge Transfer Division of NRC "Kurchatov Institute" – PNPI

Hyperfine anomaly (HFA) – the effect caused by the non-point character of atomic nucleus. As a result, the ratio of hyperfine constants for different isotopes is not equal to the ratio of corresponding magnetic moments. The main contribution to HFA is determined by the magnetization distribution in the nucleus volume. Hence, the HFA investigations allow us to obtain the information of this distribution. In addition, since the nuclear magnetic moment values are extracted from the experimental data of hyperfine constants  $a$ , it is essential to know HFA for the extraction procedure. Unknown values of HFA are the main source of uncertainties of measured nuclear magnetic moments. At last, the lack of reliable HFA calculations becomes the biggest obstacle for the interpretation of experimental results connected with search for the parity non-conservation effects, the electron electric dipole moment and the other fine effects in atomic and molecular spectra.

HFA has been known for a long time, but until now, corresponding experimental data were limited by long-lived and stable isotopes. This restriction hampers the theory progress. In our works the new experimental method for HFA studies has been used for a very long isotopic chain. The method is based on the fact that different atomic states have different sensitivity to the nuclear magnetization distribution. Measurements of hyperfine constants  $a$  for atomic states  $6s\ ^2S_{1/2}$  and  $6p\ ^2P_{1/2}$  in gold give us HFA difference for these states. HFA values relatively to the stable isotope  $^{197}\text{Au}$  (RHFA)



Hyperfine anomaly of gold isotopes

were extracted from these differences by means of atomic calculations (Fig.)

In our experiments isotope shifts and hyperfine splittings for isomer and ground states of  $^{177, 178, 187, 191, 193, 195}\text{Au}^m$ ,  $^{178, 180, 182}\text{Au}^g$  have been measured using the in-source laser resonance-ionization spectroscopy technique. Magnetic dipole moments for the gold nuclides in question have been deduced, taking into account the corresponding relative hyperfine-anomaly values. Data of HFA for a long chain of isotopes with very different properties (spherical, deformed, non-axial, with a strong Coriolis perturbation, etc.) have been obtained for the first time. New data open the possibilities for detailed theoretical analysis of factors, responsible for the nuclear magnetization distribution and for verification of atomic calculations.

1. Barzakh A.E., ..., Demidov Yu.A., ..., Fedorov D.V., ..., Kozlov M.G., ..., Molkanov P.L., ..., Seliverstov M.D. et al. // Phys. Rev. C. 2020. V. 101. Iss. 3. P. 034308.
2. Barzakh A.E., ..., Fedorov D.V., ..., Molkanov P.L., ..., Seliverstov M.D. et al. // Phys. Rev. C. 2020. V. 101. Iss. 6. P. 064321.
3. Harding R.D., ..., Barzakh A.E., ..., Fedorov D.V., ..., Molkanov P.L., ..., Seliverstov M.D. et al. // Phys. Rev. C. 2020. V. 102. Iss. 2. P. 024312.
4. Cubiss J.G., ..., Barzakh A.E., ..., Fedorov D.V., ..., Molkanov P.L., ..., Seliverstov M.D. et al. // Phys. Rev. C. 2020. V. 102. Iss. 4. P. 044332.

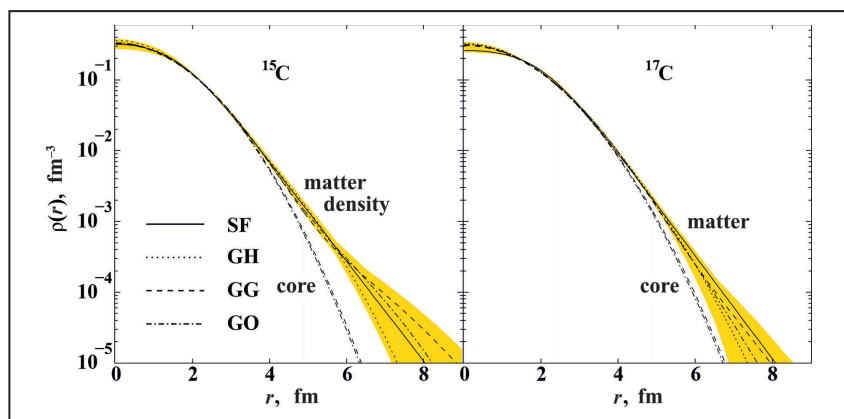
## Nuclear-matter distributions in the neutron-rich carbon isotopes $^{14-17}\text{C}$ from intermediate-energy proton elastic scattering in inverse kinematics

G.D. Alkhazov, A.A. Vorobyev, A.V. Dobrovolsky, A.G. Inglessi, G.A. Korolev, G.E. Petrov, L.O. Sergeev, A.V. Khanzadeev, V.I. Yatsoura  
High Energy Physics Division of NRC “Kurchatov Institute” – PNPI, IKAR Collaboration

In order to study the spatial matter distributions in the neutron-rich exotic nuclei  $^{14-17}\text{C}$ , absolute differential cross sections for elastic  $p^{14-17}\text{C}$  small-angle scattering were measured in inverse kinematics at an energy of 0.7 GeV/nucleon. The experiment was performed at the Helmholtz Center for Heavy Ion Research, Darmstadt. The main part of the experimental set-up was the ionization chamber IKAR, filled with pure hydrogen at a pressure of 10 bar, which served simultaneously as a gas target and a recoil proton detector. The active target IKAR was developed at NRC “Kurchatov institute” – PNPI and was originally used in experiments on small-angle hadron elastic scattering. The recoil protons were registered in IKAR in coincidence with the scattered beam particles. An analysis of the shape of the measured differential cross sections makes it possible to determine the nuclear matter distributions and radii of the nuclear core and halo.

The measured cross sections were analysed using the Glauber multiple scattering theory and applying four parameterizations of phenomenological nuclear density distributions labeled

as SF (symmetrized Fermi), GH (Gaussian–halo), GG (Gaussian–Gaussian) and GO (Gaussian–oscillator). The root-mean-square nuclear matter radii  $R_m = 2,42(5)$  fm,  $R_m = 2,59(5)$  fm,  $R_m = 2,70(6)$  fm, and  $R_m = 2,68(5)$  fm were determined correspondingly for  $^{14}\text{C}$ ,  $^{15}\text{C}$ ,  $^{16}\text{C}$ , and  $^{17}\text{C}$ . The deduced nuclear matter density distributions for  $^{15}\text{C}$  and  $^{17}\text{C}$  are shown in the Figure. The ratio of the determined valence nucleon radius  $R_v$  to the core nucleon radius  $R_c$ ,  $\kappa = R_v/R_c$ , may be used as a gauge for the halo existence in the studied nuclei. Theory typically predicts values of  $\kappa \leq 1.3$  for light non-halo nuclei, while for halo nuclei this value can be  $\kappa \approx 2$ , or even larger. According to the present work, a value of  $\kappa = 1.8$  is obtained for  $^{15}\text{C}$ , which signifies that this nucleus demonstrates a moderate halo formation. The neutron excess in  $^{17}\text{C}$  is larger than in  $^{15}\text{C}$ , and the separation energy  $S_n$  of the valence neutrons in  $^{17}\text{C}$  is rather small,  $S_n = 0.73$  MeV. Therefore, one could expect a neutron halo structure in  $^{17}\text{C}$ . However, a relatively small value of  $\kappa = 1.6$  obtained in our work for  $^{17}\text{C}$  does not support the assumption that  $^{17}\text{C}$  is a nucleus with a neutron halo.



Nuclear matter density distributions in  $^{15}\text{C}$  and  $^{17}\text{C}$  deduced from the measured cross sections using different parameterizations (GG, GO, GH and SF) of the density distributions

## Detection of solar CNO-neutrino in the Borexino experiment

A.V. Derbin, I.S. Drachnev, I.S. Lomskaya, V.N. Muratova, N.V. Niyazova, D.A. Semenov, E.V. Unzhakov – Neutron Research Division of NRC “Kurchatov Institute” – PNPI, Borexino Collaboration

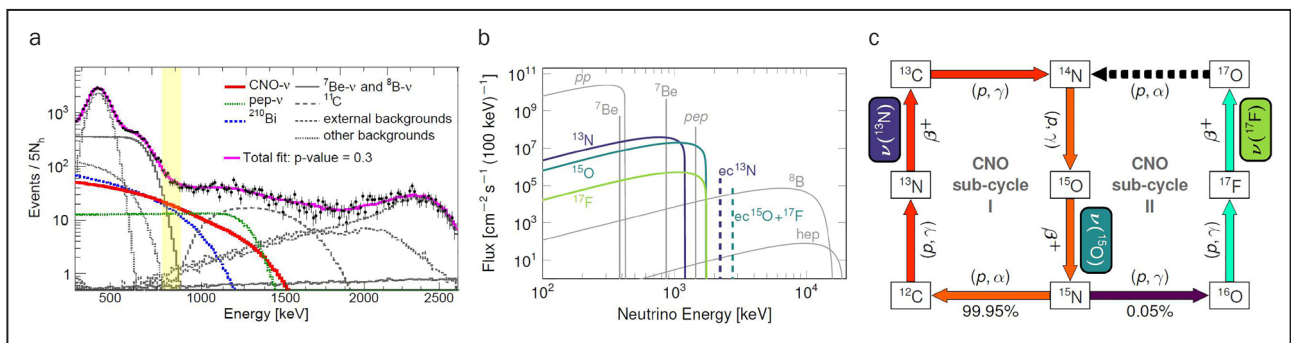
The Borexino Collaboration presented direct experimental evidence of neutrinos emitted in the so-called CNO cycle in the Sun for the first time. Scientists from NRC “Kurchatov Institute” – PNPI and NRC “Kurchatov Institute” participate in the experiment.

Nuclear fusion of hydrogen into helium in stars occurs through two processes: the proton-proton ( $pp$ ) chain, which includes only isotopes of hydrogen and helium, and the carbon-nitrogen-oxygen (CNO) cycle, in which the fusion is catalyzed by C, N and O nuclei. The CNO cycle produces only 1% of all solar energy and is secondary for the Sun. However, this cycle is decisive for more massive and hotter stars, since already for stars with 1.5 solar mass it is responsible for half of all generated energy.

The CNO cycle, which is of paramount importance for all astrophysics, was predicted theoretically and has not yet had direct experimental confirmation. The flux of solar CNO-neutrinos strongly depends on the abundance of elements heavier than helium in the Sun, which makes it possible to distinguish solar models with high or low metallicity.

A significant contribution of NRC “Kurchatov Institute” – PNPI to the obtained result is associated with the high-precision measurement of the  $\beta$ -spectrum of  $^{210}\text{Bi}$ , the knowledge of which is necessary for the analysis of the contribution of CNO-neutrinos in the measured spectrum.

The work was supported by RFBR, project No. 19-02-00097.



Borexino measured spectrum (a): the red curve shows the contribution from the scattering of CNO-neutrinos by electrons, blue line is background from  $\beta$ -decays of  $^{210}\text{Bi}$  nuclei; CNO-cycle and CNO-neutrino spectra in comparison with the spectra of neutrinos from  $pp$  chain, previously detected by the Borexino (b); layout of the most intensive reactions of the CNO cycle (c)

1. Borexino Collab., Agostini M., Derbin A., Drachnev I., Lomskaya I., Muratova V., Semenov D., Unzhakov E. et al. // Nature. 2020. V. 587. P. 577.
2. Borexino Collab., Agostini M., Derbin A., Drachnev I., Lomskaya I., Muratova V., Semenov D., Unzhakov E. et al. // Eur. Phys. J. C. 2020. V. 80. Iss. 11. P. 1091.
3. Alekseev I.E., ..., Derbin A.V., Drachnev I.S., ..., Lomskaya I.S., Muratova V.N., Niyazova N.V., Semenov D.A., ..., Unzhakov E.V. // Phys. Rev. C. 2020. V. 102. P. 064329.

# Emission of high-energy protons and photons and production of subthreshold pions in heavy-ion collisions in a hydrodynamic approach with a nonequilibrium equation of state

A.T. D'yachenko, I.A. Mitropolsky

High Energy Physics Division, Neutron Research Division of NRC "Kurchatov Institute" – PNPI

For describing the dynamics of heavy-ion collisions at intermediate energies, a hydrodynamic approach with a nonequilibrium equation of state is used, taking into account the effects of nuclear viscosity and the correction for the microcanonical distribution. The calculated double differential cross sections of the emission of protons and photons in collisions of different nuclei were in agreement with the available experimental data (Fig. 1). In this approach, it was possible to reproduce the high-momentum distributions of protons from the reaction  $^{12}\text{C} + ^9\text{Be} \rightarrow p + X$  at the  $^{12}\text{C}$  ion energies of: 300, 600, 950, and 2 000 MeV/nucleon, as well as the energy spectra of hard photons from the reaction  $^{12}\text{C} + ^9\text{Be} \rightarrow \gamma + X$  reaction at the carbon ion energies of 2 and 3.2 GeV/nucleon.

The threshold for the pion production in the collision of heavy ions falls due to collective effects and

the internal motion of the nucleons. The description of the time evolution of the resulting nonequilibrium region includes the stages of compression and expansion, taking into account the nuclear viscosity. The calculated energy spectra of pions at the subthreshold reaction energies of 84 and 94 MeV/nucleon are in agreement with the available experimental data (Fig. 2).

The inclusion in the consideration of the nuclear viscosity effects, which we found in the relaxation approximation for the kinetic equation, is new in this approach. This did not add new parameters to the description of the time evolution of nuclear collisions. When describing the emission of protons and fragments, taking into account the viscosity of the medium turned out to be insignificant, and the production of pions turns out to be very sensitive to the viscosity value.

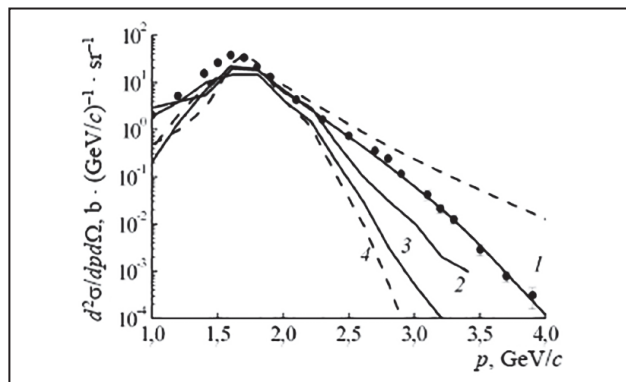


**Fig. 1.** The momentum distribution of protons emitted at an angle of  $3.5^\circ$  in the reaction  $^{12}\text{C} + ^9\text{Be} \rightarrow p + X$  at the energy 950 MeV/nucleon. *Solid curve 1* for calculation in the hydrodynamic approach; *dashed curve 2* – the same, but without taking into account the correction for the microcanonical distribution; *points* – experimental data; *curves 3–4* – the results of calculations for transport codes

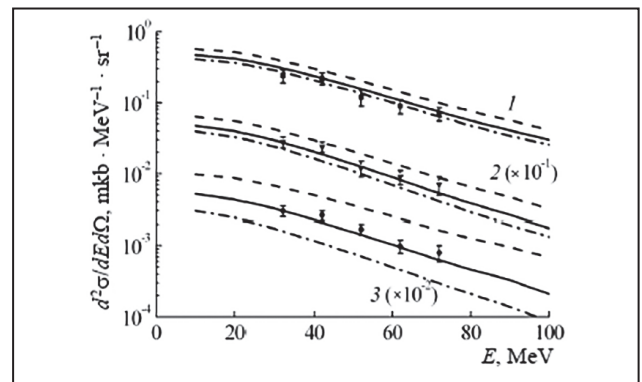
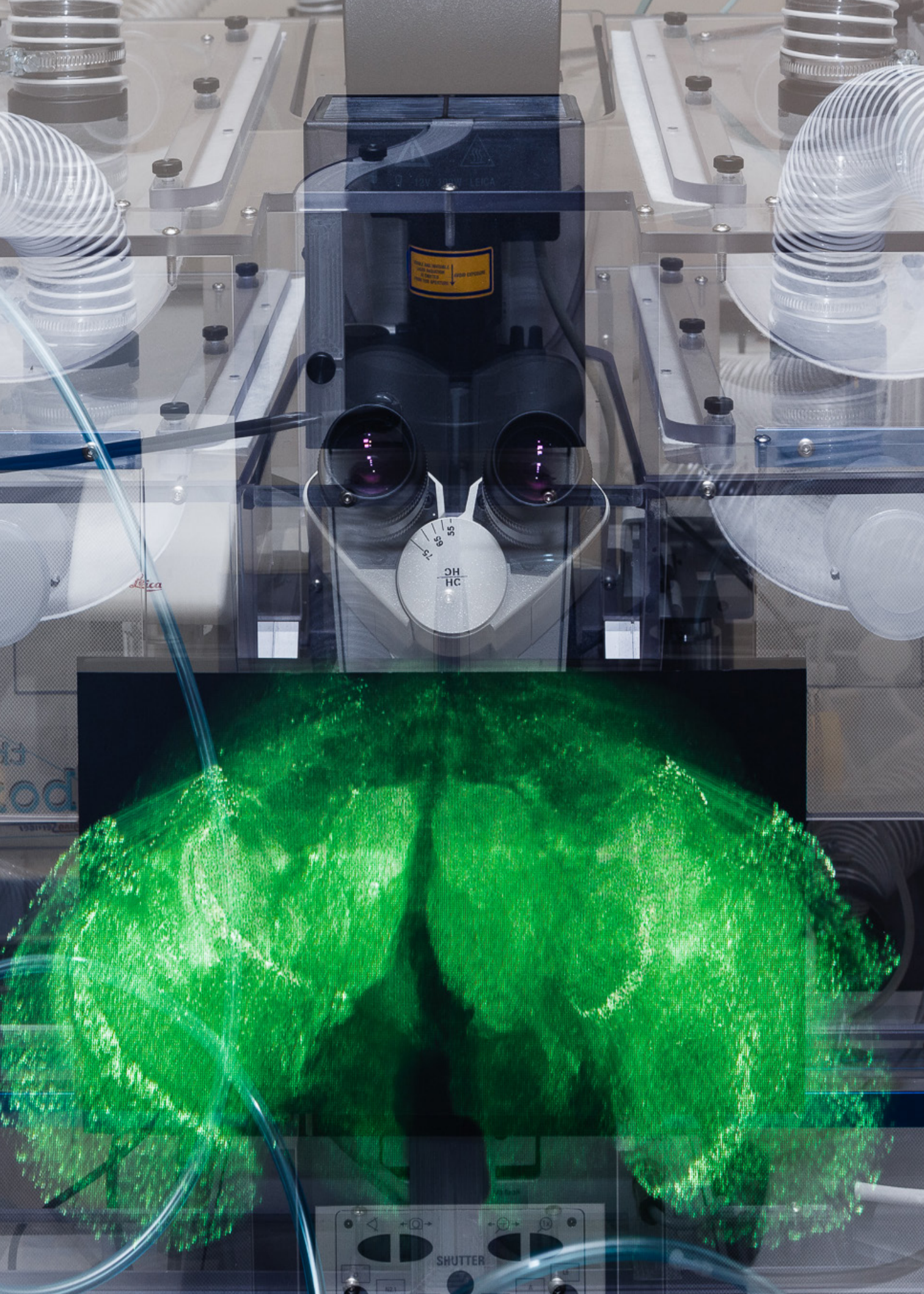


**Fig. 2.** Calculated (*solid lines*) and experimental (*points*) inclusive double differential cross-sections for the emission of  $\pi^+$  mesons at a  $90^\circ$  angle of observation for the scattering reactions of  $^{16}\text{O}$  ions with an energy of 94 MeV/nucleon at the nuclei  $^{27}\text{Al}$  (*curve 1*),  $^{58}\text{Ni}$  (*curve 2*) and  $^{197}\text{Au}$  (*curve 3*). *Solid curves* correspond to the relaxation time  $\tau = 1/(\sigma \rho v_T)$ , *dashed curves* correspond to the relaxation time  $\tau_1 = 3\tau/2$ , *dashpoint curves* correspond to the relaxation time  $\tau_2 = 2\tau/3$



## Molecular and Radiation Biophysics

- 70 Participation of the *HIM1* gene of yeast *Saccharomyces cerevisiae* in the error-free branch of post-replicative repair and role Pol $\eta$  in *him1*-dependent mutagenesis
- 71 Proteome of glioblastoma-derived exosomes as a source of biomarkers
- 72 Insights into the improved macrolide inhibitory activity from the high-resolution cryo-EM structure of dirithromycin bound to the *Escherichia coli* 70S ribosome
- 73 How the initiating ribosome copes with ppGpp to translate mRNAs
- 74 Altered level of plasma exosomes in patients with Gaucher disease
- 76 Approbation of a new method for the isolation of exosomes from human plasma
- 77 Cryo-electron microscopy of extracellular vesicles from cerebrospinal fluid in Parkinson's disease
- 79 Calcifying bacteria flexibility in induction of CaCO<sub>3</sub> mineralization
- 80 Exosomes from total blood of breast cancer patients along with plasma exosomes mediate tumor progression

## Participation of the *HIM1* gene of yeast *Saccharomyces cerevisiae* in the error-free branch of post-replicative repair and role Pol $\eta$ in *him1*-dependent mutagenesis

E.A. Alekseeva, T.A. Evstyukhina, V.T. Peshekhonov, V.G. Korolev  
Molecular and Radiation Biophysics Division of NRC "Kurchatov Institute" – PNPI

In eukaryotes, DNA damage tolerance is determined by two repair pathways, homologous recombination and a pathway controlled by the RAD6-epistatic group of genes. Monoubiquitylation of PCNA mediates an error-prone pathway, whereas polyubiquitylation stimulates an error-free pathway. The error-free pathway involves components of recombination repair; however, the factors that act in this pathway remain largely unknown.

The response to DNA damage has been well characterized in *Saccharomyces cerevisiae*. It includes three groups of proteins involved in different types of DNA repair, termed the RAD3, RAD52 and RAD6 epistasis groups.

To test the hypothesis, that *HIM1* gene may be involved in the control of the error-free branch of PRR, we deleted *MMS2* gene from *him1* mutant and the wild-type strain. UV-induced mutagenesis in *mms2* strain is markedly lower than in *him1*, but is close to the level of mutagenesis in the wild-type strain. We showed that *mms2* $\Delta$  is epistatic to *him1* $\Delta$  and *him1* $\Delta$  induced mutagenesis is *Mms2* dependent. These results strongly suggest that the *HIM1* gene is involved in the error-free branch of damage bypass.

We hypothesized that the cause of *him1*-mediated UV-induced mutagenesis is the replacement of Pol $\delta$  with highly erroneous Pol $\eta$  during the DNA synthesis in gaps after the destruction of the D-loop.

We deleted *RAD30* gene that codes for Pol $\eta$  in the wild-type strain and *him1* mutant. The UV-induced mutagenesis in the double *him1 rad30* mutant was the same as in the single *rad30* mutant.

Based on these results, it can be assumed that, in during postreplication repair the Pol $\eta$  in *him1* mutant carries out reparative synthesis in unfilled gaps. In order to get insight into the role of Pol $\eta$  in *him1*-dependent mutagenesis, mutation spectra were determined at the *CAN1* locus in *him1* and double *him1 rad30* strains for UVC. Data obtained show a significant role of Pol $\eta$  in *him1*-dependent mutagenesis.

To test the hypothesis that dNTP concentration regulates the choice of polymerase for D-loop extending, we examined UV-irradiated *him1* cells for increased *RNR3* expression. The *RNR3* expression increases in UV-irradiated wild-type sevenfold, while in mutant cells the increase did not reach twofold, and, as a consequence, the concentration of dNTP also increases by a factor of 2–3.

Our experiments demonstrated that significant increase in the dNTP levels suppress *him1*-dependent mutagenesis. Thus this study identifies the *HIM1* gene as a novel member of error-free pathway of DNA damage tolerance. Interestingly, the mechanism through *him1* mutant acts by recruiting polymerase Pol $\eta$  to carry out reparative DNA synthesis during DNA damage tolerance.

## Proteome of glioblastoma-derived exosomes as a source of biomarkers

S.N. Naryzhny, A.V. Volnitskiy, V.Yu. Bairamukov, L.A. Garaeva, T.A. Shtam –  
Molecular and Radiation Biophysics Division, Neutron Research Division  
of NRC “Kurchatov Institute” – PNPI,

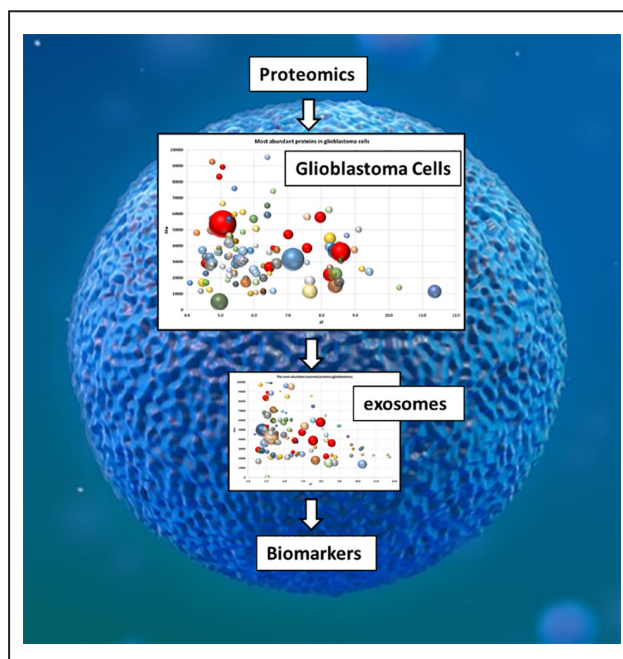
A.T. Kopylov, E.S. Zorina – V.N. Orekhovich Research Institute of Biomedical Chemistry,  
R.A. Kamyshinsky – NRC “Kurchatov Institute”,  
A.G. Shlikht – Far Eastern Federal University

Extracellular vesicles (EVs) are involved in important processes of glioblastoma multiforme, including malignancy and invasion. EVs secreted by glioblastoma cells may cross the hematoencephalic barrier and carry molecular cargo derived from the tumor into the peripheral circulation. Therefore, the determination of the molecular composition of EVs (exosomes) released by glioblastoma cells seems to be a promising approach for the development of non-invasive methods of the detection of the specific exosomal protein markers in the peripheral blood.

The aims of the present study were to determine the common exosomal proteins presented in preparations from different cell lines and search for potential glioblastoma biomarkers in exosomes. We have performed proteomics analysis of exosomes (Fig.) obtained from conditioned culture medium of five glioblastoma cell lines. A list of 133 proteins common for all these samples was generated. Based on the data obtained, virtual two-dimensional electrophoresis maps of proteins presented in exosomes of glioblastoma cells were constructed and the gene ontology analysis of exosome proteins was performed. A correlation

between the overexpression of glial cell proteins and their presence in exosomes has been found.

Thus, the existence of many potential glioblastoma biomarkers in exosomes was confirmed.



A graphical representation of the described proteomics analysis



## Insights into the improved macrolide inhibitory activity from the high-resolution cryo-EM structure of dirithromycin bound to the *Escherichia coli* 70S ribosome

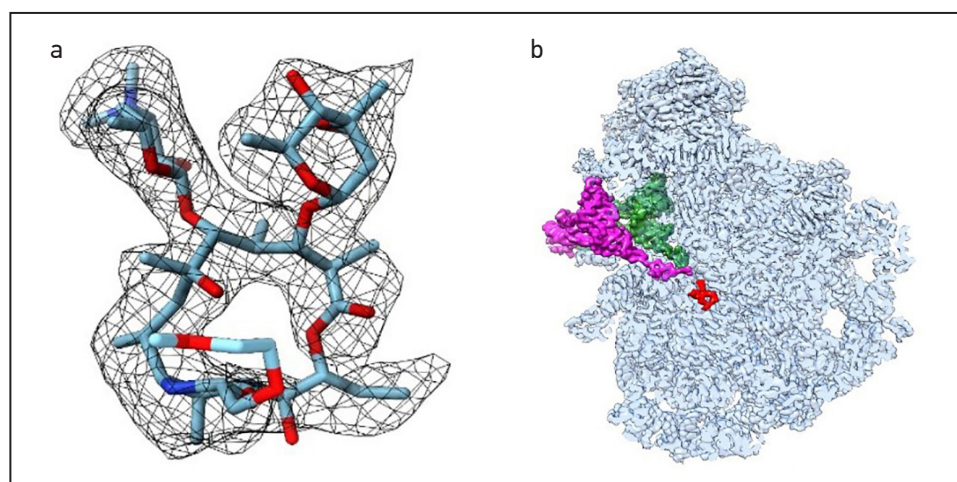
*E.B. Pichkur, A.V. Paleskava, P.S. Kasatsky, A.G. Myasnikov, A.L. Konevega*  
Molecular and Radiation Biophysics Division of NRC “Kurchatov Institute” – PNPI

The emergence and spread of bacterial strains resistant to the antibiotics used is rampant. One of the options for solving this problem is to study the molecular mechanism of action of known antibiotics for the targeted improvement of substances used in therapy. The aim of this study was to investigate the biochemical and structural aspects of the binding of the antibiotic dirithromycin (DIR) to the bacterial ribosome (Fig.) to explain the improved biological activity of DIR compared to its parental substance erythromycin (ERY).

The main distinguishing feature of DIR from ERY is the presence of a hydrophobic radical, which, obviously, is the reason for a twofold increase in the inhibitory activity of this antibiotic compared to ERY. Biochemical studies have shown that the presence of the hydrophobic radical does not lead to an increase in the binding affinity of DIR to the ribosomes, and structural data indicate

that DIR forms only canonical contacts previously found for ERY. Based on the data obtained using cryo-EM, we assume that the more pronounced inhibition of protein biosynthesis is a consequence of the location of the hydrophobic radical of DIR: it is directed into the lumen of the exit tunnel, partially closes it, which leads to disruption of the normal passage of the growing peptide through the tunnel, inhibiting synthesis of a polypeptide chain.

Thus, the analysis of the structure of the functionally active ribosomal complex by cryo-EM made it possible to elucidate the molecular mechanism of the increased inhibitory activity of the antibiotic DIR. The resolution of the obtained complex of 2.1 Å is currently a record among the published cryo-EM structures of ribosomal complexes and may serve as a basis for further studies of ribosomal complexes.



The structure of DIR in complex with the 70S ribosome: *a* – Coulomb potential map of DIR in complex with the ribosome (*black mesh*); in the fitted model of the compound carbon atoms are colored *light blue*, nitrogen atoms are *blue*, oxygen atoms are *red*; *b* – overview of the DIR (*red*) binding site on the large ribosomal subunit (*light blue*). A-site tRNA and P-site tRNA are shown in *magenta* and *green*, respectively

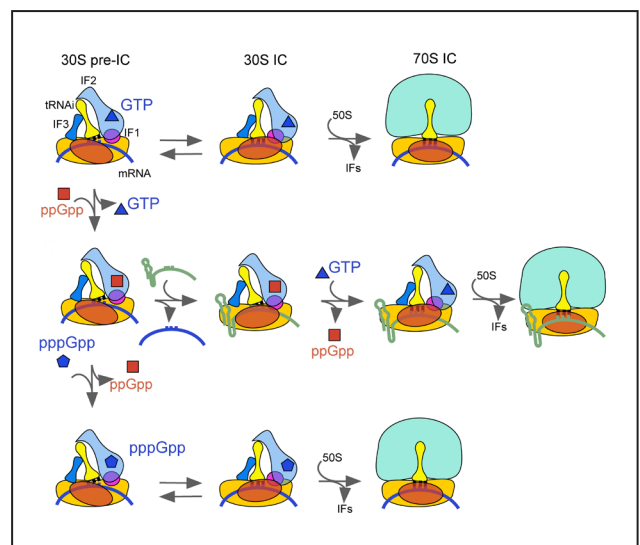
## How the initiating ribosome copes with ppGpp to translate mRNAs

*D.S. Vinogradova, E.M. Maksimova, P.S. Kasatsky, A.V. Paleskava, A.L. Konevega – Molecular and Radiation Biophysics Division of NRC “Kurchatov Institute” – PNPI, V. Zegarra, J. Alberto Nakamoto, P. Milon – Centre for Research and Innovation, Faculty of Health Sciences of Peruvian University of Applied Sciences*

To effectively fight against pathogens, we need to understand the molecular mechanism of the most vulnerable processes of the cell's vital activity. Upon stressful conditions such as amino acid starvation, sudden changes in temperature, lack of phosphorus, iron or fatty acids the stringent response mechanism is activated and the cell survives by conserving its resources. The stringent response is mediated by the accumulation of a large amount of a small regulatory molecule guanosine tetraphosphate, ppGpp in the cell. The hypothesis about the regulation of the cellular activity in unfavorable environmental conditions during the stage of transcription does not answer the question of how bacterial cells retain the ability to synthesize vital proteins.

In our work we identified a new direction of the stringent response through the translation stage and identified the key role of the messenger RNA molecule. We have shown dynamic inhibitory mechanism of the ppGpp molecule action on the translation initiation process that depends on the messenger RNA involved in the formation of the initiation complex (Fig.). In addition, for the first time we have shown that cells can use pppGpp to initiate the process of protein biosynthesis at inc-

reased concentration of the ppGpp molecule upon unfavorable conditions. In this work we have created a system of sensitive, fast and accurate analysis of the biomolecules interactions in the process of translation initiation that opens up new opportunities for studying the effect of ligands and small molecules such as antibiotics on the process of protein biosynthesis.



The model of translation initiation during the stringent response

## Altered level of plasma exosomes in patients with Gaucher disease

*T.A. Shtam, S.N. Naryzhny, D.G. Kulabukhova, L.A. Garaeva, K.A. Senkevich, S.B. Landa, E.Yu. Varfolomeeva, N.A. Verlov, T.S. Usenko, A.L. Schwarzman, E.Yu. Zakharova, A.K. Emelyanov, S.N. Pchelina – Molecular and Radiation Biophysics Division of NRC “Kurchatov Institute” – PNPI,*

*T.A. Shtam, L.A. Garaeva, R.A. Kamyshinsky, S.N. Pchelina – NRC “Kurchatov Institute”, S.N. Naryzhny, A.T. Kopylov, E.S. Zorina – V.N. Orekhovich Research Institute of Biomedical Chemistry*

Previously we demonstrated the increased levels of blood oligomeric  $\alpha$ -synuclein in patients with Gaucher disease (GD), caused by mutations in the gene encoding lysosomal enzyme, glucocerebrosidase 1 (*GBA*). We have reported an inverse correlation between plasma oligomeric  $\alpha$ -synuclein levels and leukocyte *GBA* activity in patients with GD. *GBA* mutations have been identified as the most common known genetic risk factor for the development of Parkinson's disease (PD). However, it should be noted that PD does not develop in all carriers of mutations and not in all patients with GD. Understanding the molecular basis of the development of the disease will contribute to the development of new methods of treatment of these pathologies.

The currently dominant hypothesis is the effect of lysosomal dysfunction on the formation and distribution of neurotoxic forms of the  $\alpha$ -synuclein protein. Exosomes (extracellular vesicles 40–100 nm in size) could play a key role in the transport of pathogenic forms of  $\alpha$ -synuclein. As the lysosome functionality plays a critical role for secretion of extracellular vesicles and their content, we supposed that lysosomal dysfunction associated with decreased *GBA* activity could influence the pool of extracellular vesicles of blood plasma.

Here we compared extracellular vesicles from the blood plasma of eight GD patients and eight controls in terms of amounts, size distribution, and

composition of their protein cargo. Extracellular vesicles were isolated via sequential centrifugation and characterized by cryo-electron microscopy (cryo-EM) (Fig. 1), nanoparticle tracking analysis (NTA), and dynamic light scattering (DLS). The presence of exosomal markers HSP70 and tetrasponins were analyzed by western blot and flow cytometry. Protein profiling was performed by mass-spectrometry (shotgun analysis).

Here, for the first time we reported an increased size and altered morphology in exosomes derived from blood plasma of GD patients (Fig. 2). An increased size of plasma exosomes from GD patients compared to controls was demonstrated by cryo-EM and DLS ( $p < 0.0001$ ,  $p < 0.001$ , respectively) and confirmed by mode size detected by NTA ( $p < 0.02$ ). Cryo-EM demonstrated an increased number of double and multilayer vesicles in plasma EVs from GD patients.

We found that the extracellular vesicles were enriched with the surface exosomal markers (CD9, CD63, CD81) and an exosome-associated protein HSP70 in case of the patients with the disease. Proteomic profiling of exosomal proteins did not reveal any proteins associated with PD pathogenesis. Thus, we showed that lysosomal dysfunction in GD patients leads to a striking alteration of plasma exosomes in size and morphology.

The work was supported by RFBR No. 18-015-00262A and RSF (Grants No. 19-15-00315, 19-74-20146).

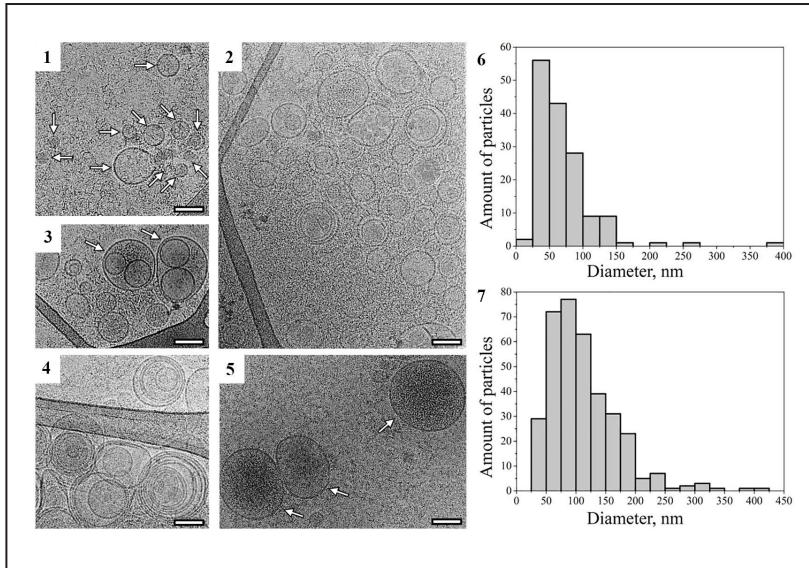


**Fig. 1.** Cryo-electron microscopy images of extracellular vesicles isolated from plasma of healthy individuals (control) and Gaucher disease patients: 1 – overview of extracellular vesicles from control; 2–5 – extracellular vesicles derived from Gaucher disease patients; 3, 5 – extracellular vesicles with electron-dense cargo; 4 – multilayer extracellular vesicles. Scale bar is 100 nm. Particle distribution according to their size: 6 – from controls; 7 – from Gaucher disease patients

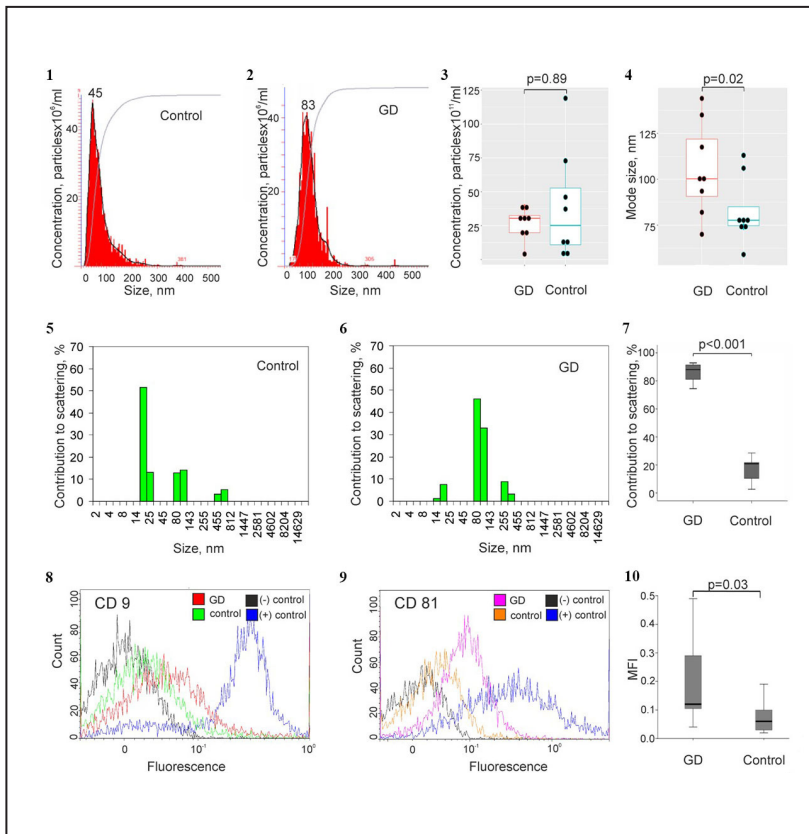


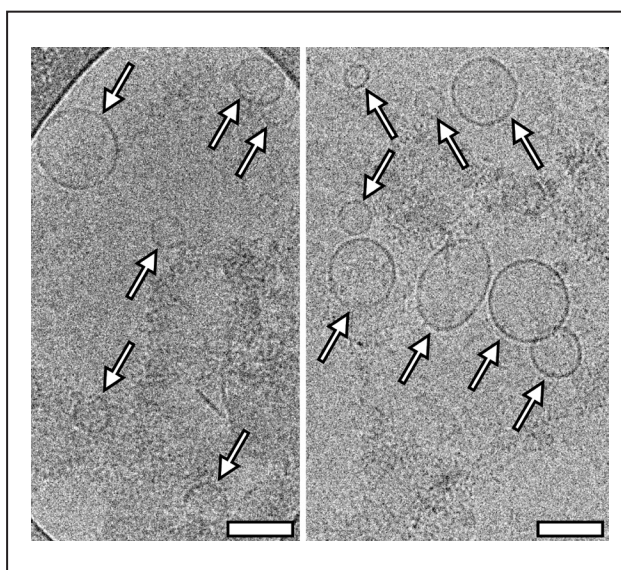
**Fig. 2.** Characterization of extracellular vesicles from the blood plasma of Gaucher disease patients and healthy donors (control): 1–4 – quantification of vesicular size and concentration by nanoparticle tracking analysis; 5, 6 – size distribution of extracellular vesicles by dynamic light scattering; 7 – contribution to the scattering of particles about 100 nm in diameter by dynamic light scattering data; 8, 9 – flow cytometry analyses of isolated extracellular vesicles for expression of the surface exosomal markers (CD9 and CD81); 10 – flow cytometry analysis estimating CD9 and CD81 markers on plasma exosomes showed that the intensity of fluorescence was higher in the group of Gaucher disease patients compared to the controls ( $p = 0.03$ ). All values in the group are represented as median (min–max)

## Approbation of a new method for the isolation of exosomes from human plasma

T.A. Shtam, Ya.A. Zabrodskay, N.A. Verlov, V.S. Burdakov, L.A. Garaeva, A.L. Konevega – Molecular and Radiation Biophysics Division of NRC “Kurchatov Institute” – PNPI, V.I. Evtushenko – A.M. Granov Russian Scientific Center for Radiology and Surgical Technologies, R.A. Kamyshinsky – NRC “Kurchatov Institute”, R.B. Samsonov, L.M. Zabegina, M.A. Slyusarenko, N.S. Nikiforova, A.V. Malek – N.N. Petrov National Medical Research Center of Oncology of MoH of Russia

Exosomes are a type of extracellular vesicles (EVs) secreted by multiple mammalian cell types and involved in intercellular communication. Numerous studies have explored the diagnostic and therapeutic potential of exosomes. The key challenge is the lack of efficient and standard techniques for isolation and downstream analysis of nanovesicles. Here we compared EVs extracted from human plasma by four different methods: 1) differential ultracentrifugation; 2) sequential ultracentrifugation in a sucrose cushion; 3) sedimentation of EVs lectin aggregates; 4) immunoprecipitation of exosomes and SubX™ technology.

This new approach to the isolation of vesicles is based on using the proprietary bi-functional compound (SubX™) that can bind clusters of phospholipids on the vesicular surface and thus oligomerize vesicles directly in biological liquids. The subsequent centrifugation precipitates [oligoEVs-SubX™] complex. The pelleted EVs dissociate back to monomers in the reconstruction buffer in a ready-to-use form for downstream applications. The vesicles isolated by the five techniques were characterized based upon size, quantity, CD63, CD81 and Calnexin protein expression, and total protein quality using several complementary methods: nanoparticle tracking analysis, dynamic light scattering, atomic force microscopy, cryo-electron microscopy (cryo-EM), and flow cytometry. The results clearly indicated the presence of the sites for the binding of SubX™ on the outer membrane of the vesicles, which confirms the possibility of EVs separation from the plasma using SubX™ technology. In order to confirm the vesi-



Cryo-electron microscopy images of extracellular vesicles isolated from plasma by SubX™ reagent. The white arrows point to the vesicles with a double membrane. Scale bars are 100 nm

cular nature of particles isolated with SubX™, these samples were analyzed by cryo-EM. As seen in Figure, isolated particles are indeed formed by a characteristic lipid bilayer, which has an average thickness of ~ 10 nm, and have a round-shaped vesicular morphology. The visualized particles with a lipid bilayer generally varied in size from 50 to 220 nm.

Summarizing all the data, we can assume that SubX™ allows obtaining relatively pure populations of exosomes, while the concentration of isolated vesicles is rather low. Undoubtedly, this method is suitable for the isolation of EVs from human blood plasma.

## Cryo-electron microscopy of extracellular vesicles from cerebrospinal fluid in Parkinson's disease

A.K. Emelyanov, T.A. Shtam, L.A. Garaeva, N.A. Verlov, I.V. Miliukhina, S.N. Pchelina, A.L. Konevega – Molecular and Radiation Biophysics Division of NRC “Kurchatov Institute” – PNPI,  
A.K. Emelyanov, I.V. Miliukhina, A.V. Kudrevatykh, S.N. Pchelina – Pavlov First Saint Petersburg State Medical University,  
T.A. Shtam, R.A. Kamyshinsky, L.A. Garaeva, N.A. Verlov, S.N. Pchelina, A.L. Konevega – NRC “Kurchatov Institute”,  
R.A. Kamyshinsky – Federal Scientific Research Center “Crystallography and Photonics” of the RAS, Moscow Institute of Physics and Technology,  
L.A. Garaeva, A.L. Konevega – Peter the Great Saint Petersburg Polytechnic University,  
I.V. Miliukhina, A.V. Kudrevatykh, S.N. Pchelina – Institute of Experimental Medicine,  
G.V. Gavrilov – S.M. Kirov Military Medical Academy,  
Yu.M. Zabrodskaya – A.L. Polenov Russian Scientific Research Neurosurgical Institute

The formation of  $\alpha$ -synuclein fibrils is currently believed to play a key role in the pathogenesis of Parkinson's disease (PD). Aggregates of this protein have been shown to be transmissible and may spread from cell to cell via extracellular vesicles. The size and morphology of extracellular vesicles have been shown to affect the diffusion properties of vesicles and they might affect the spread of  $\alpha$ -synuclein pathology in PD. The study of these characteristics seems to be an urgent task for understanding the role of extracellular vesicles in the pathogenesis of PD.

In the present study, we used extracellular vesicles purified by ultracentrifugation from cerebrospinal fluid of seven patients with PD (mean age  $67.6 \pm 7.8$  years) and seven individuals in the comparison group (mean age  $48 \pm 7$  years). The comparison group consisted of patients with various non-PD neurosurgical pathologies: epidermoid cyst ( $N = 1$ ), neurovascular conflict ( $N = 2$ ), post-hypoxic encephalopathy ( $N = 2$ ), subarachnoidal hemorrhage ( $N = 1$ ), arachnoid cyst ( $N = 1$ ). All extracellular vesicles were characterized using

nanoparticle tracking analysis, flow cytometry and cryo-electron microscopy. Vesicular size and the presence of exosomal marker CD9 on the surface provided evidence that most of the extracellular vesicles were exosome-like vesicles. Cryo-electron microscopy allowed us to visualize a large spectrum of extracellular vesicles of various size and morphology with lipid bilayers and vesicular internal structures (Figs. 1, 2) both in the PD patients group and in the comparison group. At the same time, the majority of vesicles of a certain shape were found in both study groups. Also, in the extracellular vesicles samples of both patients with PD and those in the control group, an increase in the size of multilayer extracellular vesicles compared to single vesicles was revealed ( $p < 0.0001$ ).

Thus, we described the diversity and new characteristics of the extracellular vesicles from human cerebrospinal fluid including that of the PD patients suggesting that subpopulations of extracellular vesicles with different and specific functions may exist.

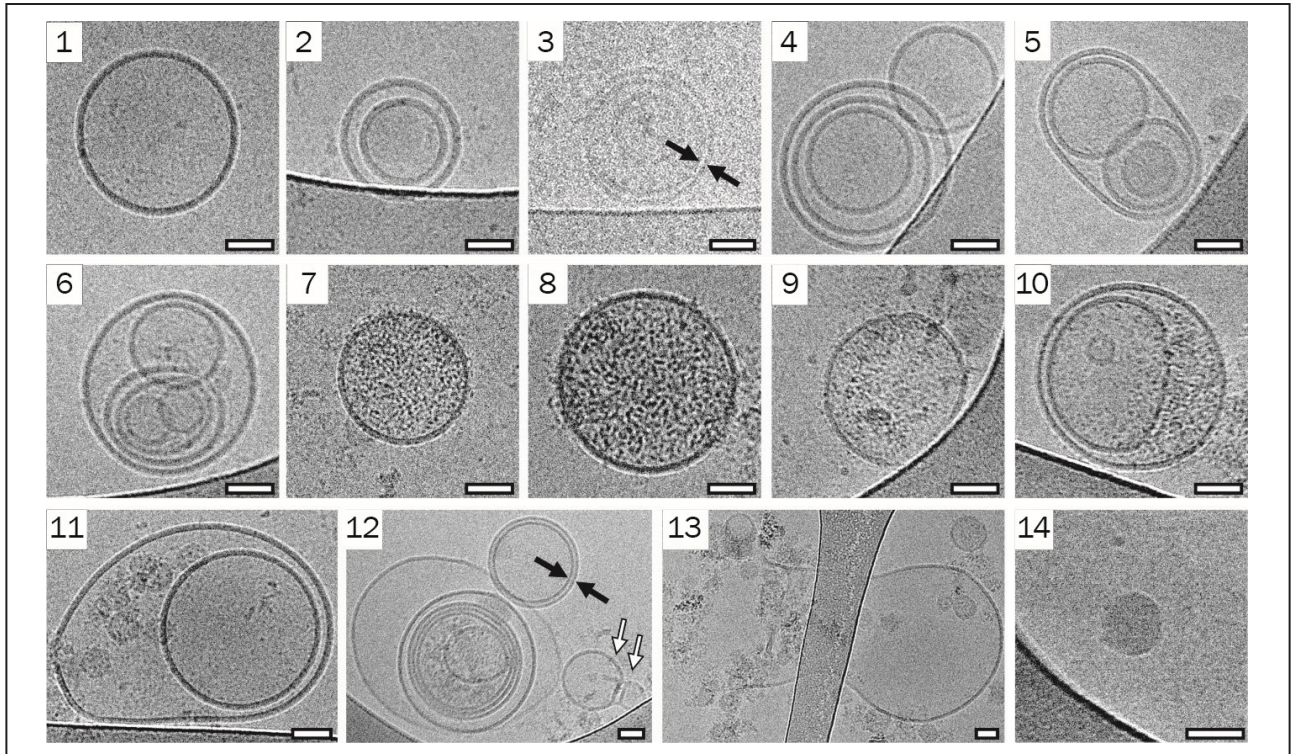


**Fig. 1.** Cryo-electron microscopy images of extracellular vesicles isolated from pooled cerebrospinal fluid of Parkinson's disease patients: 1 - single vesicles; 2, 11 - double vesicles; 3, 12 - double-membrane vesicles; 3-6, 12 - multilayer vesicles; 7-10, 12 - vesicles with electron dense cargo in lumen; 11, 13, 14 - vesicles with broken membrane. The arrows point to vesicle with double membrane (*black arrow*) and "bowling pin" vesicle (*white arrow*). Scale bars are 50 nm

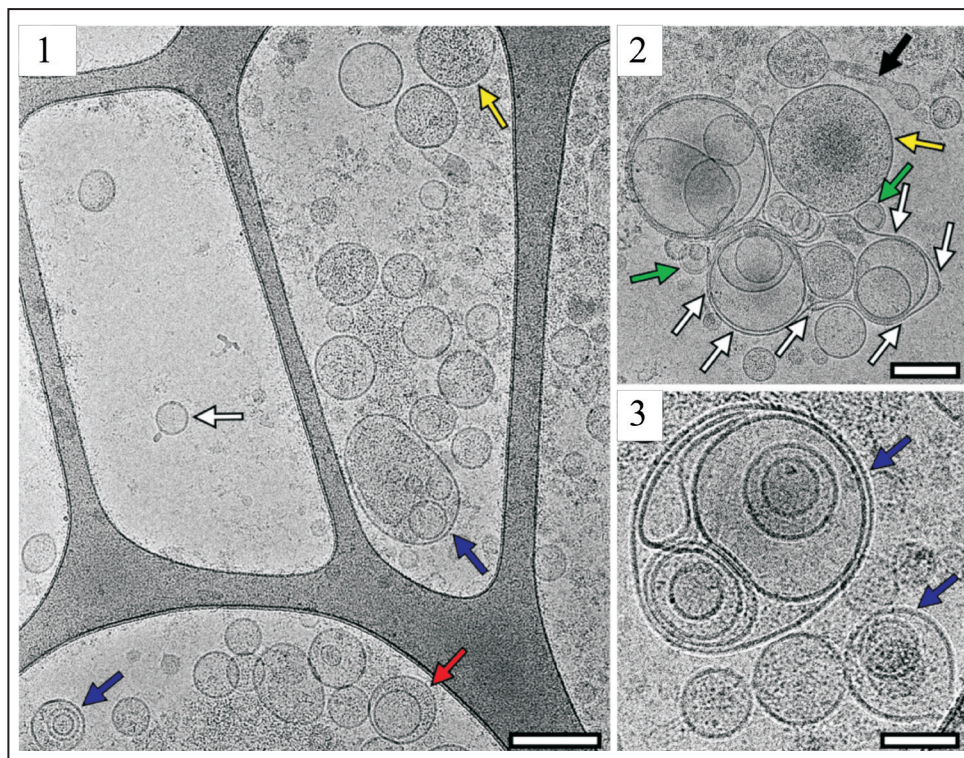


**Fig. 2.** Cryo-electron microscopy images of extracellular vesicles isolated from pooled cerebrospinal fluid sample from individuals of the comparison group: 1 - micrograph of single (*white arrow*), double (*red arrow*), multilayer (*blue arrow*) vesicles and vesicles with electron dense cargo in lumen (*yellow arrow*); 2 - micrograph of double-membrane vesicles (*green arrow*), vesicles with electron dense cargo in lumen (*yellow arrow*), vesicle in the form of a sack (*white arrow*), distinctly elongated vesicle (*black arrow*); 3 - micrograph of multilayer vesicles (*blue arrows*). Scale bars are 200 nm for Figures 1, 2 and 100 nm for Figure 3

## Calcifying bacteria flexibility in induction of CaCO<sub>3</sub> mineralization

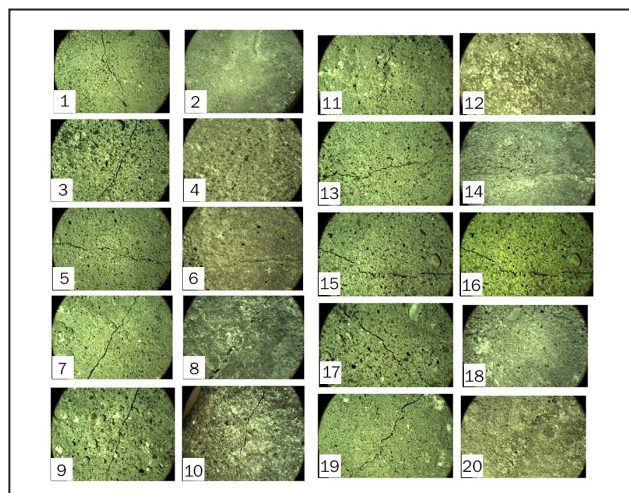
D.A. Golovkina, E.V. Zhurishkina, L.A. Ivanova, K.S. Bobrov, A.A. Kulminskaya, A.Ye. Sokolov, G.P. Kopitsa – Molecular and Radiation Biophysics Division, Neutron Research Division, Kurchatov Genome Center of NRC “Kurchatov Institute” – PNPI, A.Ye. Baranchikov – N.S. Kurnakov Institute of General and Inorganic Chemistry of the RAS, A.E. Masharsky – Research Resource Center for Molecular and Cell Technologies of the Research Park of Saint Petersburg State University, N.V. Tsvigun – Federal Scientific Research Center “Crystallography and Photonics” of the RAS

Microbially induced CaCO<sub>3</sub> precipitation (MICP) is considered as an alternative “green” technology for cement self-healing and a basis for the development of new biomaterials. However, some issues about the role of bacteria in the induction of biogenic CaCO<sub>3</sub> crystal nucleation, growth and aggregation are still debatable. Our aims were to screen for ureolytic calcifying microorganisms and analyze their MICP abilities during their growth in urea-supplemented and urea-deficient media. Nine candidates showed a high level of urease specific activity and sharp increase of the urea-containing medium pH resulted in efficient CaCO<sub>3</sub> biomineralization. In the urea-deficient medium, all ureolytic bacteria also induced CaCO<sub>3</sub> precipitation although at lower pH values. Five strains (*Bacillus licheniformis* DSMZ 8782, *B. cereus* 4b, *Staphylococcus epidermidis* 4a, *Micrococcus luteus* BS52, *M. luteus* 6)

were found to completely repair micro-cracks in the cement samples (Fig.).

Detailed studies of the most promising strain *B. licheniformis* DSMZ 8782 revealed a slower rate of the polymorph transformation in the urea-deficient medium than in urea-containing one. We suppose that a ureolytic microorganism retains its ability to induce CaCO<sub>3</sub> biomineralization regardless the origin of carbonate ions in a cell environment by switching between mechanisms of urea-degradation and metabolism of calcium organic salts.

The work was carried out with financial support of Kurchatov Genome Center of NRC “Kurchatov Institute” – PNPI within the framework of the program for the development of world-class genetic research centers, agreement No. 075-15-2019-1663.



Typical micro-images of micro-cracks filled with the selected strains. Unfilled cracks are on the left hand side and the same cracks on the right after bacterial cultivation on the sample surface within a month: 1, 2 – *B. licheniformis* DSMZ 8782; 3, 4 – *B. cereus* 4b; 5, 6 – *B. cereus* 168; 7, 8 – *B. cereus* BSP; 9, 10 – *E. coli* DH5 $\alpha$ , negative control; 11, 12 – *S. epidermidis* 4a; 13, 14 – *M. luteus* 6; 15, 16 – *B. subtilis* 170; 17, 18 – *M. luteus* BS52; 19, 20 – *B. subtilis* K51



## Exosomes from total blood of breast cancer patients along with plasma exosomes mediate tumor progression

*T.A. Shtam – Molecular and Radiation Biophysics Division of NRC “Kurchatov Institute” – PNPI, M.Yu. Konoshenko, K.V. Proskura, O.S. Tutanov, S.N. Tamkovich – Institute of Chemical Biology and Fundamental Medicine of SB RAS, G.D. Sagaradze, A.Yu. Efimenko – Lomonosov Moscow State University, E.I. Orlova, A.Yu. Alexandrova – N.N. Blokhin National Medical Research Center of Oncology, R.A. Kamyshinsky – NRC “Kurchatov Institute”, N.V. Yunusova – Cancer Research Institute of Tomsk National Research Medical Center of the RAS*

Extracellular vesicles (EVs) are widely present in human body fluids, contain proteins, nucleic acids and lipids and can participate in the delivery of biological information to recipient cells, thereby modulating their behavior and potentially participating in the pathogenesis of many human diseases, including cancer. Exosomes are key players in the intercellular communication and have been shown to be involved in tumorigenesis through paracrine signaling. It has been recently discovered that blood circulating exosomes contain distinguishable fractions of free and cell-surface-associated vesicles. Here, we compared the effect of total blood (contains plasma exosomes and blood cell-surface-associated exosomes) and plasma exosomes from breast cancer patients (BCPs) and healthy females (HFs) on important steps of tumor progression, such as epithelial-to-mesenchymal transition, cell migration and stimulation of angiogenesis.

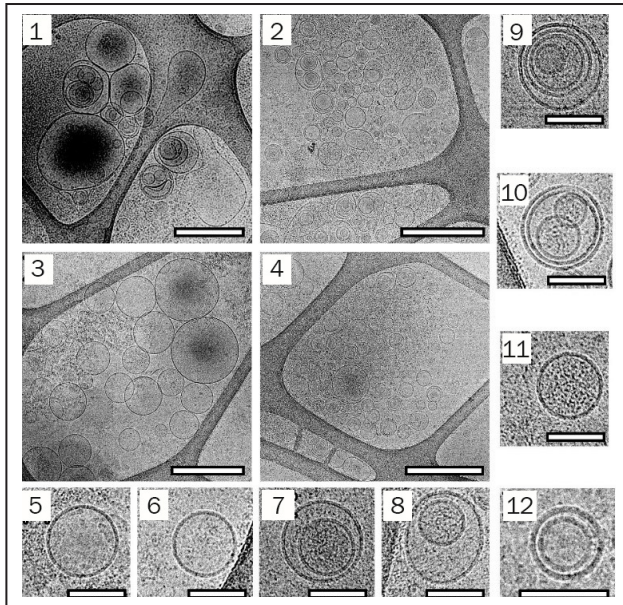
The research was initiated at the Institute of Chemical Biology and Fundamental Medicine of SB RAS and carried out by a team of authors from several research centers. Both extracellular vesicles from blood plasma and vesicles from total blood of HFs and BCPs were isolated by ultrafiltration and ultracentrifugation and then characterized using cryo-electron microscopy (cryo-EM), nanoparticle tracking analysis and flow cytometry. Vesicular size and the presence of exosomal markers on the surface provided evidence that most of the extracellular vesicles were exosomes. Cryo-EM has revealed a wider spectrum of exosome morphology with lipid bilayers and vesicular internal structures in the HF

total blood exosomes in comparison with plasma exosomes (Fig.).

Thus, for the first time, the morphology of exosomes isolated from the total blood of BCPs and HFs was characterized in detail. An *in vitro* study demonstrated the effect of a pool of human whole blood exosomes on the main stages of breast cancer development: angiogenesis, the ability of cells to migrate, invasion, and the formation of intercellular contacts. Some molecular participants of these processes have been identified. In particular, this study demonstrated that the plasma exosomes and total blood exosomes of BCPs had different expression levels of tumor-associated miR-92a and miR-25-3p, induced angiogenesis and epithelial-to-mesenchymal transition (EMT), and increased the number of migrating pseudo-normal breast cells (MCF10A) and the total migration path length of SKBR-3 breast cancer cells. The multidirectional effects of HF total blood exosomes on tumor dissemination were revealed; they suppress the angiogenesis and total migration path length of MCF10A, but stimulate EMT and increase the number of migrating MCF10A and the total path length of SKBR-3 cells. In addition, HF plasma exosomes enhance the metastasis-promoting properties of SKBR-3 cells and stimulate angiogenesis.

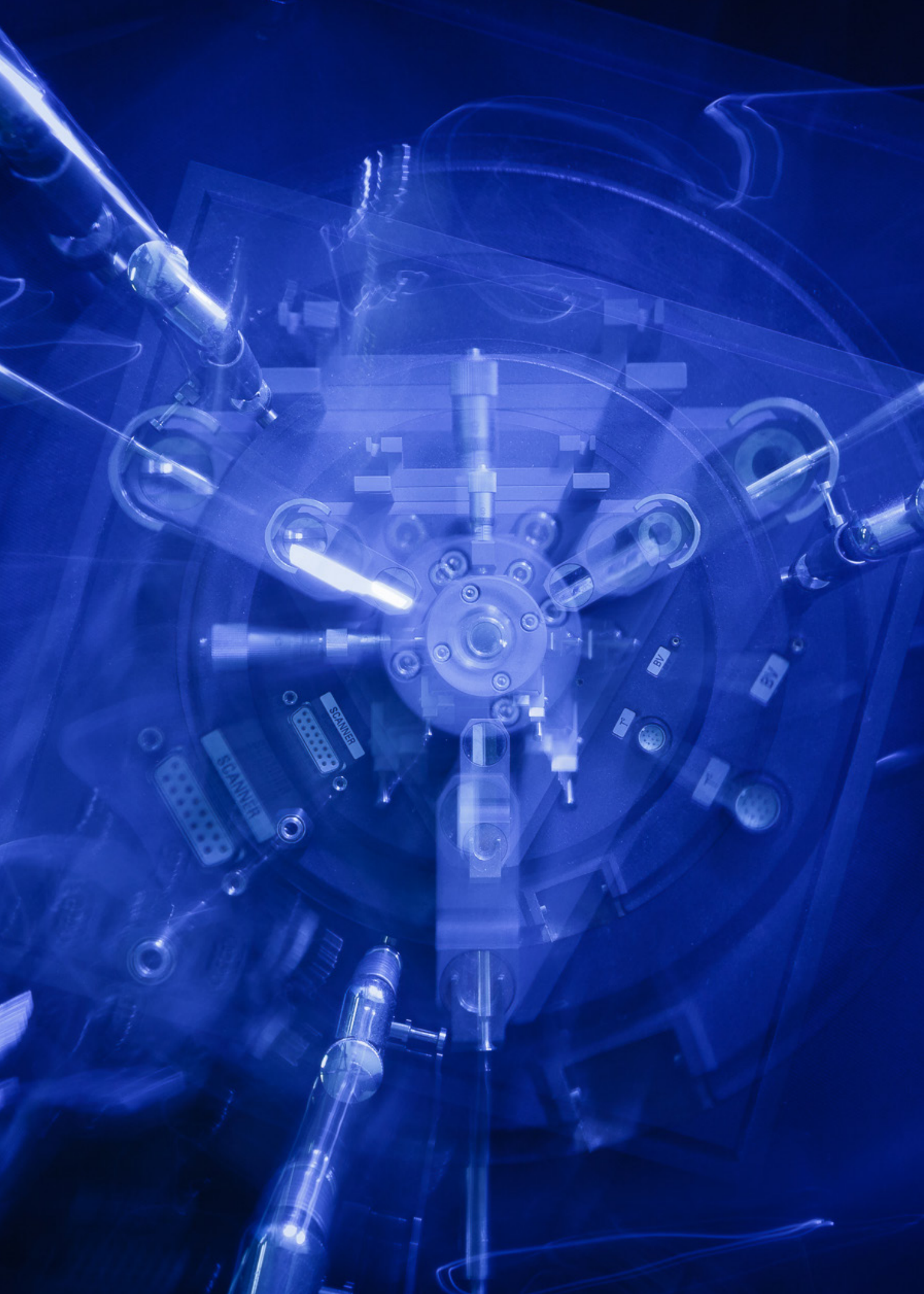
Thus, all subpopulations of human blood exosomes analyzed in this study can potentially be involved in the main stages of carcinogenesis: epithelial-to-mesenchymal transition, cell migration and stimulation of angiogenesis.

Studies of vesicle morphology by cryo-EM were supported by the RSF (No. 19-74-20146).



Representation of exosomes with various morphologies. Exosomes isolated from pooled samples of the plasma (1, 3) and total blood (2, 4) of healthy females (1, 2) and breast cancer patients (3, 4). Vesicles are shown: a single vesicle (5, 6); double vesicles (7, 8, 12); multilayer vesicles (9, 10); double-membrane vesicle (9–11); vesicles with an electron-dense cargo in lumen (7, 9, 11). Scale bars are 500 nm for micrographs (1–4) and 100 nm for micrographs (5–12)

1. Tutanov O., Proskura K., Kamyshinsky R., Shtam T., ..., Tamkovich S. // *Front. Oncol.* 2020. V. 10. P. 580891.
2. Konoshenko M., Sagardze G., Orlova E., Shtam T., Proskura K., Kamyshinsky R., Yunusova N., Alexandrova A., Efimenko A., Tamkovich S. // *Int. J. Mol. Sci.* 2020. V. 21. Iss. 19. P. 7341.



## Nuclear Medicine (Isotope Production, Beam Therapy, Bio- and Nanotechnologies for Medical Purposes)

- 84 A new method of generator radionuclide  $^{212}\text{Pb}/^{212}\text{Bi}$  production
- 85 Development of a proton therapy planning system, dose calculation algorithm

## A new method of generator radionuclide $^{212}\text{Pb}/^{212}\text{Bi}$ production

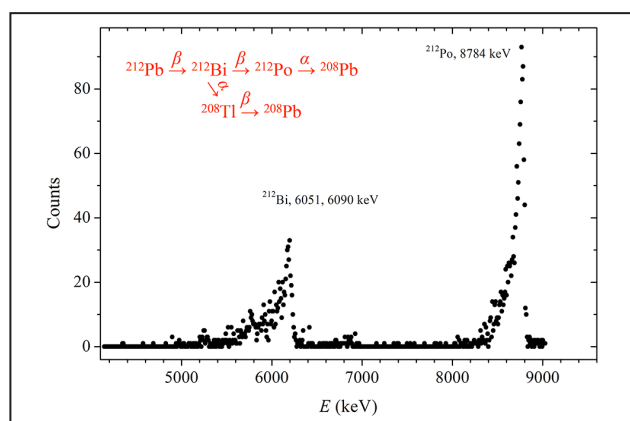
V.N. Pantelev, A.E. Barzakh, D.V. Fedorov, V.S. Ivanov, P.L. Molkanov,  
S.Yu. Orlov, M.D. Seliverstov, Yu.M. Volkov – High Energy Physics Division  
of NRC “Kurchatov Institute” – PNPI

The use of uranium or thorium targets irradiated by proton beams of different energies can be very effective for the production of radionuclides decaying by  $\alpha$ -particle emission. Pharmaceuticals based on  $\alpha$ -emitter radionuclides are the safest and most effective tools for the treatment of different kinds of malignant tumors at the early stage of their formation. One of the main advantages of  $\alpha$ -particles is their very short range (50–90  $\mu\text{m}$ ) in biological tissue. Therefore, the action of a radionuclide emitting  $\alpha$ -particles is very local and does not destroy the surrounding healthy tissues. Radionuclides used for  $\alpha$ -therapy are  $^{223}\text{Ra}$  ( $T_{1/2} = 11.4$  days),  $^{224}\text{Ra}$  ( $T_{1/2} = 3.66$  days),  $^{225}\text{Ac}$  ( $T_{1/2} = 10.0$  days) and radioisotopes  $^{212}$ ,  $^{213}\text{Bi}$ ,  $^{212}\text{Pb}$  as well. These radionuclides can be produced by proton irradiation of uranium or thorium targets.

One of the main goal of radioisotope complex RIC-80, which is being presently constructed at NRC “Kurchatov Institute” – PNPI, is the production of high purity radionuclides for medicine, including the aforementioned  $\alpha$ -particle emitters. This work presents the results of development of a new method on the selective extraction of  $^{212}\text{Pb}$  from a high-density thorium carbide target at a high

temperature. This target material also will be utilized for the mass-separator target construction to produce high purity beams of mass-separated  $\alpha$ -emitting isotopes. In the experiments carried out, a thorium carbide target of a density of about  $6 \text{ g/cm}^3$  was irradiated during 24 h by the 1-GeV proton beam of the SC-1000 synchrocyclotron with an intensity of  $0.1 \mu\text{A}$ . The target mass was about 1 g. After one month of radiation cooling the target was placed into a graphite cavity which was inserted into a tungsten oven heated by resistant heating at the vacuum test bench. During the target heating the evaporated radionuclides were collected on the copper collector cooled by the flowing water. In experiments for selective  $^{212}\text{Pb}$  separation the target material was kept at a temperature of  $1230 \text{ }^\circ\text{C}$  for one hour in a high vacuum of about  $10^{-5}$  mbar. The value of evaporation efficiency of  $^{212}\text{Pb}$  above 90% was obtained. In Figure  $\alpha$ -spectrum of  $^{212}\text{Bi}$  and  $^{212}\text{Po}$ , which are the daughter isotopes of  $^{212}\text{Pb}$  are presented.

This work can be considered as the first stage of the thorium carbide target material investigation, which will be used at RIC-80 for the production of heavy radionuclides  $\alpha$ -emitters.



Alpha spectrum of the daughter isotopes of  $^{212}\text{Pb}$  ( $^{212}\text{Bi}$  and  $^{212}\text{Po}$ ) measured on the copper collector

## Development of a proton therapy planning system, dose calculation algorithm

*N.I. Mamedova, F.A. Pak, A.I. Khalikov, D.L. Karlin, N.A. Kuzora, D.S. Brozhik, O.M. Zhidkova, A.A. Vasiliev – Department of Medical Radiology of NRC “Kurchatov Institute” – PNPI*

Currently, the Medical Proton Complex based on the SC-1000 synchrocyclotron uses a proton beam with an energy of 1 GeV for research activities, which has also been successfully used for radiation therapy of localized intracranial diseases.

Previously, before radiation therapy, the absorbed dose in the therapeutic focus and critical structures was evaluated by simple mathematical calculations, however, rapid progress over the past decades in the field of medical diagnostics and the development of computer technologies has led to the emergence of three-dimensional computer radiation planning, which makes it possible to calculate the conformal dose distribution and assess the likelihood of complications in critical structures.

In 2020, the development of a dose-anatomical treatment planning system (TPS) for 1 GeV proton radiation therapy was started. The main component of the TPS is a dose calculation algorithm using modern calculation methods, taking into account: 1) convergence/divergence of the beam, 2) scattering of protons in matter, 3) change in the linear energy transfer along the trajectory, 4) “blurring” of the dose distribution due to secondary particles. To implement this algorithm, the Monte Carlo simulation with further analytical parameterization was chosen. The Monte Carlo simu-

lation is implemented using a Geant4 libraries, in particular, the hadrontherapy open source. Figure 1 shows the trajectory of primary protons, as well as emerging secondary particles, in a 3 m thick water model phantom calculated in Geant4. When validating the Monte Carlo simulation for a proton energy of 1 GeV, good agreement with the literature data was obtained.

In addition to the dose calculation algorithm, the TPS implements a three-dimensional reconstruction of DICOM images with the ability to visualize structures of various types (skeletal, muscle, connective tissue). Manual and semi-automatic contouring of structures on diagnostic images, as well as automatic contouring of inhomogeneities (Fig. 2) are under development. Work is underway to combine DICOM images of various modalities (CT, MRI, PET) for the most reliable determination of the location and size of target volumes.

In addition to the dose calculation algorithm, taking into account the Monte Carlo simulation, a mathematical method was proposed for calculating the depth dose distributions from a monodirectional beam of protons with an energy of 1 GeV with a rotary irradiation technique. A model of a proton beam is considered in the first approximation without taking into account its interaction

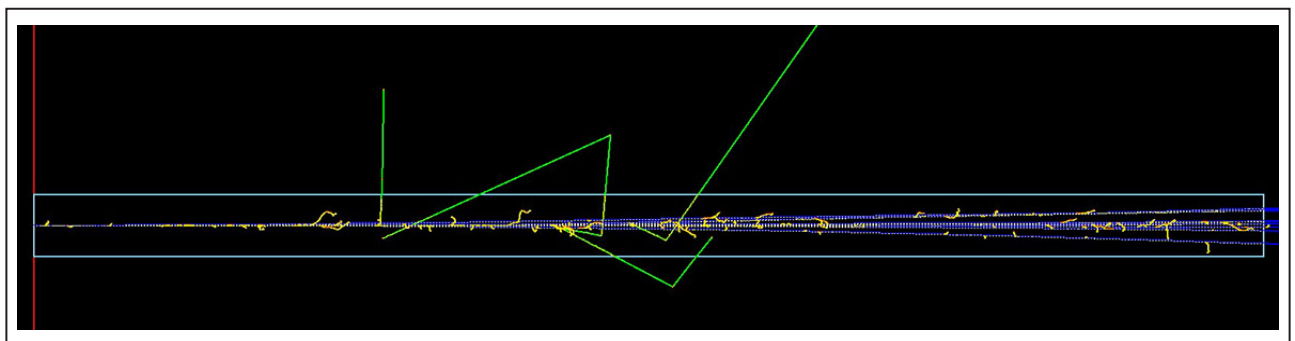


**Fig. 1.** Simulation of the passage of 1 GeV protons through the water layer (blue – primary protons; yellow – electrons; green – photons; red – secondary protons)

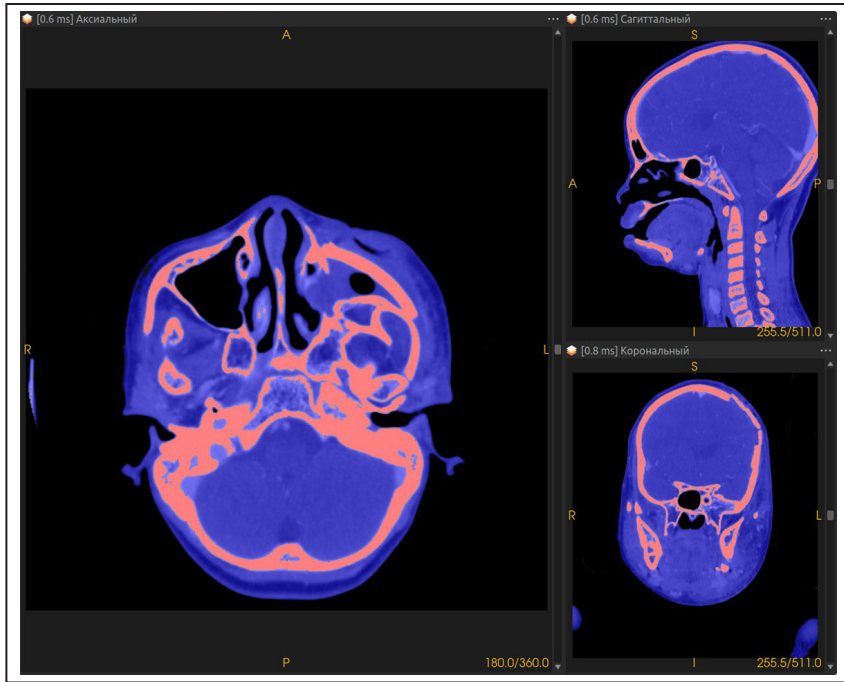


Fig. 2. Contouring of inhomogeneities

with the matter. Comparison of the calculation results with experimental dose distributions obtained by thermoluminescent dosimetry was carried out (Fig. 3). Comparison of the data showed that the deviation of the calculation from the experiment is no more than 10% in the central region of interest. In the future, it is planned to introduce adjustments to the theoretical model to take into

account the physical features of the interaction of protons with matter, increase statistics and determine the scope of the developed calculation method.

In 2020, the scientific staff of the Laboratory of Medical Physics published five articles, including in the Scopus database, five abstracts, and also presented seven reports at scientific conferences.

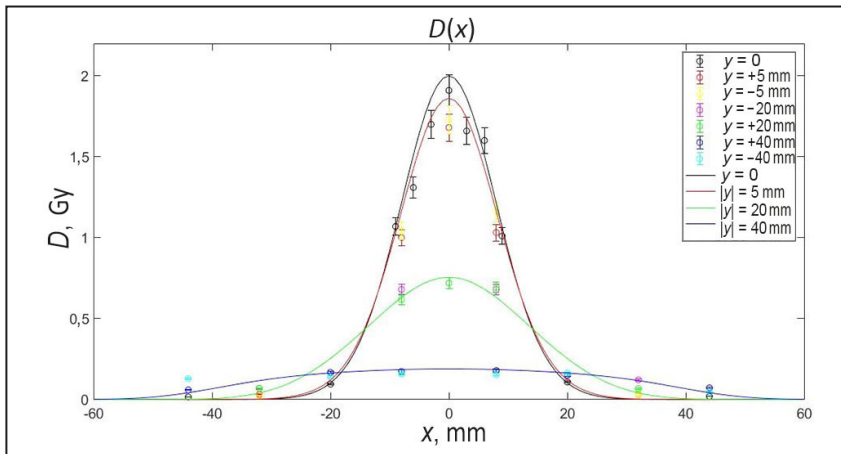


Fig. 3. Comparison of the calculation results (solid lines) with those of the experiment







# Nuclear Reactor and Accelerator Physics

- 90 The status of the heavy water detritiation facility at NRC “Kurchatov Institute” – PNPI
- 91 Investigation of corrosion resistance of aluminum materials for experimental channels of the reactor PIK
- 93 Estimation of the possibility of accumulation of isotopes Es and Bk at reactor PIK
- 94 Comparison of neutron fluxes measured by  $^3\text{He}$ -gaseous proportional detectors and calculated with the PHITS package

## The status of the heavy water detritiation facility at NRC “Kurchatov Institute” – PNPI

S.D. Bondarenko, I.A. Alekseev, T.V. Vasyanina, O.A. Fedorchenko

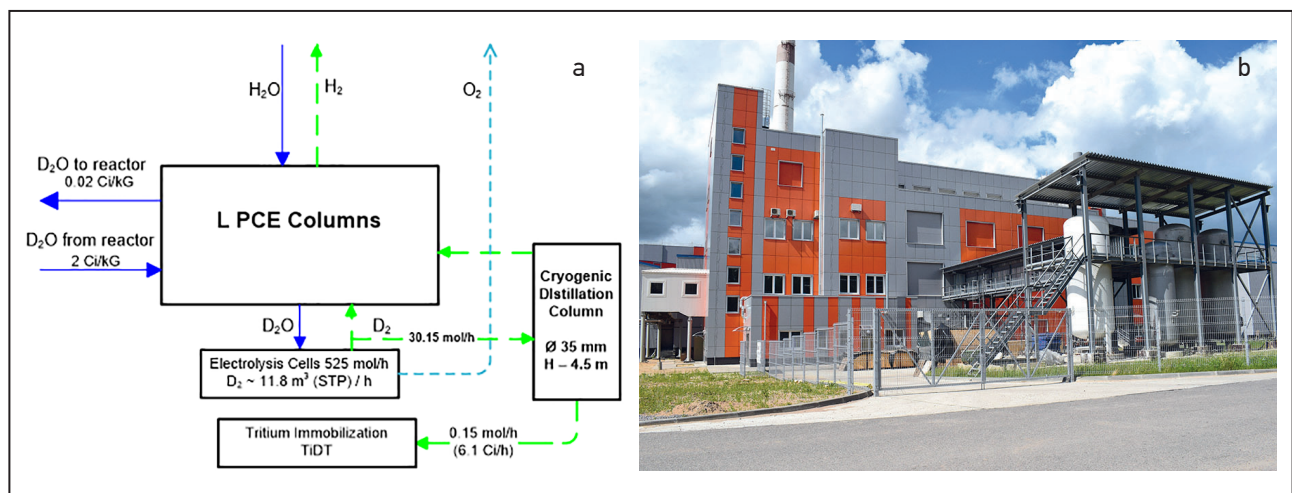
Department of Commissioning of the PIK Reactor, Department of Reactor Physics and Technology of NRC “Kurchatov Institute” – PNPI

The multi-functional tritium removal facility (TRF) has been designed for the heavy water research reactor PIK in Russia. The facility will maintain the tritium concentration in the heavy water of the PIK reactor at a level of no more than  $7.4 \cdot 10^{10}$  Bq/kg (2 Ci/kg), for which it is necessary to extract up to  $1.1 \cdot 10^{16}$  Bq (30 000 Ci) of tritium from the reactor heavy water circuit per year. The TRF will maintain the deuterium concentration of reactor heavy water at a level of at least 99.8 at. % also.

Research work on the development of technology for the isotope purification of heavy water and the creation of the TRF have been carried out at our Institute. A block diagram of the TRF for PIK reactor is shown in Fig. a. The main elements of TRF are a set of isotopic exchange columns with hydrophobic catalyst (LPCE columns), a cryogenic distillation column, an electrolyser, and a system for tritium

immobilization in TiDT form. TRF can also process heavy water waste to obtain conditioned heavy water, including heavy water deeply purified from tritium. The possibility of heavy water waste processing simultaneously with the extraction of tritium and protium from reactor heavy water will improve the functionality and economic efficiency of the TRF.

In 2020, the construction of the TRF building (Fig. b) and external networks were completed. Equipment and devices were purchased. The installation of instruments and pipelines of analytical laboratories was completed. The equipment of the main technology has been installed, and the pipelines are being installed. The installation of general technological systems, ventilation systems, special sewerage systems, and a special network has been completed. Commissioning is scheduled to start next year.



Heavy water detritiation facility of the PIK reactor: a – flowchart; b – building

## Investigation of corrosion resistance of aluminum materials for experimental channels of the reactor PIK

*T.V. Voronina, S.R. Friedmann – Department of Nuclear and Radiation Safety, Department of Reactor Physics and Technology of NRC “Kurchatov Institute” – PNPI, R.M. Ramazanov – Central Research Institute of Structural Materials “Prometey” named by I.V. Gorynin of NRC “Kurchatov Institute”*

The purpose of these works was to validate the corrosion resistance of aluminum materials for experimental channels of the reactor PIK of NRC “Kurchatov Institute” – PNPI in heavy water ( $D_2O$ ) with test specimens from alloys AMg3 and AD1 with different passivating coatings.

The timeliness of this work was due to the uncertainty in pitting growth rates in experimental channels operating in heavy water, and the need to increase the operation time of experimental channels after operation in the heavy water reflector during the first criticality of PIK and under a long-term shutdown mode within six years.

For corrosion tests 30 samples from aluminum alloys AMg3 of GOST 17232-99 and AD1 of GOST 4784-97 with dimensions of  $5 \times 30 \times 50$  mm and different surface treatment were used. The appearance of the samples is presented in Fig. 1.

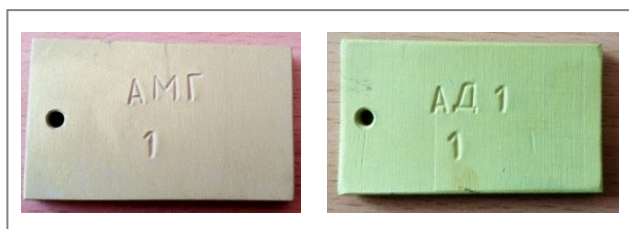


Fig. 1. Appearance of corrosion test samples

For tests the corrosion test stand with a stainless steel (12Cr18Ni10Ti) tank in the amount of  $\sim 100$  l was designed and produced. The tank was equipped with a sealed detachable cover, preheating and temperature control systems, a water decanting boot. Inside the tank the stainless steel (12Cr18Ni10Ti) hangoff system for samples was placed. It excludes the contact of the samples with one another (Fig. 2).



Fig. 2. Appearance of a corrosion test stand

Heavy water for tests was prepared according to the regulations for the reactor PIK. During the tests carried out at 6500 h at the temperature of  $60^\circ C$  an inspection, investigation of samples and chemical analysis of heavy water were performed.

Virtually all samples including samples with pittings have significant weight increase after exposure during  $\sim 1500$ ,  $\sim 3500$  and  $\sim 6500$  h in media. On average, for all samples the specific overweight was in limits of  $0.7\text{--}1.0$  mg/cm<sup>2</sup> and weakly depended upon a holding time in water. Under operation conditions similar to those in the heavy water reflector tank, according to indirect data, the rate of total corrosion was in the range of  $0.03\text{--}0.2$   $\mu\text{m}/\text{year}$ .

The two cases of operational occurrences for the experimental channels with pittings were chosen. The first one is the loss of tightness. One or more pittings grow with a high rate and result in failure

of a channel under pitting regrowth through wall thickness. When this happens the given case does not have an effect on the channel strength. When assessing the ultimate behavior at tightness loss conditions (limiting thickness of a pitting is 0.75 from the initial wall thickness) the upper estimate of the pitting growth rate of 1.20 mm/year can be recommended.

The second case is the loss of strength. It is conservatively assumed that pittings on the channel surfaces keep growing at an average rate. In that case the chain of pittings can form a crack shape. In this case, the strength of channels with a hypothesized crack needs to be assessed. When assessing the ultimate behavior of experimental channels in terms of strength (limiting thickness of a pitting from the initial wall thickness) the pitting growth of 0.25 mm/year rate was recommended.

The chemical analysis of heavy water on intermediate final stages of tests confirmed high corrosion

resistance of sample materials with all different surface treatments. The absence of visible corrosion damage on the samples in the given tests is basically owing to the low content of ferrous ions in heavy water.

According to the test results, an anticorrosion coating using the chromate anodizing technology was recommended for newly manufactured aluminum channels.

The reactor facility PIK has experimental equipment, and long-time corrosion test procedures for different materials in heavy water were developed. It allows to carry out necessary investigations. In particular, the continuation of work in this area would be the investigation of welded joint serviceability AMg3 + AMg5 in a sample slope state in light and heavy water containing ferrous ions  $\text{Fe}^{2+}$  in quantity of 0.1–0.5 mg/l and not containing them.

## Estimation of the possibility of accumulation of isotopes Es and Bk at reactor PIK

M. S. Oegin

Theoretical Physics Division of NRC "Kurchatov Institute" – PNPI

There are only two high flux reactors in the world where the production of transcurium isotopes is possible. They are the HFIR reactor (Oak Ridge, USA) and the SM-3 reactor (Dimitrovgrad, Russia). At reactor PIK in the central experimental channel the record thermal neutron flux takes place which makes it possible to produce transcurium isotopes there. Presently the design of the core for reactor operation after full power startup is under consideration. The additional places for isotopes production in the reactor core can be organized besides the central experimental channel.

The irradiation conditions in the central experimental channel and in the core are compared. For this purpose we have calculated the neutron spectra, neutron fluxes and cross sections of the main reactions at these places, which affect the isotope production. We made the approximation of the mean reaction cross sections using thermal cross sections, resonance integral and Westcott factors. For the realistic isotope targets we have calculated the amount of produced einsteinium and berkelium. Also we compare the accumulation speed of these two elements in the central water trap and in the reactor core. We have made the verification of the MCNP code calculations of the isotope production using analytic calculations and code SCALE.

It was demonstrated that for targets with the raw isotopes placed in the core the amount of

einsteinium and berkelium produced can be 4–5 times greater than for targets placed in the central experimental channel. However, the time for isotope production in the core can be about two times longer. We also discuss the main ambiguities in the reaction cross section which influence the amount of the einsteinium produced in the target. The main ambiguity in the calculations of the produced amount of rather long-lived isotope  $^{254}\text{Es}$  is introduced by the neutron reaction cross sections of  $^{253}\text{Es}$  nuclei, especially by the isomeric ratio of the reaction of the neutron radiation capture.

Isotopes of berkelium and einsteinium in macroscopical quantities are needed for the synthesis of the super heavy elements. The production of such elements in Dubna at the super heavy elements factory gives the opportunity to confirm the hypothesis of the existence of the island of stable neutron enriched isotopes. Another application concerns the  $^{252}\text{Cf}$  isotope as an intensive neutron source. The  $^{249}\text{Bk}$  isotope can be also obtained as a byproduct of the production of  $^{252}\text{Cf}$  isotope in the central experimental channel of the reactor PIK.

As a result the reactor PIK as well as the reactor SM-3 can be used for accumulation of transcurium isotopes for the fundamental and applied purposes.

## Comparison of neutron fluxes measured by $^3\text{He}$ -gaseous proportional detectors and calculated with the PHITS package

L.A. Axelrod, G.P. Didenko, K.V. Ershov, V.G. Zinoviev, I.A. Mitropolsky – Neutron Research Division of NRC «Kurchatov Institute» – PNPI, S.E. Belov – V.G. Khlopin Radium Institute

Development of the radiation protection system and neutron moderator for the Pu-Be neutron source gives rise to a special problem for modeling the spectrum of such a source. The neutron flux from a radioactive source depends on the energy of primary  $\alpha$ -particles, the amount of impurities, the size of plutonium dioxide grains, and other technological factors. The simulation of the Pu-Be source was performed using the PHITS version 3.10 program in accordance with the factory specification datasheet. This program describes the transport of charged particles, neutrons,  $\gamma$ -quanta and heavy ions by the Monte Carlo method. The behavior of the calculated spectrum also depends on the grain size of plutonium dioxide (Fig. 1).

To test the simulation, we used a stand presented in Fig. 2 which consisted of the container made from borated polyethylene but instead

of the conventional cover we used a moderator with various combinations of “pure” and borated polyethylene. The source had an  $\alpha$ -decay activity of  $2.4 \cdot 10^{11}$  Bq and produced the isotropic flux of  $10^7 \text{ cm}^{-2} \cdot \text{s}^{-1}$  at the time of manufacture (two years before our experiment).

Experiments were carried out with a variety of moderators and in various configurations. All the amplitude spectra obtained as a result of measurements turned out to be similar and differed only in amplitude. To determine the background, polyethylene sheets were placed between the source and the detector until the counting rate stopped changing. The latter value was taken as the background. In our measurements we also used a position-sensitive  $^3\text{He}$ -filled detector manufactured by NRC “Kurchatov Institute” – PNPI to test and prepare it for inclusion in the instrument suite of the PIK reactor.

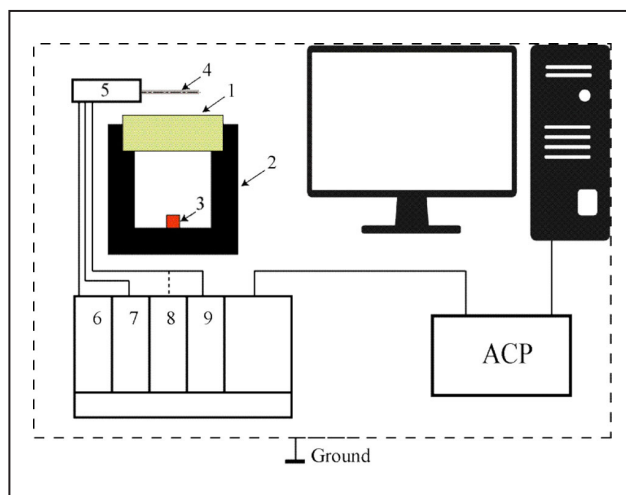


**Fig. 1.** The experimental stand: 1 – moderator; 2 – container; 3 – source; 4 – counter SNM-50; 5 – preamplifier; 6, 7 – low and high-voltage power; 8 – digital counter; 9 – spectrometric amplifier

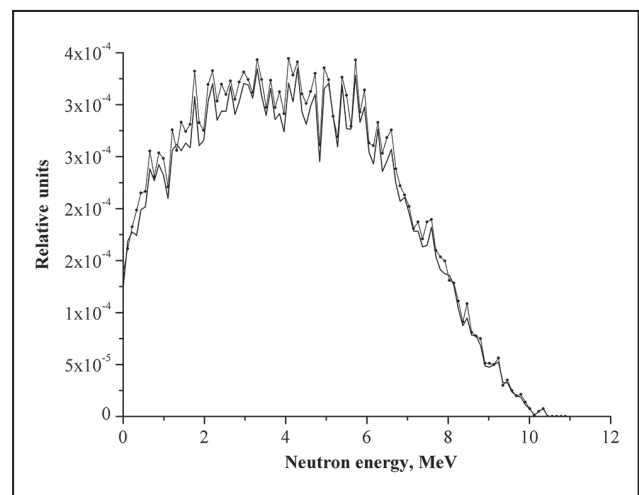


**Fig. 2.** Calculated neutron spectra of the Pu-Be source: the solid line for 5.6  $\mu\text{m}$  grains of Pu dioxide, the line with dots for 5.0  $\mu\text{m}$  grains of Pu dioxide

The calculations performed using the PHITS program package qualitatively describe the experimental data obtained, but a good quantitative agreement could not be reached. One of the reasons for this is that the composition of the materials is not exactly known and may include impurities that absorb neutrons.

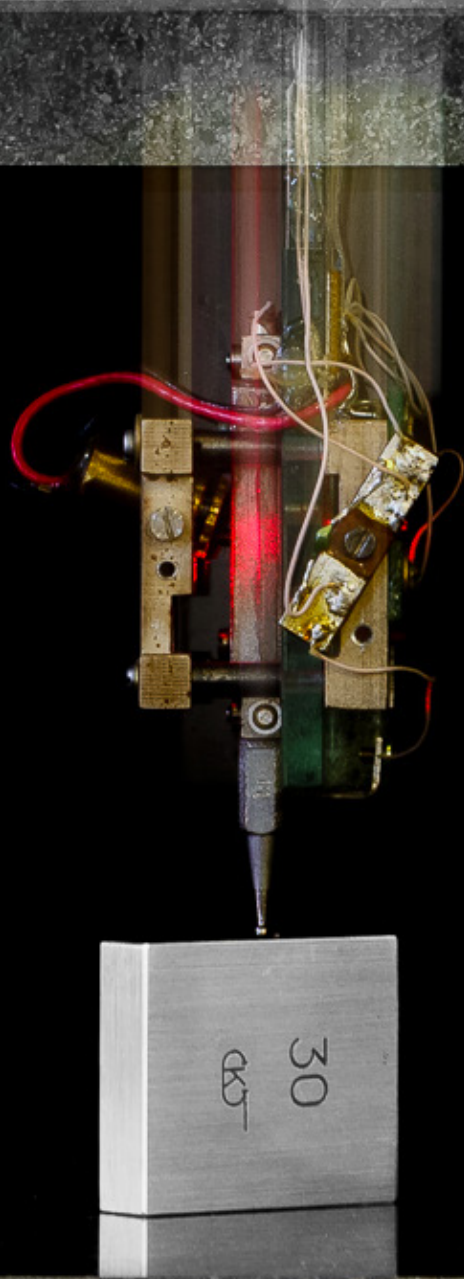
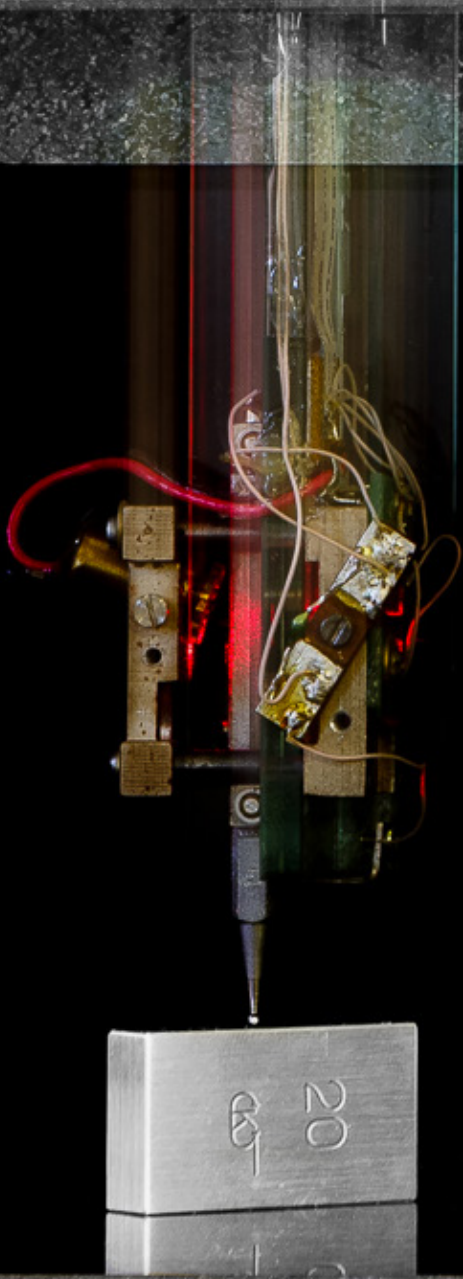
Model calculations showed the maximum neutron absorption is carried out when the boron content in polyethylene is at the level of 2–4%. Furthermore, the number of neutrons leaving the system increases with increasing boron concentration, *i. e.* absorption decreases (due to high-energy neutrons). It is possible to find out whether this fact has a physical reason or it is a feature of the software package using an experiment with a detector

that allows registering fast neutrons, or in an experiment at a synchrocyclotron (GNEISS stand), where you can use a time-of-flight technique.

A comparison of the calculated and experimental data allowed us to draw the following conclusions:

- The modeling method used proved to be quite reliable;
- The coincidence of the experimental and calculated results depends only on the weighted average neutron energy, and not on their energy distribution;
- To measure the spectrum of a Pu-Be source, a fast neutron detector must be used, and such an experiment is planned;
- The concentration of boron in the protection has a value close to the optimal one.





## Applied Research and Developments

- 98 Crystal and supramolecular structure of bacterial cellulose hydrolyzed by cellobiohydrolase from *Scytalidium candidum* 3C: a basis for development of biodegradable wound dressings
- 99 A database for inventory of proteoform profiles: “2DE-pattern”
- 100 Composite proton-conducting membranes with nanodiamonds
- 101 Upgrade of the ATLAS muon spectrometer
- 102 Information on the work of Holographic Information and Measuring Systems Laboratory in 2020

## Crystal and supramolecular structure of bacterial cellulose hydrolyzed by cellobiohydrolase from *Scytalidium candidum* 3C: a basis for development of biodegradable wound dressings

L.A. Ivanova, E.V. Eneyskaya, V.S. Burdakov, N.A. Verlov, A.A. Kulminskaya, G.P. Kopitsa – Molecular and Radiation Biophysics Division, Neutron Research Division of NRC “Kurchatov Institute” – PNPI,  
A.Ye. Baranchikov, K.B. Ustinovich – N.S. Kurnakov Institute of General and Inorganic Chemistry of the RAS,  
T.V. Khamova – I.V. Grebenshchikov Institute of Silicate Chemistry of the RAS,  
Y.E. Gorshkova – Frank Laboratory of Neutron Physics of Joint Institute for Nuclear Research,  
N.V. Tsvigun – Federal Scientific Research Center “Crystallography and Photonics” of the RAS,  
E.V. Zinoviev, M.S. Asadulaev, A.M. Fedyk, A.S. Shabunin – Laboratory for Experimental Surgery of Saint Petersburg State Pediatric Medical University

The bacterial cellulose (BC) synthesized by the *Gluconacetobacter hansenii* ATCC 10821 strain was treated with cellobiohydrolase isolated from the yeast *Scytalidium candidum* 3C. The crystal and supramolecular structure of the bacterial cellulose has been studied at different stages of cellobiohydrolase hydrolysis using various physical and microscopic methods. Enzymatic hydrolysis significantly affected the crystal and supramolecular structure of native BC, in which 3D polymer network consisted of nanoribbons with a thickness  $T \approx 8$  nm and a width  $W \approx 50$  nm and with a developed specific surface  $S_{\text{BET}} \approx 260$  m<sup>2</sup> · g<sup>-1</sup>. Biodegradation for 24 h led to 10% decrease in the mean crystal size  $D_{\text{hkl}}$  of BC, to two-fold increase in the sizes of nanoribbons and in the specific sur-

face area  $S_{\text{BET}}$  up to  $\approx 100$  m<sup>2</sup> · g<sup>-1</sup>. Atom-force and scanning microscopy images showed BC microstructure “loosening” after enzymatic treatment, as well as the formation and accumulation of submicron particles in the cells of the 3D polymer network. Experiments *in vitro* and *in vivo* did not reveal cytotoxic effect by the enzyme addition to BC dressings and showed a generally positive influence on the treatment of extensive III degree burns, significantly accelerating wound healing in rats.

Thus, in our opinion, the results obtained can serve as a basis for further development of effective biodegradable dressings for wound healing.

This research was funded by the NRC “Kurchatov Institute” (project No. 1363).

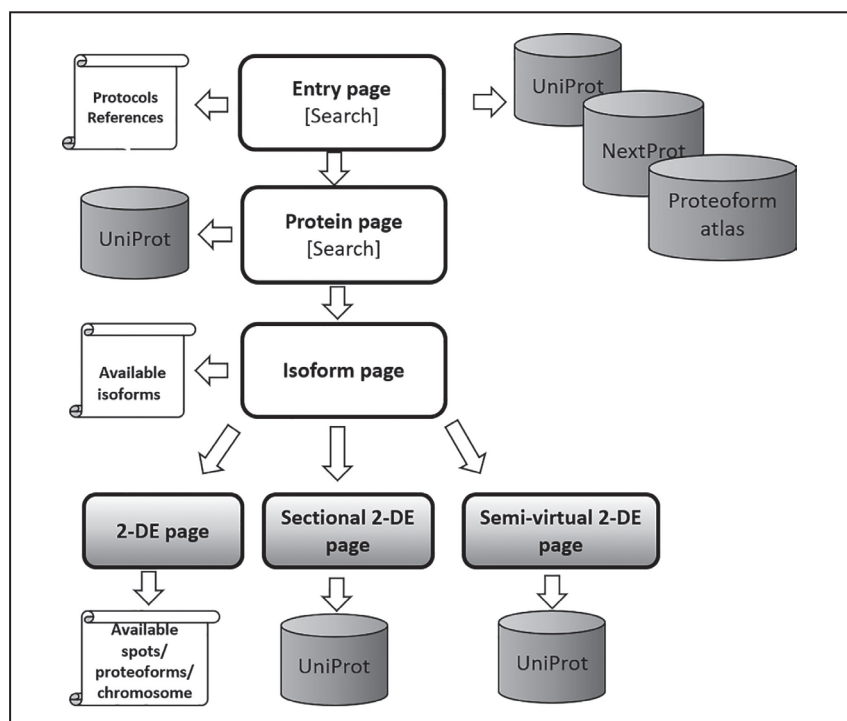
## A database for inventory of proteoform profiles: “2DE-pattern”

S.N. Naryzhny, N.V. Klopov, N.L. Ronzhina, O.A. Kleyst, N.V. Belyakova, O.L. Legina – Molecular and Radiation Biophysics Division of NRC “Kurchatov Institute” – PNPI, E.S. Zorina, V.G. Zgoda – V.N. Orekhovich Research Institute of Biomedical Chemistry

The human proteome is composed of a diverse and heterogeneous range of gene products/proteoforms/protein species. Because of the growing amount of information about proteoforms generated by different methods we need a convenient approach to make an inventory of the data. Here, we present a database of proteoforms that is based on information obtained by separation of proteoforms using two-dimensional electrophoresis (2DE) followed by shotgun ESI LC-MS/MS. The principles and structure of the database are described. The database is called “2DE-pattern”

(Fig.) as it contains multiple isoform-centric patterns of proteoforms separated according to 2DE principles. The database can be freely used at <http://2de-pattern.pnpi.nrcki.ru>.

A user starts from the top, “Entry page”, where a choice of search parameters can be found. According to the choice, a “Protein page” of the desired protein will be opened. Beneath, a choice of isoform for this protein is available. From “Isoform page”, a selection of three types of 2DE pattern for the isoform is available: “2-DE page”, “Sectional 2-DE page”, or “Semi-virtual 2-DE page”.



A flow chart of the proteoform database “2DE pattern”

## Composite proton-conducting membranes with nanodiamonds

Yu.V. Kulvelis, V.T. Lebedev, V.Yu. Bayramukov  
Neutron Research Division of NRC "Kurchatov Institute" – PNPI

A new approach was applied to improve the proton conductivity mechanism in perfluorinated membranes for hydrogen fuel cells. The membranes based on short-side chain copolymer (Aquivion®) were modified with functionalized diamond nanoparticles. Carboxylated nanodiamonds embedded in the polymer matrix provide an increase in conductivity at a moderate nanodiamond content, while the mechanical strength of the membranes remains high (Fig. 1). The casting method of compositional membranes preparation from suspensions in *N,N*-dimethylformamide allowed saving the general channel structure in membranes at the presence of nanodiamonds, in agreement with neutron scattering data (the ionomer peak remains) (Fig. 2).

We propose the formation of additional areas of conductivity, formed controllably, due to nanodiamond particles associated with polymer chains,

on the surface of which accelerated diffusion of protons through the hopping Grotthuss mechanism from the centers of proton adsorption proceeds with the transition to proton-conducting channels of the polymer matrix covered with sulfonic groups. The composite perfluorinated Aquivion®-type membranes with nanodiamonds, prepared by casting method, provide temperature-dependent effect of modified proton conductivity mechanism. Carboxylated nanodiamonds serve as proton reservoirs, accumulating protons at low temperatures. At higher temperatures the additional protons penetrate to the conducting channel system, thus, increasing the conductivity. The measured effect of raising the proton conductivity at 50 °C and good mechanical properties allow us to be sure of improving the performance of this type of membranes at real working temperatures in fuel cells up to 130 °C.

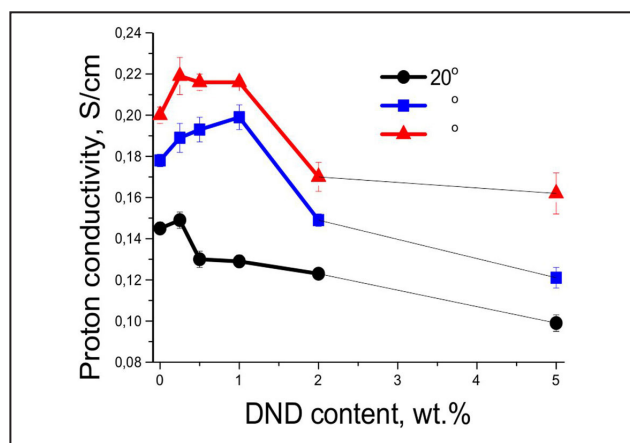


Fig. 1. Proton conductivity of compositional membranes at 20, 35 and 50 °C vs. Content of nanodiamonds

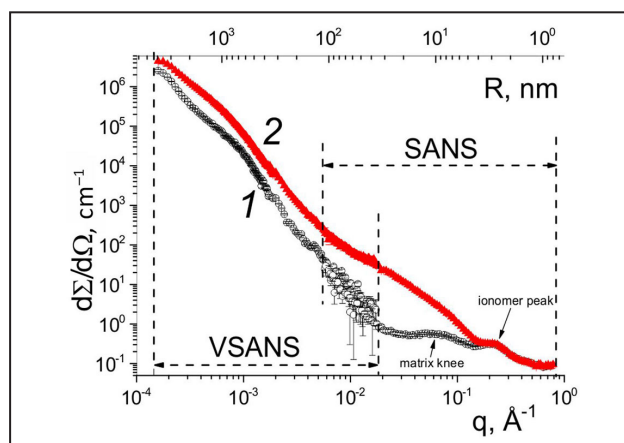


Fig. 2. Small and very small angle neutron scattering on membranes in dry condition: 1 – sample without nanodiamonds; 2 – compositional membrane with 5 wt. % of nanodiamonds

## Upgrade of the ATLAS muon spectrometer

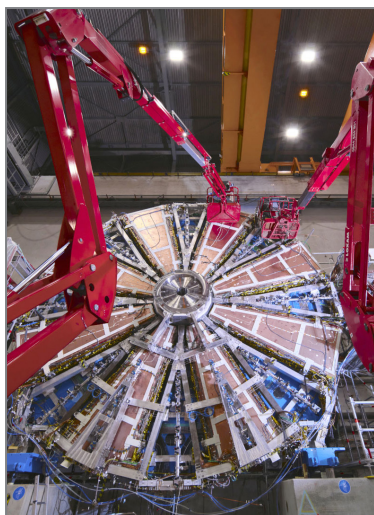
S.G. Barsov, V.T. Grachev, A.E. Ezhilov, M.P. Levchenko, V.P. Maleev, Yu.G. Naryshkin, D. Pudzha, V.M. Solovyev, O.L. Fedin, V.A. Schegelsky – High Energy Physics Division of NRC “Kurchatov Institute” – PNPI, ATLAS Collaboration

The instantaneous luminosity of the Large Hadron Collider (LHC) at the European Organization for Nuclear Research (CERN) will be increased up to a factor of five with respect to the design value by undergoing an extensive upgrade program over the coming years. The motivation for this upgrade is to precisely study the Higgs sector and to extend the sensitivity to new physics to the multi-TeV range. In order to achieve these goals, the ATLAS experiment has to maintain the capability to trigger on moderate momentum leptons under background conditions much harder than those currently present at the LHC. For the muon spectrometer (MS) such requirements necessitate the replacement of the forward muon-tracking region (called the muon Small Wheel) with new detectors capable of precision tracking and triggering simultaneously. The New Small Wheel (NSW) upgrade is designed to cope with the high luminosity that is expected at  $L = (2-5) \cdot 10^{34} \text{ cm}^{-2} \cdot \text{s}^{-1}$  during Run 3 and the high luminosity LHC (HL-LHC).

The NSW utilizes two detector technologies: small-strip thin gap chambers (sTGC) as the primary trigger and micromegas (MM) as the primary precision tracker. sTGCs are multiwire proportional chambers with thin gas volume with an anode-cathode spacing of 1.4 mm, while the spacing between the anode wires, which are made of gold-plated tungsten, is 1.8 mm. The cathode planes are a 1.3 mm thick printed circuit board with a 200  $\mu\text{m}$  thick layer of pre-preg on top of them. Over this, the cathode planes are sprayed with a graphite to build a resistive layer. One of the cathode planes is segmented into rectangular

pads that are used in the trigger system to identify regions of interest in the strips and wires. The other cathode plane is segmented into 3.2 mm pitch strips in the azimuthal direction. The chambers are operating in the quasi-saturated mode at 2.85 kV with a gas amplification of  $2 \cdot 10^5$ . Individual sTGC layers are then assembled into modules consisting of four sTGC layers, known as quadruplets.

sTGC quadruplets for the NSW are produced in Russia, Israel, Canada, China and Chile. NRC “Kurchatov Institute” – PNPI was in charge of producing 36 of the largest quadruplets QL3 with surface area of 2.3 m<sup>2</sup>. NRC “Kurchatov Institute” – PNPI successfully finished the production and testing of all detectors in November 2020. Currently, all the detectors produced in NRC “Kurchatov Institute” – PNPI have been shipped to CERN, where the NSW wheels are currently being assembled (Fig.).



Mounting of the first NSW wheel (wheel A) at CERN

## Information on the work of Holographic Information and Measuring Systems Laboratory in 2020

*B.G. Turukhano*

*Knowledge Transfer Division of NRC "Kurchatov Institute" – PNPI*

In 2020, the Holographic Information and Measuring Systems Laboratory (HIMSLab) continued the development of a universal angle measuring machine – UIM. The basic design of the UIM was created, and the nano-measuring linear and angle holographic encoders LHE and AHE, which are part of the UIM, were developed and manufactured. A special program has been developed for the motion control system for linear and radial sensors.

The LHE linear movement transducer allows you to increase the accuracy and resolution when measuring linear dimensions in the entire measured movement range up to a meter or more, regardless of the quality of the system guides. As a result, here we deal with an expansion of the range of processed or studied objects while maintaining high accuracy and resolution of the measuring system. The task of the proposed invention is to estimate the error introduced into the movement measurement value due to the occurrence of moire fringes from inaccurate LHE guides.

Inaccuracies of fabrication of LHE guides along which one of the gratings moves, affects the value of the fringe (Moire fringe) period, and consequently, the value of the movement itself, therefore, not this value but the value of the obturation bands is used to measure the length, since they are independent (invariable) from the quality of the guides.

The task is solved not by improving the quality of the guides through their mechanical processing, which is expensive, extremely difficult and practically impossible, especially in case of large lengths (up to a meter or more), but by real-time digital compensation of the error introduced by the appearance of moire fringes resulting from the movement of a carriage containing one of the sensor gratings along its guide by the amount of movement or length

of the product to be calibrated or being manufactured.

In connection with the need to study the accuracy characteristics of the LHE and AHE sensors, a metrological system was created and equipped in the underground part of the vibration-proof and temperature-controlled laboratory of the HIMSLab. In addition, the precision linear transducer of the Japanese company "Mitutoyo", which is used in experiments by High Energy Physics Division of NRC "Kurchatov Institute" – PNPI was certified using the same device. The certification was carried out using a precision metrology linear holographic sensor LHE-700 HIMSLab. The accuracy of the Japanese sensor was three times less than that of the HIMSLab sensor.

In the HIMSLab a high-precision spindle was designed, manufactured and tested. Using the NANO IPS-2 stand (Fig. 1), the radial runouts of the spindle of a nano-measuring single-axis holographic rotary table were studied. The radial runouts of the spindle vary from 0.05 to 0.38  $\mu\text{m}$  per revolution, and the axial ones – from 0.2 to 0.45  $\mu\text{m}$ .

Also, the spindle was tested using a nano-measuring holographic length meter DG-30 (Fig. 2), recognized as a measuring instrument according to the Verification Certificate issued by the State Committee of the Russian Federation for Standardization and Metrology No. 112511-7-121/10, and the Certificate approving the type of the measuring instrument RU.C.27.001.A No. 100899, issued by the Federal Agency for Technical Regulation and Metrology.

The accuracy of DG-30 is  $\pm 0.05 \mu\text{m}$ , the resolution is 0.01  $\mu\text{m}$  at a length of 30 mm. The values of the runout of this spindle turned out to be no more than 0.2  $\mu\text{m}$ .

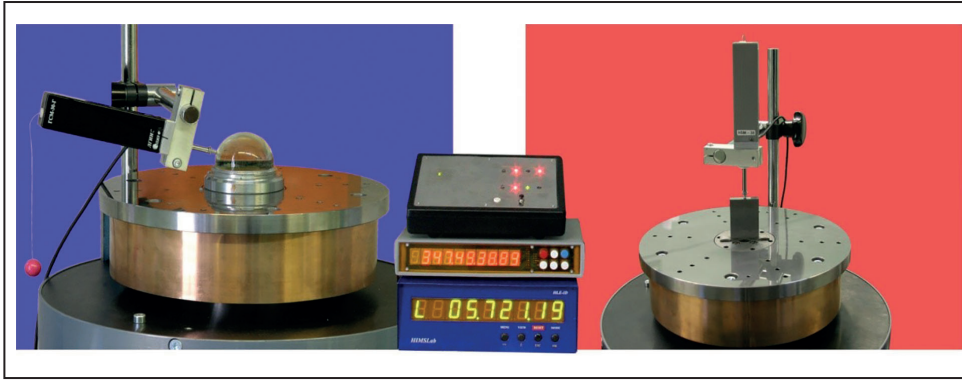


**Fig. 1.** NANO IPS-2 test stand to study of the roundness of parts, their radial and axial runouts using a holographic DG-100 length meter



**Fig. 2.** Holographic DG-30 length meter with access to an autonomous display unit

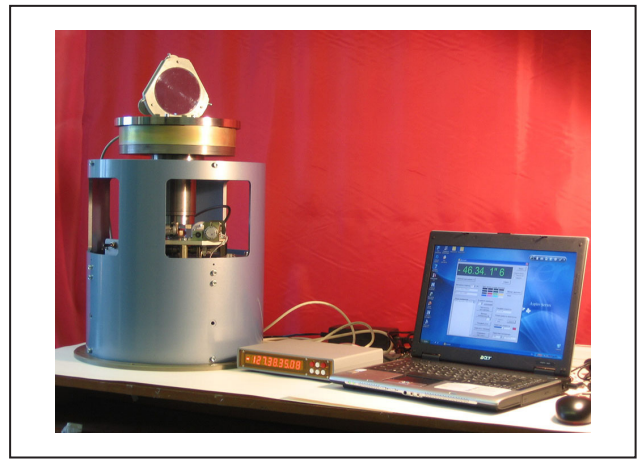


**Fig. 3.** Nano-measuring two-spindle mirror goniometer NANO DZG

Studies of radial and axial runouts of a spindle with nano-accuracy are necessary for the calibration of spindles built into ultra-precision angle measuring systems:

- Angular nano-measuring sensors (see Fig. 1) based on high-precision holographic gratings R, which have a potential accuracy of up to one-hundredths of an arcsecond;
- Angle measuring machines required for certification and calibration of code disks;
- High-precision nano-measuring rotary tables used in guidance systems, as well as for calibration

of electric motors for space systems: ultra-precision nano-measuring two-spindle mirror goniometer NANO DZG (Fig. 3) and ultra-precision two-spindle nano-measuring holographic rotary table – single-axis test stand NANO IPS-2;

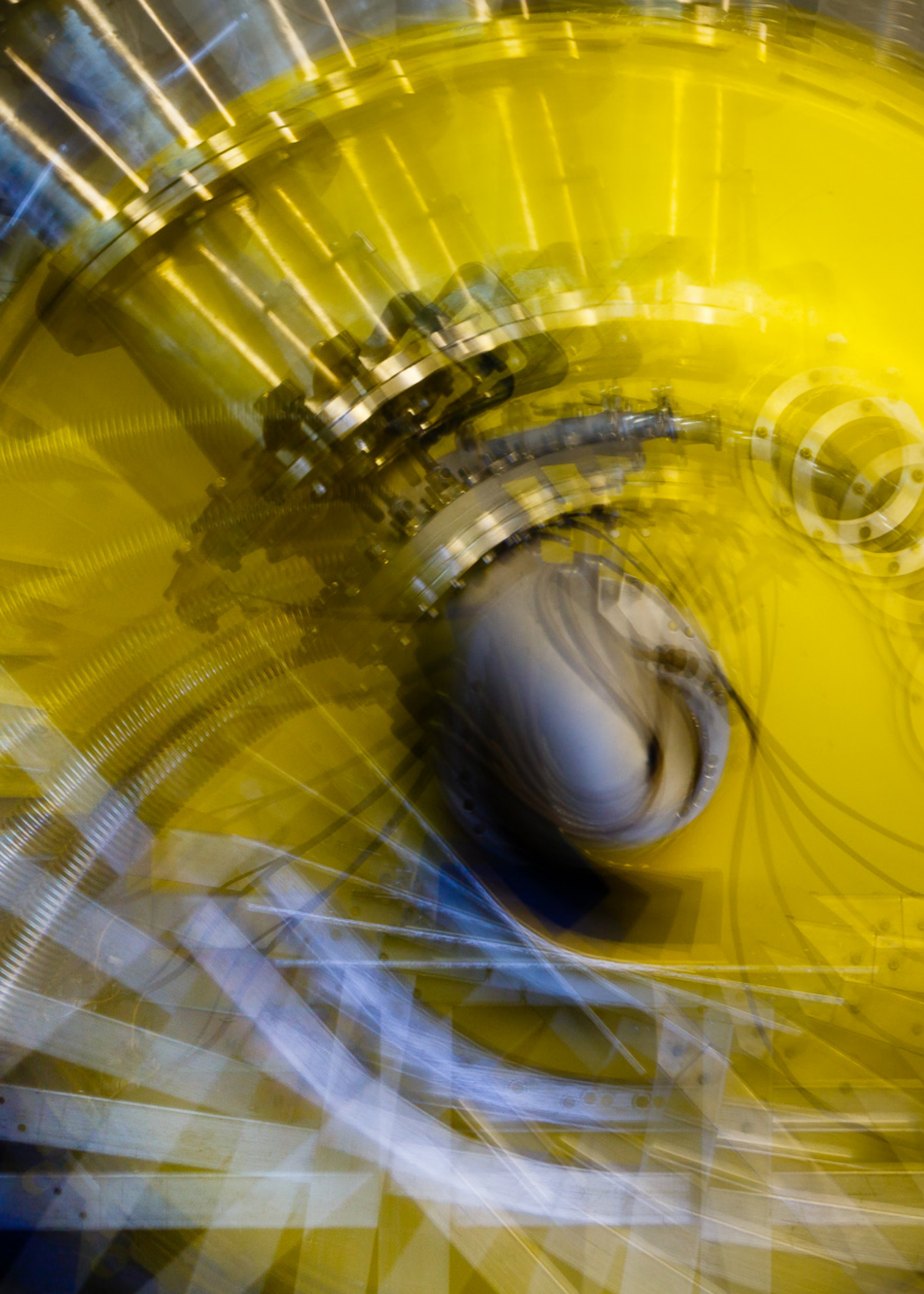
- Systems in C-class high-precision machines under the Standard of Council of Mutual Economic Assistance 3111-81 with digital-program control, which produce units and spare parts for space systems in order to increase their accuracy and reliability.

1. B.G. Turukhano et al. // Instrum. Systems: Monitor., Control, Diagnost. 2020. No. 9. P. 24–28.

2. Turukhano B.G. et al. // Nanoindustry. 2020. No. 6. P. 384–390.

3. Linear Movement Transducer: RF Utility Model Patent No. 201730 / Turukhano B.G., Turukhano I.A., Turukhano N.; Priority Data 29.10.2020.





## Basic Installations

- 106** Power Start-up Program of the PIK reactor at a power of 10 MW
- 107** Commissioning of experimental stations at the PIK reactor
- 108** The work of SC-1000 synchrocyclotron to ensure the scientific and experimental activities of NRC “Kurchatov Institute” – PNPI in 2020

## Power Start-up Program of the PIK reactor at a power of 10 MW

*A.S. Zakharov, A.S. Poltavskii*

*Department of Reactor Physics and Technology, Department of Nuclear and Radiation Safety of NRC “Kurchatov Institute” – PNPI*

In March–April 2019, hydraulic tests with fuel assembly simulators were conducted, during which the characteristics of the primary circuit and its main equipment were measured at various configurations of core loading for validation of design models of the PIK research nuclear installation.

Reports have been prepared on the verification of all computer programs used to justify the safety of the next stage of power start-up – reaching a power of 10 MW. As part of the implementation of the Power Start-up Program of the PIK research nuclear installation, a test program in the low power testing mode up to 10 MW has been developed, which determines the procedure for reaching the power up to 10 MW, the volume and methods of performing tests and experiments, as well as the procedure for the core unloading when the tests are over.

A special feature of the experiments in the low power testing mode up to 10 MW is the limitation of energy yield of 2–5 MW · day, which provides safe conditions for the performance of works on modernization of safety-critical elements and systems, and the scheduled replacement of individual channels in the reflector within the framework of the project “Creation of the Instrument Suite of the PIK Neutron Research Facility of NRC “Kurchatov Institute” – PNPI” before the transition to the stage of 100 MW power ascension.

Tests and experiments including those listed below were started in 2020:

- Placement of neutron activation detectors in inclined and vertical experimental channels, reaching a critical state with twelve fuel assemblies and

- six aluminum fuel assembly simulators in the core, irradiation of neutron activation detectors at power, primary calibration of neutron flux monitoring equipment;

- Checking the symmetry and actual position of the heavy control members and protection system devices (shutters) according to the results of overcompensation in critical condition;

- Measuring the reactivity effects when filling the circuit of a liquid regulator with a heavy-water coolant;

- Measuring the barometric, consumption and temperature coefficients of reactivity;

- Automatic power controller functioning test;

- Alignment of scientific equipment and carrying out of experiments at five research neutron stations.

The works are performed by the teams of the following institutions:

- NRC “Kurchatov Institute” (principal scientific organization),

- Joint Stock Company “N.A. Dollezhal Research and Development Institute of Power Engineering” (principal design agency),

- ZAO “NPO “Spetsprekt” (principal engineering company),

- NRC “Kurchatov Institute” – PNPI (operating company).

The results obtained at the stage of the low power testing mode up to 10 MW will serve as the basis for justifying the safety and reliability of the systems at the next stage of power start-up – reaching the nominal capacity of 100 MW.

## Commissioning of experimental stations at the PIK reactor

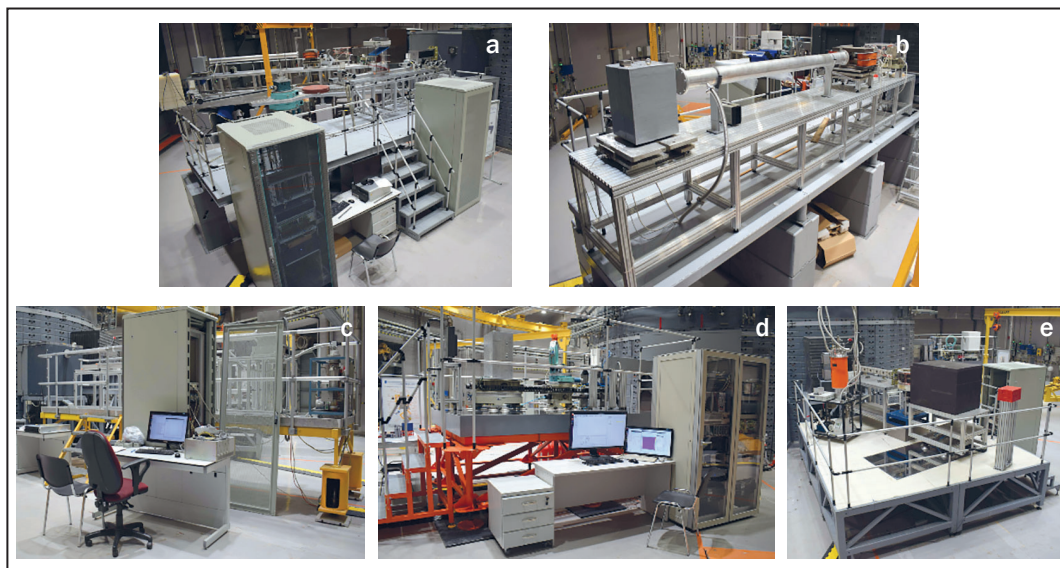
V.V. Tarnavich, P.S. Matveev, D.A. Ipatov, A.E. Sokolov, K.A. Pshenichnyj,  
A.V. Sizov, A.O. Polyushkin, S.V. Gavrilov, I.A. Zobkalo, V.A. Ulianov, M.A. Diachkov,  
S.O. Sumbaev, V.A. Matveev, D.V. Tyts, V.A. Solovei, M.R. Kolhidashvili  
Neutron Research Division, Knowledge Transfer Division,  
Engineering Center “Neutron Technologies” of NRC “Kurchatov Institute” – PNPI

The aim of the work – creation and commissioning of five first-stage experimental stations at the PIK reactor. The work is an integral part of addressing the problem of developing of synchrotron and neutron research, ensuring the creation and development of research infrastructure in the Russian Federation; it was carried out in accordance with the Decree of the President of the Russian Federation No. 356 of July 25, 2019.

Five research experimental stations were installed on neutron beams and put into operation in the hall of horizontal experimental channels of the PIK reactor. These are polarized neutron reflectometer NERO-2, test neutron reflectometer TNR, test neutron spectrometer T-Spectrum, neutron texture diffractometer TEX-3 and polarized neutron

diffractometer DPN (Fig.). The five experimental stations put into operation provide a basic set of neutron techniques: diffraction, reflectometry and spectrometry.

Neutron physical tests of the stations were carried out, and test experiments were performed. The staff for the operation of the stations has been trained, the operational infrastructure has been established, and the mechanisms of interaction with technical support services have been created. The scientific-technical and technological groundwork has been established for the subsequent implementation of a full-scale experimental complex, which will be created in the framework of the project “Creation of the Instrument Suite of the PIK Reactor Facility” (execution period 2019–2024).



First-stage instruments of the PIK Neutron Facility:  
a – reflectometer NERO-2;  
b – test neutron reflectometer TNR; c – test spectrometer T-Spectrum;  
d – texture diffractometer TEX-3;  
e – polarized neutron diffractometer DPN

# The work of SC-1000 synchrocyclotron to ensure the scientific and experimental activities of NRC “Kurchatov Institute” – PNPI in 2020

*E.M. Ivanov, S.A. Artamonov, L.A. Suhorukov  
Knowledge Transfer Division of NRC “Kurchatov Institute” – PNPI*

Synchrocyclotron SC-1000 (Fig. 1) is one of the main facilities of NRC “Kurchatov Institute” – PNPI. It has been successfully operated since 1970s. The main parameters of the synchrocyclotron are given in the Table.



Fig. 1. SC-1000 synchrocyclotron

Table. Main parameters of SC-1000

Characteristic	Value
Pole diameter	7.0 m
Winding current	5 400 A
Accelerating particle	Protons
Beam energy	1 000 MeV
Ejected beam current	Up to 1 $\mu$ A

The SC-1000 synchrocyclotron is used for fundamental research in elementary particle physics, the study of the structure of atomic nuclei and the mechanisms of nuclear reactions, in various fields of solid state physics. The SC-1000 is also widely used for applied work, for example, for radiation testing and nuclear medical research. SC-1000 is

a reliable installation in regular operation in Russian Federation in the range of variable energies 100–1 000 MeV, but most of the time the SC-1000 operates in the 1 000 MeV mode. From November 2019 to November 2020 the synchrocyclotron was in operation for 1 497 h for performing experiment. Figures 2 shows the breakdown of operating time of SC-1000 by months, and Fig. 3 shows its breakdown by lines of research.

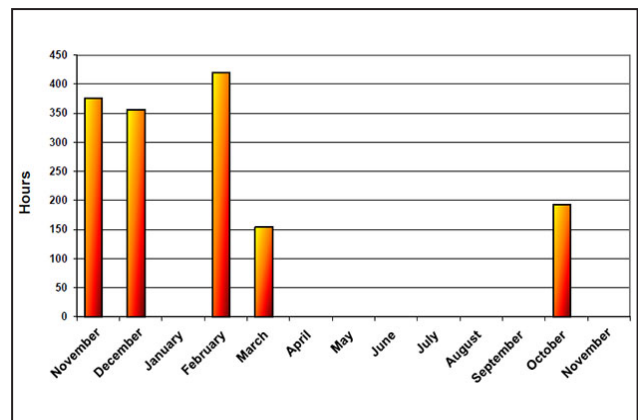


Fig. 2. Running time of SC-1000 in 2019–2020

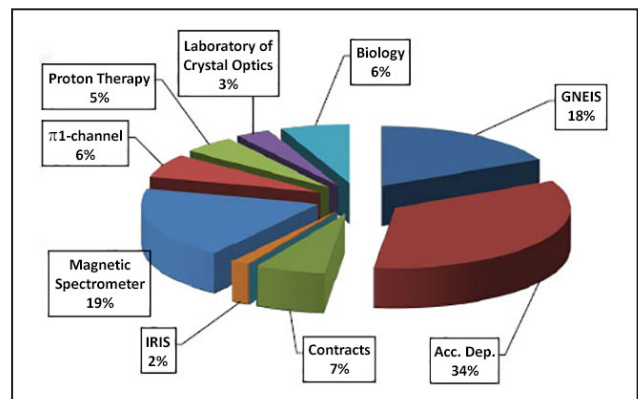


Fig. 3. The breakdown of operating time of SC-1000 by different lines of research

### The following studies were conducted at proton beams of SC-1000

1. Under RFBR grant No. 19-02-00005 on line and off line tests of a new target-ion unit with an ion source made from single-crystal tungsten with increased work function were continued. The study was conducted at a mass-separator IRIS.

2. In the framework of the research and development (R&D) projects the MAP&NES two-arm magnetic spectrometer was used to perform a number of studies of the structure of atomic nuclei with mass numbers 9, 28, 56 and 90.

3. In the framework of the R&D project on a comprehensive topic “Biomedical Technology”, there was a study of the influence of medications containing  $^{11}\text{B}$  on the effectiveness of therapeutic effect of a proton beam on animal models of malignant neoplasms.

4. The following works were performed under various contracts:

– Research works “Development and Creation of Prostate Cancer Models Expressing Prostate-Specific Membrane Antigen (PSMA), and Models of the Squamous Cell Carcinoma of the Head and Neck in Research Animals” were performed on a contractual basis for the use of A.M. Granov Russian Scientific Center for Radiology and Surgical Technologies.

– A study “Methodological and Technical Support of Radiation Studies and Trials of Pituitary Tumors on Proton Beams of a Synchrocyclotron SC-1000”.

5. As part of R&D project “Modernization of Stereotaxic Proton Therapy Installation” the following studies were performed:

– Measurement of dose fields with thermoluminescent dosimeter;

– Operation tests of new radiation-measuring equipment.

6. According to R&D roadmap in the framework of state assignment for 2020 and for the planned period of 2021–2022 the synchrocyclotron SC-1000 was used to continue the studies of radiation hardness of fullerenes and their derivatives.

7. According to R&D roadmap in the framework of state assignment for 2020 it was decided to continue the development of the project of RIC-80 complex on the production of radioactive isotopes for medical application on the basis of the C-80

cyclotron. We obtained new results on the basis of an innovative high-temperature method for the extraction of medical radionuclides of  $\alpha$ -emitters  $^{212}\text{Pb}$  and  $^{224}\text{Ra}$  from a high-density thorium carbide target.

8. It was proposed to continue the program of cooperation with the Roscosmos State Corporation and Ministry of Defense of the Russian Federation in the field of heavy-ion radiation resistance tests of electro-radio items.

### The following studies were conducted at neutron beams of SC-1000

Studies in the field of fundamental and applied nuclear physics were performed at a neutron time-of-flight spectrometer GNEIS:

– Within the framework of the RFBR grant No. 18-02-00571 (2018–2020), measurements of the angular distributions and anisotropy of fragments during the fission of heavy nuclei by intermediate-energy neutrons were carried out. The simulation study of results obtained was carried out. The study is performed in cooperation with the Neutron Research Division and High Energy Physics Division of NRC “Kurchatov Institute” – PNPI and NRC “Kurchatov Institute”.

– Under the RFBR grant No. 19-02-00116 (2019–2021) the structure of the fission barrier and the properties of transition states in neutron resonances were studied. The study is performed in cooperation with the Neutron Research Division and High Energy Physics Division of NRC “Kurchatov Institute” – PNPI.

– Under the agreement with A.I. Leypunsky Institute of Physics and Power Engineering No. 984-600-2/2019/6659 (2019–2021) “Experimental Studies of the Interaction of Neutrons with Actinide Nuclei for the National Library of Nuclear Physics Data of the Fourth Generation BROND” measurements of the cross sections for neutron-induced fission of  $^{240}\text{Pu}$  and  $^{237}\text{Np}$  in the energy range from 1 to 200 MeV were performed. The relevance of the conducted study is related to the continuously growing requirements for the accuracy and completeness of nuclear data systems that are used in the development of the latest nuclear technologies, primarily in nuclear power industry;

- Within the framework of the Federal target program No. 14.607.21.0200 “Creation of Innovative Technology for the Production of the Latest Neutron Radiation Detection Systems for Solving Problems in Condensed Matter Physics” (2018–2020), a transmission monitor of the thermal neutron flux with an energy of 0.01–1 eV was tested for experiments on the beams of the PIK reactor.

#### The following studies were performed at beams of $\pi$ - и $\mu$ -meson channels of SC-1000

In NRC “Kurchatov Institute” – PNPI a series of experiments is planned to study isotopic invariance in the processes of  $\eta$ -meson formation near the threshold and the CUSP effect in the charge-exchange reaction. For this purpose, the creation of a magnetic spectrometer based on the  $\pi$ -meson channel of the SC-1000 synchrocyclotron was continued. A pulse resolution of  $\sim 0.5\%$  of the channel is going to be achieved, which was confirmed by the Monte Carlo simulation of the optics of the  $\pi$ -meson channel. Experimental setting of the proton triplet has been performed to focus the proton beam on the meson-forming target. Focusing in the horizontal plane  $\sigma = 2$  mm has been obtained. Work on creating a magnetic spectrometer will continue.

#### The following papers published as a result of works carried out at SC-1000 synchrocyclotron

1. Amerkanov D.A., Artamonov S.A., Ivanov E.M., Mikheev G.F., Ryabov G.A., Tonkikh V.A. // Scientific and Technical Book Conf. “Radiation Resistance of Electronic Systems” (Resistance-2020). M., 2020. Iss. 23. P. 46–47.

2. Amerkanov D.A., Ermakov K.N., Ivanov E.M., Ivanov N.A., Lobanov O.V., Pashuk V.V. // VANT. 2020. No. 1. P. 13–17.

3. Artamonov S.A., Ivanov E.M., Ryabov G.A., Tonkikh V.A., Amerkanov D.A. // Nucl. Phys. Eng. 2020. V. 83. No. 10. P. 1–5.

4. Vrozhik D.S., Zhidkova O.M., Ivanov E.M., Karlin D.A., Kuzora N.A., Lazarev V.I., Maksimov V.I., Mamedova N.I., Pak F.A., Ryabov G.A., Khalikov A.I. Preprint NRC “Kurchatov Institute” – PNPI 3045. Gatchina, 2020. 48 p.

5. Brozhik D.S., Mamedova N.I., Pak F.A., Vasiliev A.A., Khalikov A.I. // Youth Conf. on Theor. and Exp. Phys. (YSCONF-2020). 2020. V. 2. P. 7.

6. Vasiliev A.A., Golikov I.G., Mamedova N.I., Pak F.A., Zhigalova M.V., Karlin D.L., Brozhik D.S., Khalikov A.I., Vasilevskaya I.V. // Med. Phys. 2020. No. 5. P. 5–12.

7. Volnitsky A.V., Garaeva L.A., Burdakov V.S., Razgildina N.D., Lebedev D.V., Amerkanov D.A., Pak F.A., Verlov N.A., Konevega A.L., Shtam T.A. // Book of Abstracts of the XXI Winter Youth School on Biophys. and Mol. Biol. Gatchina, 2020. P. 48–49.

8. Vorobyev A.S., Gagarski A.M., Shcherbakov O.A., Vaishnene L.A., Barabanov A.L. // JETP Lett. 2020. V. 112. Iss. 6. P. 343–351.

9. Kotb O.M., Brozhik D.S., Verbenko V.N., Gulevich E.P., Ezhov V.F., Karlin D.L., Pak F.A., Paston S.V., Polyanichko A.M., Khalikov A.I., Chikhirzhina E.V. // Biophysics. 2021. V. 66. No. 2. P. 240–247.

10. Razgildina N.D., Garaeva L.A., Volnitsky A.V., Burdakov V.S., Verlov N.A., Amerkanov D.A., Pak F.A., Lebedev D.V., Konevega A.L., Shtam T.A. // Book of Abstracts of the XXI Winter Youth School on Biophys. and Mol. Biol. Gatchina, 2020. P. 183–184.

11. Artamonov S.A., Ivanov E.M., Riabov G.A., Tonkikh V.A., Amerkanov D.A. // Phys. At. Nucl. 2020. V. 83. No. 12. P. 1700–1704.

12. Barabanov A.L., Vorobyev A.S., Gagarski A.M., Shcherbakov O.A., Vaishnene L.A. // Bull. Russ. Acad. Sci. Phys. 2020. V. 84. No. 4. P. 397–402.

13. Lebedev D., Garaeva L., Burdakov V., Volnitskiy A., Razgildina N., Garina A., Amercanov D., Pack E, Shabalin K., Ivanov E., Ezhov V., Konevega A., Shtam T. // Rad. Conf. Proc. 2020. V. 4. P. 1–4.

14. Miklukho O.V., Kisselev A.Yu., Amalsky G.M., Andreev V.A., Barsov S.G., Gavhlov G.E., Zhdanov A.A., Izotov A.A., Ilyin D.S., Kozlenko N.G., Kravchenko P.V., Maysuzenko D.A., Murzin V.I., Novinskiy D.V., Shvedchikov A.V. // Phys. At. Nucl. 2020. V. 83. No. 3. P. 431–441.

15. Panteleev V.N., Barzakh A.E., Batist L.Kh., Fedorov D.V., Ivanov V.S., Moroz F.V., Molkanov P.L., Orlov S.Yu., Seliverstov M.D., Volkov Yu.M. // Nucl. Inst. Meth. Phys. Res. B. 2020. V. 463. P. 364.

16. Seliverstov M., Barzakh A., ..., Fedorov D., Fedoseev V., ..., Molkanov P., Panteleev V. et al. // Hyperf. Interact. 2020. V. 241. P. 40.

17. Vorobyev A.S., Gagarski A.M., Shcherbakov O.A., Vaishnene L.A., Barabanov A.L. // JETP Lett. V. 112. No. 6. P. 323–331.

18. A Device for Rapid Radiation Irradiation of Aerospace Electronics with Protons Using a Synchrocyclotron: pat. RF for invention No. 2720494 / Artamonov S.A., Ivanov E.M., Mikheev G.F., Anashin V.S., Krylov D.G., Chubunov P. A.; Priority Date 02.10.2019.; Publ. 30.04.2020.

19. A Program for Searching for Static Equilibrium Orbits and Motion Parameters in an Iso-

chronous Cyclotron on a Super Period. Certificate of state registration of a computer program No. 2020612261 / Artamonov S.A.; Date of State Reg. 19.02.2020.

20. The READ PSI Program. Certificate of state registration of a computer program No. 2020661440 / Getalov A.L., Vorobyov S.I., Komarov E.N., Kotov S.A., Shcherbakov G.V.; Date of State Reg. 23.09.2020.





## Management and Research

- 114** Full-time personnel
- 116** Quantitative characteristics of scientific and educational activities
- 120** Awards. Prizes
- 124** Scientific events

## Full-time personnel

### Staff number

Professional qualification groups of positions	2018	2019	2020
Total not including part-time workers	1 973	1 962	1 987
Researchers, total	490	473	473
<i>Of which holding the position of</i>			
head	65	68	66
chief researcher	9	9	9
leading researcher	43	42	44
senior researcher	157	151	146
researcher	97	86	83
junior researcher	55	58	59
other researchers	64	59	66
<i>With a science degree</i>			
Doctor of Sciences	66	66	62
Candidate of Sciences	230	218	215
<i>With an academic rank</i>			
Academician	-	-	-
Corresponding Member	2	2	2
Professor	12	9	8
Docent	90	87	80

### Information on scientific experience of NRC “Kurchatov Institute” – PNPI researchers

Position	Total	Including with the experience		
		less than 5 years	more than 5 years	more than 10 years
Heads of laboratories and departments	38	2	2	34
Chief researchers	9	-	-	9
Leading researchers	44	2	-	42
Senior researchers	146	10	10	126
Researchers	83	10	23	50
Junior researchers	59	28	22	9

### Information on age distribution of NRC “Kurchatov Institute” – PNPI researchers

Professional qualification groups of positions	Age, years old					
	20–29	30–39	40–49	50–59	60 and older	mean age
Researchers, total	84	88	47	65	189	52
<i>With a science degree</i>						
Doctor of Sciences	-	-	6	10	46	69
Candidate of Sciences	5	36	28	41	105	58
<i>W/o science degree</i>	79	52	13	14	38	40
<i>With an Academic rank</i>						
Academician	-	-	-	-	-	-
Corresponding Member	-	-	-	-	2	83
Professor	-	-	-	-	8	82
Docent	-	-	-	4	76	72

### The number and average age of researchers of NRC “Kurchatov Institute” – PNPI by position

Position	2018		2019		2020	
	Number	Mean age	Number	Mean age	Number	Mean age
Chief researcher	9	81	9	82	9	83
Leading researcher	43	68	42	69	44	68
Senior researcher	157	61	151	62	146	62
Researcher	97	51	86	51	83	50
Junior researcher	55	31	58	32	59	32
Heads	65	64	68	63	66	62
Other researchers	64	26	59	27	66	27

### Structure and staffing for 5 years

Category of staff	2016	2017	2018	2019	2020
Scientific workers	529.4	503.9	489.2	435.5	450.2
Scientific and engineering staff	244.5	241.8	251.8	290.7	296.05
Office and management personnel	1 158.8	1 121.9	1 181.4	1 253.1	1 290.15
Junior service staff	24.5	32.5	32.5	32.5	31.5
Total	1 957.2	1 900.1	1 954.9	2 011.8	2 067.9

## Quantitative characteristics of scientific and educational activities

NRC “Kurchatov Institute” – PNPI has completed all events and achieved all target indicators intended for 2020, owing to, in particular, the state assignment implementation subsidies for 2020.

In 2020 the employees of NRC “Kurchatov Institute” – PNPI were the authors and co-authors of 674 papers including 473 publications indexed in Web of Science database and associated with NRC “Kurchatov Institute” – PNPI, which constitutes 70.2% of the total number of published articles.

### Dynamic pattern of the number of publications affiliated with NRC “Kurchatov Institute” – PNPI for 5 years

Year	Total number of publications / publications including those indexed in Web of Science database
2016	569/398
2017	592/426
2018	689/507
2019	714/465
2020	674/473

### Dynamic of participation in scientific events for 5 years

Year	Number of facts of participation of employees in exhibition activities, conferences, forums and other similar events
2016	340
2017	466
2018	420
2019	422
2020	387

### Number of international and Russian patents, whose holder is NRC “Kurchatov Institute” – PNPI obtained in 2020 depending on the title of protection type

Objects of patent law by title of protection type			
Patent for invention	Utility patent	Certificates of registration of computer software	Total
5	8	13	26

### Dynamic pattern of titles of protections whose right holder is NRC “Kurchatov Institute” – PNPI for 5 years

Type of title of protection	2016	2017	2018	2019	2020
Patents for invention	3	4	7	10	5
Utility patents	4	5	4	2	8
Certificates of registration of computer software	5	6	25	12	13
Database certificates	2	1	1	-	-
Registered know-how	1	-	3	-	-
Total	15	16	40	24	26

In 2020 the scientific research of Institute's employees was financed by RFBR (34 grants) and RSF (14 grants). The Ministry of Education and Science of the Russian Federation also supported the Institute in the framework of Federal Special Purpose Program “Research and Development in Priority Development Fields of Russia’s Science and Technology Sector for the Period of 2014–2020”.

In 2020 the employees of Institute defended 6 Candidate of Sciences dissertations and 3 Doctor of Science dissertations in line with the Program of Activities of NRC “Kurchatov Institute” – PNPI for 2018–2022. In 2020 the employees of NRC “Kurchatov Institute” – PNPI defended six Candidate of Sciences dissertations and three Doctor of Science dissertations in line with the Program of Activities of NRC “Kurchatov Institute” – PNPI for 2018–2022.

### Training of highly qualified personnel for 5 years

Year	Total number of dissertations / number of Doctor of Science dissertations
2016	13/2
2017	11/1
2018	8/2
2019	7/-
2020	9/3

Pursuant to the Order of the Federal Education and Science Supervision Agency of 06.07.2020 No. 722 the Institute obtained the State Accreditation Certificate for higher education programs – post-graduate training program of highly trained academic and teaching staff (serial number 90A01 No. 0003632, registration No. 3414 of 06.07.2020) in post-graduate courses in compliance with the requirements of the Federal Educational Standards of the Higher Education within the following training programs:

- 03.06.01 “Physics and Astronomy”  
subfields: 01.04.02 “Theoretical Physics”, 01.04.07 “Condensed Matter Physics”, 01.04.16 “Nuclear and Particle Physics”, 03.01.02 “Biophysics”;



- 06.06.01 “Life Sciences”  
subfields: 03.02.07 “Genetics”.

This means that for the next 6 years, all postgraduate programs of the NRC “Kurchatov Institute” – PNPI have state accreditation. Information about the availability of the Institute’s certificate of state accreditation of postgraduate programs is officially entered in the register of organizations engaged in educational activities for state-accredited educational programs.

In 2020 11 students entered the post-graduate course for the full time mode of study: 4 students for the training program 06.06.01 “Life Sciences” (subfield 03.02.07 “Genetics”) and 7 students for the training program 03.06.01 “Physics and Astronomy” (subfields: 01.04.02 “Theoretical Physics”, 01.04.07 “Condensed Matter Physics”, 01.04.16 “Nuclear and Particle Physics”, 03.01.02 “Biophysics”).

The total number of postgraduate students by the end of 2020 is 49 people.

In 2020 NRC “Kurchatov Institute” – PNPI took part in an open competition of the Ministry of Education and Science of the Russian Federation on the distribution of admission quotas for post-graduate course training financed from Federal budget allocations for 2021/22. The following admission quotas were obtained: 03.06.01 “Physics and Astronomy” – 8 places, 06.06.01 “Life Sciences” – 4 places.

In 2020 the proportion of young scientists (researchers without a degree, Candidates of Sciences under 35 years old and Doctors of Sciences under 40 years old) in the total number of employees involved in research and development amounted to 28%.

In 2020 more than 150 students of Russia’s institutions of higher education conducted academic and research work, did practical training, prepared final qualification works for Bachelor’s and Specialist’s degree and Master’s theses in the laboratories of the Institute.

### The total number of students of field-oriented universities who did practical training in the Institute as part of implementing the Program of Activities of NRC “Kurchatov Institute” – PNPI for 5 years

Year	Number of students
2016	105
2017	101
2018	122
2019	127
2020	154

In an effort to popularize science and get young people interested in getting an education in physics and biology, NRC “Kurchatov Institute” – PNPI organizes and conducts excursions in the Institute and to the facilities of NRC “Kurchatov Institute” – PNPI (including excursions to the accelerator facility SC-1000 and C-80, PIK Neutron Facility, WWR-M Reactor, the Molecular and Radiation Biophysics Division as well as other scientific divisions) and carries out occupational guidance for high-school children.

Under the Cooperation Agreement between the administration of the Gatchina Municipal District of the Leningrad region and the NRC “Kurchatov Institute” – PNPI and within the framework of existing

cooperation agreements with educational institutions in Gatchina (Lyceum No. 3 named after the Hero of the Soviet Union A.I. Peregudov, Secondary School No. 9 with in-depth study of individual subjects, Secondary School “Apex”, Center for Information Technologies, Secondary School No. 2) employees of the NRC “Kurchatov Institute” – PNPI are working with high school student which includes delivering popular science lectures by employees of the Institute, selecting of promising students and conducting practical training in physics, mathematics and biology.

Research and Educational Center of NRC “Kurchatov Institute” – PNPI organizes lectures and extracurricular classes for the in-depth study of some topics in physics and biology for the students of schools of Gatchina and Gatchina region. During these classes the students become acquainted with the advances of modern science and technology. There is occupational guidance for schoolchildren of major schools of Saint Petersburg and Leningrad region as well as university students of the entire Northwestern District of Russia. We are conducting popular science lectures (including those when the scientists of the Institute visit schools), excursions to the primary Divisions of the Institute, where the advances of Russian science are discussed, thus increasing the interest in academic field and the activity of NRC “Kurchatov Institute” – PNPI among schoolchildren.

Under the Collaboration Agreement between Saint Petersburg University (SPbU) and NRC “Kurchatov Institute” – PNPI the employees of NRC “Kurchatov Institute” – PNPI conduct lectures and laboratory practicals in the frame of the academic program “Convergence and High-End Technologies” for students of 10th and 11th grade of D.K. Faddeev Academic Gymnasium of SPbU.

NRC “Kurchatov Institute” – PNPI carries out a unique project called “School Environmental Initiative” – “Young Talents”, whose goal is the environmental education of children and teenagers and which celebrated its 30th anniversary in 2020. In 2020, a lot of creative competitions, contests, environmental actions were held. Around five thousand young residents of Gatchina and Gatchina region took part in the project events. In total, around 100 000 children participated in the “School Environmental Initiative” – “Young Talents” project over its 30-year history.





## Awards. Prizes

NRC “Kurchatov Institute” – PNPI is an actively functioning institution, which keeps pace with the current world trends, as evidenced by numerous prizes and scholarships of its employees.

The active participation of the Institute’s employees in the competition for the **I.V. Kurchatov Prize** has already become a good tradition. It is especially pleasant that not only leading and young scientists and engineers but also students are allowed to participate in the competition. In 2019 studies and teams of authors from NRC “Kurchatov Institute” – PNPI were among the winners of Kurchatov Prize as well.

**In the field of scientific research** the study “Spin chirality and energy landscape of cubic helicoidal magnets” was recognized as one of the best studies conducted. It was carried out by the team of authors consisting of *S.V. Grigoriev, E.V. Altyntbaev, K.A. Pshenichnij, E.V. Moskvina, S.V. Maleev*.

**Among the works of young scientists and engineers the study** conducted by *O.I. Utesov* “Phase transitions in multiferroics with a spiral magnetic structure” was voted one of the best studies.

**Among the works performed by students** the list of top-prize winners includes the Master's thesis of *L.A. Azarova* “An investigation of the fractal properties of zirconium dioxide xerogels at various annealing temperatures”, *A.O. Petrova* “Selection of optimal parameters of a time-of-flight neutron spectrometer based on stationary and pulsed sources” and *A.O. Koptyukhov* “Thermal mode of ultracold neutron source at the WWR-M reactor”.

In 2020 in the **field of scientific research** the study “Structure-function studies of the effect of antibiotics on prokaryotic ribosomes” carried out by the team of authors *A.L. Konevega, A.V. Paleskava, P.S. Kasatskii, A.G. Myasnikov, E.B. Pichkur* was recognized as one of the best.

**Among the works of young scientists and engineers** the list of winners includes the studies conducted by *E.G. Iashina* “Spin-echo small-angle neutron scattering study of the structure organization of the chromatin in biological cell”, *L.V. Skripnikov* and *D.V. Chubukov* “Study of the effects of violation of fundamental discrete symmetries in heavy atoms and two-atom molecules”.

**Among the works performed by students** the study conducted by *N.V. Surina* “Analysis of the morphology and functions of glial cells on the *Drosophila melanogaster* model for Alzheimer’s disease” was included in the list of winners.

### Dynamics of receiving the I.V. Kurchatov Prize by the employees of the NRC “Kurchatov Institute” – PNPI in 2012–2020

Contest nomination	2012	2013	2014	2015	2016	2017	2018	2019	2020
In the field of scientific research	1	1	1	1	3	–	2	1	1
In the field of engineering and technological developments	1	–	2	1	–	1	1	–	–
Among the works of young scientists and engineers	–	1	2	2	3	1	3	1	2
Among the works performed by students	–	–	3	4	5	2	1	3	1
Total	2	2	8	8	11	4	7	5	4

In the annual competition of scientific papers for the 2020 **A.P. Aleksandrov Prize** at NRC “Kurchatov Institute”, the winners were: *A.P. Serebrov, V.A. Lyamkin, A.K. Fomin, A.O. Koptukhov* and *D.V. Prudnikov* with the work “A source of ultracold neutrons based on superfluid helium for PIK neutron facility”.

### Dynamics of receiving the A.P. Aleksandrov Prize by the employees of the NRC “Kurchatov Institute” – PNPI in 2015–2020

Contest nomination	2015	2016	2017	2018	2019	2020
Main section of the competition	1	-	1	1	-	1
Youth section of the competition	-	2	-	-	-	-
Total	1	2	1	1	-	1

In 2020 the Government of Leningrad region supported 8 projects of employees of NRC “Kurchatov Institute” – PNPI who were awarded scientific **scholarships of the governor of Leningrad region**: 4 scientists got a scientific scholarship in the “Young Scientists” category and 4 researchers – in the “Leading Scientists” category.

#### **Holders of scientific scholarships of the governor of Leningrad region in the “Leading Scientists” category:**

- *A.K. Emel'ianov*, senior scientist of MRBD. “Epigenetic disorders in Parkinson’s disease”;
- *N.S. Mosyagin*, senior scientist of KTD. “Producing a new generation of relativistic effective core potentials for light elements of the periodic table, designed for high-precision predictions of the properties of their compounds”;
- *S.I. Vorobyov*, acting head of a laboratory of HEPD. “Investigation of nanostructured magnetic systems using the  $\mu$ SR-method at the synchrocyclotron of NRC “Kurchatov Institute” – PNPI”;
- *D.V. Fedorov*, deputy head of a laboratory of HEPD. “Laser-spectroscopic studies of the evolution of the nuclear shapes on mass-separator complexes”.

#### **Holders of scientific scholarships of the governor of Leningrad region in the “Young Scientists” category:**

- *K.A. Ivshin*, researcher at HEPD. “Development and creation of a recoil proton detector for precision measurement of the proton radius (“Proton” experiment)”;
- *R.M. Samoilov*, junior researcher at NRD. “The “Neutrino” instrument complex at the PIK research reactor”;
- *P.A. Melentiev*, post-graduate student, laboratory assistant at MRBD. “Study of the genetic basis of molecular and cellular mechanisms of aging”;
- *T.S. Usenko*, researcher at MRBD. “Lysosomal dysfunction in synucleinopathies”.

Names of recipients of the **award of the Governor of Leningrad region** were announced on the eve of the New Year. This is the award recognizing the contributions to the development of science and technology in the Leningrad region and for the best research project.

A senior researcher at the Division of Advanced Research, Candidate of Physical and Mathematical Sciences *L.V. Skripnikov* is the recipient of the the award of the Governor of Leningrad region for contribution to the development of science and technology



in the Leningrad region “For achievements in the field of fundamental and applied research” in the category “Natural and Technical Sciences”.

*T.S. Usenko*, a researcher at MRBD, Candidate of Biological Sciences, became the winner of the award of the Governor of Leningrad region of the third degree for the best research work for young scientists.

**A scholarship program** for young scientists and specialists of NRC “Kurchatov Institute” – PNPI was established in recognition of outstanding achievements and in memory of distinguished scientists S.E. Bresler, V.N. Gribov, G.M. Drabkin and V.M. Lobashev whose academic career is inextricably linked to the Institute. Scholarships are awarded annually in the following categories:

- S.E. Bresler scholarship for works in the field of biology;
- V.N. Gribov scholarship for works in the field of theoretical physics;
- G.M. Drabkin scholarship for works in the field of condensed matter physics;
- V.M. Lobashev scholarship in the field of nuclear physics.



In 2020 4 young scientists of the Institute were the recipients of these scholarships.

**V.N. Gribov scholarship** for works in the field of theoretical physics was awarded to junior researcher of the laboratory of quantum chemistry of KTD *D.V. Chubukov*. **S.E. Bresler scholarship** for works in the field of biology was awarded to laboratory assistant of the Laboratory of Experimental and Applied Genetics of MRBD *E.V. Ryabova*, laboratory assistant of the Laboratory of Protein Biophysics of MRBD *N.V. Kolchina* and laboratory assistant of the Laboratory of Protein

Biosynthesis *O.V. Shulenina*. In 2020, **V.M. Lobashev scholarship** for works in the field of nuclear physics and **G.M. Drabkin scholarship** for works in the field of condensed matter physics were not awarded.

The work “The EXP-T program package for high-precision modeling of molecular electronic structure”, the results of which were presented by *Alexander Oleinichenko*, a junior researcher at the KTD, performed jointly with other employees of the KTD: a chief researcher, Doctor of Physical and Mathematical Sciences *A.V. Zaitsevsky*, and a senior researcher, Candidate of Physical and Mathematical Sciences *L.V. Skripnikov*, as well as Professor *E. Eliav* from Tel Aviv University (Israel) was awarded a diploma for the best scientific report at the scientific conference “Supercomputing Days in Russia – 2020”.



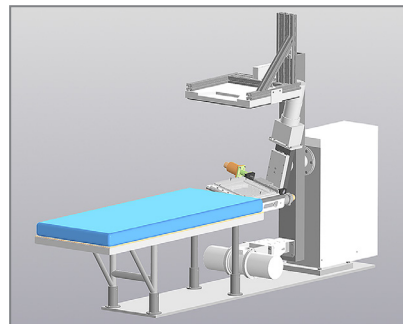
Head of Physics of Exotic Nuclei Laboratory of HEPD Prof. *Yu.N. Novikov* achieved the “trusted reviewer” status of the “IOP Publishing”, the Headquarters of which is located in Bristol, UK. Yuri Nikolaevich was one of the first to achieve this status in the established nomination based on the results of the rating and without any confirming trainings and certificates. The diploma and the cover letter of the “IOP Publishing” state that the “IOP Trusted Reviewer” status confirms that Professor *Yu.N. Novikov* has demonstrated “an exceptionally high level of peer review competence”.

Junior researcher of the Laboratory of Medical Physics of the Department of Medical Radiology *Fedor Pak* won the international contest for enterprises for future whizzes of 3D computer modeling in the nomination “Young



expert”. At the competition, he presented a project for the facility for proton-based stereotactic body radiation therapy (SBRT), which is intended for the treatment of patients. The treatment table can rotate around the vertical axis by  $40^\circ$ , and the head immobilizer can perform pendulum movements at an angle of  $36^\circ$  around the horizontal axis.

The competition is held annually by “Ascon” for enterprises that use the “Compass-3D” software and welcomes experts from different industries who are ready to demonstrate their engineering skills. Only the top ten projects were selected out of thousands. Fedor Pak received a diploma and a cup.



At the competition of scientific works of NRC “Kurchatov Institute” – PNPI 2020, the commission considered 34 works in 8 scientific areas of the Institute’s activities.

Based on expert assessments after a comprehensive discussion the commission decided that:

- The first prize in the field of high energy nuclear physics was awarded for the work “Investigation of the energy dependence of the cross-section of the hard QCD process  $\gamma p \rightarrow J/\Psi p$  in the LHCb and ALICE experiments on

the LHC” (G.D. Alkhazov, N.F. Bondar, A.A. Vorobyev, A.A. Dzyuba, M.B. Zhalov, V.V. Ivanov, S.N. Kotryakhova, E.L. Kryshen, O.E. Maev, M.V. Malaev, V.N. Nikulin, M.G. Ryskin, V.G. Ryabov, Yu.G. Ryabov, N.R. Sagidova, V.M. Samsonov, A.V. Khazadeev, A.D. Chubykin (LHCb, ALICE Collaborations).

- In the field of theoretical physics, the work “Non-Abelian strings in  $N = 1$  supersymmetric QCD” (E.A. Ilev, A.V. Yung) was recognized as the best.

- In the field of condensed matter physics, the winner was the work “Magnetism of two-dimensional layered oxides with a honeycomb-like superstructure of magnetic ions” (A.N. Korshunov, A.I. Kurbakov, A.L. Malyshev, S.Yu. Podchezertsev, A.N. Vasiliev, T.M. Vasilchikova, M.A. Evstigneeva, E.A. Zvereva, V.B. Nalbandyan, G.V. Raganyan, M.I. Stratan, I.L. Shukaev, F. Damay, R. Klingeler, C. Koo, J. Park, I. Safiulina).

- In the field of biological research, the first prize was awarded for the work “Features of the interaction of dirithromycin with ribosomes of two bacterial species” (A.L. Konevega, A.V. Paleskava, P.S. Kasatsky, E.B. Pichkur, A.G. Myasnikov, N.F. Khabibullina, A.G. Tereshchenkov, E.S. Komarova, E.A. Syroegin, D.I. Shiryayev, V.G. Kartsev, A.A. Bogdanov, O.A. Dontsova, P.S. Sergiev, I.A. Osterman, Yu.S. Polikanov).

- The work “Protective membranes on horizontal experimental channels of the PIK reactor” (K.A. Konoplev) was named the best one in the field of applied research.

Overall 23 works were recognized the winners of the competition.



## Scientific events

### Institute Seminars

**9 January. Seminar of MRBD.** *Yu.S. Polikanov* (Department of Biological Sciences Department of Pharmaceutical Sciences University of Illinois at Chicago, USA). “Seminar on molecular visualisation using PyMOL and creation of images for publications”.

**14 January. Nuclear seminar of HEPD.** *D.A. Ivanishchev*. “Perspectives of thermal photon study in the MPD experiment at NICA collider”.

**21 January. Nuclear seminar of HEPD.** *M.V. Smirnov* (Sun Yat-sen University, Guangzhou, China). “JUNO experiment: status and physics”.

**28 January. Nuclear seminar of HEPD.** *A.L. Getalov*. “ $\mu$ SR-investigation of the ferro fluids with cobalt ferrite nanoparticles of 3%”.

**4 February. Nuclear seminar of HEPD.** *G.D. Shabanov*. “Gatchina’s discharge in China and in Russia – investigation is continued”.

**6 February. Theoretical seminar on CSP.** *S.V. Andreev*. “Pairing of dipole excitons in semiconductor heterostructures”.

**11 February. Nuclear seminar of HEPD.** *S.I. Manaenkov*. “Does pentaquark  $\theta^+$  exist?”

**13 February. Combined seminar of HEPD and TPD.** *M.G. Ryskin*. “Physics of DGLAP and BFKL”.

**18 February. Nuclear seminar of HEPD.** *A.E. Shevel’*. “Information Infrastructure trends in large nuclear and high energy physics centers”.

**20 February. Theoretical seminar on CSP.** *A.N. Poddubny* (Ioffe Institute). “The interaction of two photons with an array of atoms in a waveguide”.

**20 February. Combined seminar of HEPD and TPD.** *M.G. Ryskin*. “Physics of DGLAP and BFKL (part 2)”.

**25 February. Nuclear seminar of HEPD.** *Yu.G. Naryshkin*. “New physics search in the  $t$ -quark pair production at ATLAS”.

**27 February. Theoretical seminar on CSP.** *S.V. Maleev*. “Spin chirality and polarized neutrons”.

**3 March. Nuclear seminar of HEPD.** *V.A. Guzej*. “The project of an Electron-Ion Collider in the USA”.

**4 March. Seminar of KTD.** *N.V. Kamanina*. “Modification of the properties of inorganic and organic materials by laser nanotechnology methods”.

**5 March. Theoretical seminar on CSP.** *A.S. Scherbakov*. “The magnon spectrum and spin resonance in an antiferromagnet with a large single-ionic anisotropy of the “light plane” type”.

**10 March. Nuclear seminar of HEPD.** *V.A. Kuznetsov*. “Time-of-flight detectors based on plastic scintillators: overview, principles of operation and calibration”.

**12 March. All-Institute seminar on CSP.** *N.K. Pleshanov*. “Neutron spin optics (on the basis on Doctoral Thesis)”.

- 17 March. Nuclear seminar of HEPD.** *A.E. Barzakh.* “Laser ion source. History, status and prospects”.
- 10 June. Seminar of MRBD.** *N.V. Tsygan.* “The effect of COVID-19 on the nervous system: pathogenesis and clinical features”.
- 15 September. Nuclear seminar of HEPD.** *I.A. Mitropolsky.* “Systematization of nuclear radii based on neuron net application”.
- 17 September. Theoretical seminar on CSP.** *S.E. Andreev.* “Spin-orbital decay of dipole biexitons in the superfluid phase”.
- 17 September. Combined seminar of HEPD and TPD.** *A.P. Serebrov.* “The analysis of the results of the “Neutrino-4” experiment on search for sterile neutrino and comparison with results of other experiments”.
- 22 September. Nuclear seminar of HEPD.** *A.A. Dzyuba.* “New LHCb results on tetraquark study”.
- 23 September. Seminar of MRBD.** *N.V. Kolchina.* “Molecular mechanisms of binding of short peptides to dnDNA and globular proteins”.
- 29 September. Nuclear seminar of HEPD.** *E.N. Komarov, S.G. Sherman.* “Bilinear decomposition of cross sections of reactions  $dd \rightarrow n^3\text{He}$ ,  $dd \rightarrow p^3\text{H}$  in terms of partial amplitudes”.
- 6 October. Nuclear seminar of HEPD.** *A.B. Gridnev.* “Threshold anomalies in nuclear reactions”.
- 20 October. Nuclear seminar of HEPD.** *D.E. Sosnov.* “First observation of diffraction in proton-lead collisions at the LHC with the CMS detector”.
- 29 October. Theoretical seminar on CSP.** *N.E. Savitskaya.* “Dynamic phase transitions in a decision-making model on a time-varying network”.
- 3 November. Nuclear seminar of HEPD.** *D.V. Novinsky.* “Polarization research program at the U-70 accelerator in Protvino: the SPASCHARM experiment”.
- 10 November. Nuclear seminar of HEPD.** *M.D. Seliverstov.* “Multi-purpose highly efficient ion source. Applications in medicine and nuclear physics”.
- 25 November. Seminar of KTD.** *K. Reih* (Ioffe Institute). “Electronic properties of highly doped semiconductor nanostructures”.
- 26 November. Seminar of MRBD.** *S.V. Grigoriev.* “Switch of fractal properties of DNA in chicken erythrocytes nuclei by mechanical stress”.
- 3 December. Theoretical seminar on CSP.** *M. Zvonarev.* “Mobile impurity in a quantum fluid”.
- 24 December. Theoretical seminar on CSP.** *O.I. Utesov.* “Sequences of phase transitions in frustrated anisotropic antiferromagnets in an external magnetic field”.

## Conferences

Within the context of a wide variety of areas of scientific research conducted in NRC “Kurchatov Institute” – PNPI we are convening our own conferences, lecture courses and workshops attended by scientists from leading research centers of Russia and abroad.

In 2020 the Institute organized 11 scientific events (meetings, conferences, schools).

### The list of organized events

1. Day of Science. **6–7 February.**
2. XXI Winter Youth School of Biophysics and Molecular Biology. **24–29 February.**
3. The 54th PNPI Winter School in Nuclear and Elementary Particle Physics. **10–15 March.**
4. The 54th PNPI Winter School in Condensed Matter Physics “FKS-2020”. **16–21 March.**
5. Environmental Holiday “Ecoshow-2020”. **25 September.**
6. V Reactor PIK Youth Scholl “Professionalism. Intelligence. Career. PIK-2020”. **7–25 September.**
7. International Conference “Drosophila in Genetics and Medicine”. **30 September – 2 October.**
8. 5th Workshop on Inelastic Neutron Scattering “Spectrina-2020”. **11–12 November.**
9. VII All-Russian Youth Science Forum “Open Science 2020”. **18–20 November.**
10. An anniversary conference “Young Talents – 2020” of the program “School Environmental Initiative”. **9 December.**
11. IX School on Polarized Neutron Physics “FPN-2020”. **10–11 December.**



